The axonal transcript *Tp53inp2* mediates the development of the sympathetic nervous system

Hamish Crerar

Thesis submitted for the degree of Doctor of Philosophy

Riccio Lab

MRC Laboratory for Molecular Cell Biology

University College London

November 2017

I, Hamish Crerar, confirm that the work presented in this thesis is my own. Where information has been derived from other sources, I confirm that this has been indicated in the thesis.

Abstract

Nerve Growth Factor (NGF) is a neurotrophin essential for the survival of sympathetic and sensory neurons. Localisation of mRNA in axons of NGF-dependent neurons supports growth and maintains axon integrity, however how localised transcripts regulates most axonal functions remains unknown. To characterise the 3'UTR of transcripts localised in sympathetic neuron axons, we performed a 3'end RNA-Seq on mRNA isolated from either axons or cell bodies of neurons cultured in compartmentalised chambers. We identified *Tp53inp2* as the most abundant transcripts in axons, accounting for almost one third of the reads. Interestingly, despite the abundance of its RNA, the protein for Tp53inp2 is not detectable within axons of sympathetic neurons. We observe that *Tp53inp2* is not actively translated, held in a strictly repressed state mediated by its UTRs. Deletion of Tp53inp2 in sympathetic neurons *in vivo* and *in vitro* affects both cell survival and axon growth, suggesting a critical role for Tp53inp2 in neuronal development, despite the lack of translation. That this phenotype can be rescued by transfecting a non-translatable form of the transcript, suggests that instead *Tp53inp2* acts as an atypical non-coding RNA, whose function is mediated through interaction with the NGF receptor TrkA. We conclude that *Tp53inp2* mRNA regulates sympathetic neuron survival and axon growth in a coding-independent manner by interacting with TrkA receptor and enhancing axonal NGF-dependent signalling.

Acknowledgements

I would like to start by expressing my sincere gratitude to my supervisor Professor Antonella Riccio. Her guidance, motivation and support have been incredible throughout my time in the lab, and she has constantly encouraged me to push beyond what I thought I was capable of.

I extend my gratitude to the excellent collaborators I have had throughout this project. Dr. Raphaëlle Luisier and Dr. Nicholas Luscombe for their work on the RNAseq and to Dr. Marco Gaspari for the mass spectrometry analysis. Special thanks goes to Professor Rejji Kuruvilla, Chantal Bodkin-Clarke and Emily Scott-Solomon with whom it has been a pleasure to work on the knockout mouse, both at home and overseas.

I would like to thank Dr. Catia Andreassi for her selfless technical assistance and guidance during my time in the lab. I am also very grateful to all other members of the Riccio lab, both past and present: Dr. Luca Crepaldi, Dr Marife Cano, Dr. Emily Brookes, Dr. Justyna Nitarska, Dr. Jacob Smith, Dr. Cristina Policarpi, Dr. William Sherlock, Sarah Aldous, Sarah French and Emilie Logie for making the lab a truly fantastic environment to work in. It has been my privilege to work with such a dedicated and passionate group. Special thanks goes to Emilie for her invaluable assistance with the 3'UTR constructs and Marife for her extensive work on the antibody validation.

Thanks goes to all those who have read and edited drafts of the thesis, their suggestions and discussions have been invaluable.

Thank you to my family and friends for their support. A special thanks to my parents who have supported me in every way during my PhD. Finally, I am indebted to Hilary for her unwavering support and encouragement through the tough times and excitement during the good. Without her help this would have been very difficult indeed.

Table of Contents

List of Figures

List of Tables

Abbreviations

ANS	Autonomic nervous system
Ago2	Argonaute-2
AKT (PKB)	Protein Kinase B
APA	Alternative polyadenylation
ARE	AU-rich element
ARE-BP	ARE-binding protein
Atf4	Activating transcription factor 4
AUF1	AU-binding factor 1
AV	Adenovirus
BDNF	Brain derived neurotrophic factor
BMP	Bone morphogenetic proteins
CDS	Coding sequence
ceRNA	Competing endogenous RNA
Cox4	Cytochrome c oxidase 4
CPSF	Cleavage and polyadenylation specificity factor
CREB	cAMP response element-binding protein
CPEB1	Cytoplasmic polyadenylation element binding protein
CTSF	Cleavage-stimulating factor
DAG	Diaglycerol
DCC	Deleted in colorectal cancer
DOR	Diabetes and obesity regulator
DRG	Dorsal root ganglia
eEF1A-1	Eukaryotic elongation factor 1A-1
eIF4E	Eukaryotic initiation factor 4E
ERK	Extracellular signal-regulated kinase
FMRP	Fragile x mental retardation protein
FUS	Fused in sarcoma
IMPA1	Inositol monophosphatase1
IP3	Inositol triphosphate
Ig	Immunoglobin-like
HITS-CLIP	High throughput sequencing-crosslinking immunoprecipitation
HuD (Elavl4)	ELAV-like protein 4
HuR	Hu-antigen R
LE	Localisation element
MAPK	Mitogen activated protein kinase
MEF2D	Myocyte enhancer factor 2D
myrdEGFP	Myristoylated destabilised EGFP
NGF	Nerve Growth Factor
NFAT	Nuclear factor of activated T-Cells
NT-3	Neurotrophin-3
NT-4	Neurotrophin-4
ORF	Open reading frame
$p75^{NTR}$	p75 neurotrophin receptor
PAS	polyadenylation signal
PI3K	Phophoinositide 3-kinase
PC12	Pheochromocytoma-12
PLC-γ	Phospholipase C gamma
PNS	Parasympathetic nervous system
PolI	Polymerase 1 transcription machinery
PTENP1	PTEN pseudogene
RACE	Rapid amplification of cDNA ends
RBP	RNA binding protein
RISC	RNA-induced silencing complex
RGC	Retinal ganglion cell
SAGE	Serial analysis of gene expression
SCG	Superior cervical ganglia
SFPQ	Splicing factor poly-glutamine rich
SNS	Sympathetic nervous system
STAT3	Signal transducer and activation 3
TERC	Telomerase RNA component
TH	Tyrosine hydroxylase
TNF	Tumour necrosis factor
Tp53inp2	Tumour protein p53 inducible nuclear protein 2
TRAP	Translating ribosome affinity purification
TRICK	Translating RNA imaging by coat protein knock-off
TrkA/B/C	Tropomyosin receptor kinase A/B/C
TSS	Translational start site
UTR	Untranslated region
Ube3a	Ubiquitin-protein ligase E3A
Upf1 (RENT)	Regulator of nonsense transcripts 1
YB-1	Y-box-protein 1
ZBP1	Zipcode binding protein 1

1. Introduction

1.1 The sympathetic nervous system

The development of the mammalian autonomic nervous system (ANS) is a complex process that must be completed faithfully to ensure the establishment of the neuronal circuitry that regulates a wide range of involuntary body responses. The ANS includes the sympathetic (SNS) and parasympathetic nervous systems (PNS) that act antagonistically to maintain the body's homeostasis by regulating blood pressure, heart and respiration rate, body temperature and sexual arousal. The PNS is responsible for the body's "rest and digest" responses that ensure a constant basal heart and respiration rate to minimise energy expenditure under normal conditions. It also regulates vital functions, such as digestion and sexual arousal. Conversely, the SNS mediates the body's "fight or flight" response to perceived threats by triggering physiological actions designed to maximise the individual's chances of survival. These include increased heart and respiration rate, diversion of blood to skeletal muscle, suppression of digestion and sexual arousal, and dilation of the pupils. The ANS mediates these actions by innervating a number of targets throughout the mammalian body, including the heart, lungs, eyes, kidneys, skin, smooth and cardiac muscle, and endocrine and exocrine glands (**Fig.1.1**).

Neuronal and glial cells of the SNS derive from progenitor cells located in the neural crest that generate pre- and post-ganglionic neurons. During SNS development, the neural crest cells migrate ventrally to the dorsal aorta and form a column of ganglion primordial cells. Upon reaching the dorsal aorta,

the progenitor cells encounter bone morphogenetic proteins (BMP), which regulates the expression of transcriptional regulators required for noradrenergic differentiation, including *Mash1*, *Phox2a/b* and *HAND2* (Lo *et al.* 1991, Lo *et al.* 1997, Lo *et al.* 1999, Ernsberger *et al.* 2000, Howard 2005). These cells eventually coalesce into discrete ganglia that in the case of postganglionic neurons are the superior cervical ganglia (SCG) and the prevertebral ganglia (Young *et al.* 2011). The neuroblasts undergo several rounds of proliferation to populate the ganglia followed by terminal differentiation into neurons capable of elaborating dendrites and axons (Glebova and Ginty 2005). The regulated outgrowth of these processes and final innervation of correct targets is critical for the SNS' function.

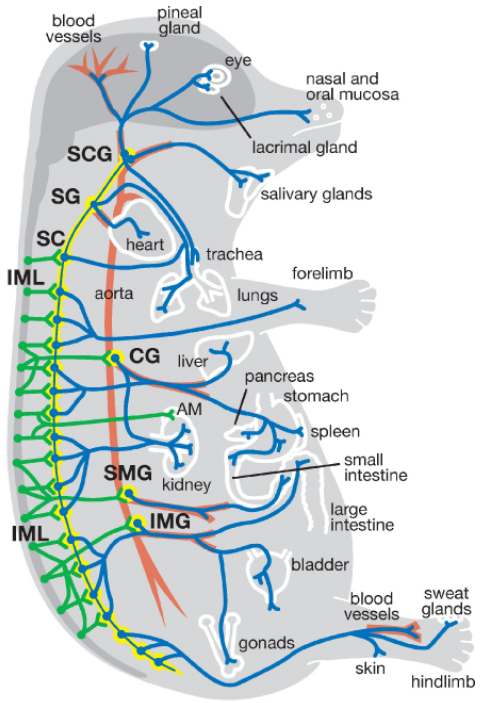

Fig.1.1 The rodent sympathetic nervous system Schematic illustration of the ganglia and target tissues of the rodent SNS. Stellate ganglion (SG), sympathetic chain (SC) intermediolateral column (IML), superior mesenteric ganglion (SMG) and inferior mesenteric ganglion (IMG). Taken from (Glebova and Ginty 2005).

1.1.1 Neurotrophins mediate SNS development

In rodents, SNS target innervation occurs over a relatively wide time frame, with the first axonal projections detectable at embryonic day (E) 12 in rats (Rubin 1985, Young *et al.* 2011). Sympathetic axons reach the lacrimal gland and eye as early as E15, while other tissues, such as the skin and sweat glands, are not fully innervated until after birth (Rubin 1985, Young *et al.* 2011). The growth of sympathetic neuron axons can be roughly divided into two stages, which are the initial axon outgrowth and final target innervation. Both stages are dependent upon extracellular signalling molecules, such as the neurotrophins. Neurotrophins are a family of small peptide growth factors that includes the nerve growth factor (NGF), brain derived neurotrophic factor (BDNF) and neurotrophin-3 and -4 (NT-3, NT-4). Initial axonal growth depends on Artemin and NT-3. Artemin is a member of the GDNF family of trophic factors that in rodents is expressed and released from the arterial smooth muscle cells (Honma *et al.* 2002). At E14, Artemin is highly expressed in the vicinity of sympathetic ganglia, including the SCG, and induces initial growth of sympathetic neuron axons (Baloh *et al.* 1998, Nishino *et al.* 1999, Honma *et al.* 2002). Consistent with this finding, *in vitro* stimulation of sympathetic neurons with Artemin induces axonal outgrowth and genetic disruption of either Artemin or its co-receptor GFRα3/RET inhibits axon growth (Enomoto *et al.* 2001, Honma *et al.* 2002).

Similarly, NT-3 is expressed in the arterial vasculature at E15, at a time coinciding with the early growth of sympathetic neuron axons, and exposure to NT-3 induces neurite development *in vitro* (Maisonpierre *et al.* 1990,

Scarisbrick *et al.* 1993, Belliveau *et al.* 1997, Francis *et al.* 1999). Evidence for the role of NT-3 in regulating axonal outgrowth *in vivo* was provided by the analysis of the phenotype of mice lacking NT-3 (Francis *et al.* 1999, Kuruvilla *et al.* 2004). NT-$3^{-/-}$ animals develop to term but display reduced activity and food intake relative to wildtype littermates, and typically die within 24 hours. This is primarily due to neuronal cell death, as there is a 48% reduction in the number of SCG neurons in perinatal NT-$3^{-/-}$ mice when compared to wildtype littermates (Farinas *et al.* 1994). Interestingly, at E15.5, there is no difference in the number of ganglionic neurons in NT-$3^{-/-}$ mice compared to wildtype, however these neurons exhibit impaired axonal growth and target innervation (Kuruvilla *et al.* 2004). Thus, the neuronal cell death observed in NT-3-/- mice is due to a lack of target innervation and exposure to the essential target-derived survival factor, NGF.

1.1.2 Signalling to survive: the Nerve Growth Factor (NGF)

The first indication that a target-derived trophic factor controlled neuronal growth and survival was provided by Viktor Hamburger and Rita Levi-Montalcini. When fragments of the mouse sarcoma 180, a tumour that produces NGF, were grafted onto the developing limb bud of chick embryos, sensory neuron axons projected into the neoplastic tissue at very high density, indicating that the tumour provided a stimulating environment for axonal growth (Bueker 1948, Levi-Montalcini and Hamburger 1951). Moreover, the ganglia grown with mouse sarcoma cells were six times larger than controls, suggesting the tumours secreted a factor capable of mediating cell survival and growth (Levi-Montalcini and Hamburger 1951, Levi-

Montalcini 1987). The discovery of NGF as the trophic factor responsible for these effects occurred when Rita Levi-Montalcini and Stanley Cohen observed that a protein fraction obtained from snake venom stimulated cultured chick sensory ganglia to produce a large halo of axons (Cohen and Levi-Montalcini 1956, Levi-Montalcini and Cohen 1956). This was followed four years later by the purification of mammalian NGF from the submaxillary salivary glands of mice, and the demonstration of axonal growth promoting effect both *in vitro* and *vivo* (Cohen 1960, Levi-Montalcini 1987). In addition to promoting growth, NGF is also necessary to regulate the development and maintenance of the SNS. Injection of anti-NGF antibodies in neonatal rats resulted in loss of sympathetic neurons (Levi-Montalcini and Booker 1960). More recently, analysis of $NGF^{-/-}$ knockout mice revealed a near complete loss of neurons in the ganglia of the sympathetic and sensory nervous systems (Crowley *et al.* 1994).

Early studies from the Hendry laboratory demonstrated that axotomy of SCG neurons resulted in dramatic atrophy of the ganglia, suggesting that the axons were transmitting a survival signal to the cell bodies. Importantly, NGF applied exogenously to axotomised sympathetic neurons promoted cell survival (Hendry 1975). This pivotal study provided the basis for the hypothesis that target derived NGF is required for neuronal survival and that the signal initiated at the distal axons is retrogradely transmitted to the cell bodies. Further support to this hypothesis was provided by the work of Robert Campenot, utilising a compartmentalised chamber system (**Fig.1.2**). In this system, the chamber is attached to the culture dish by a thin layer of grease. Neurons are plated in the central compartment and are able to project axons

under the Teflon dividers, through the grease, into the lateral compartments. However, the grease does not allow significant diffusion of fluids and therefore the three compartments are physically separated from one another (Campenot 1977). Two major findings regarding the nature of NGF signalling arose from experiments utilising sympathetic neurons cultured in these chambers. First, NGF in the media of the lateral compartments was necessary for axonal projection into the lateral compartments and, withdrawal of NGF from the lateral compartments induced axon degeneration, regardless of whether NGF was present in the cell body compartment. Second, neurons survived NGF withdrawal from cell bodies as long as NGF was supplied to axons (Campenot 1977). Thus, local NGF stimulation was necessary and sufficient to promote and maintain axonal growth, and more importantly, target-derived NGF signalling supported neuronal survival.

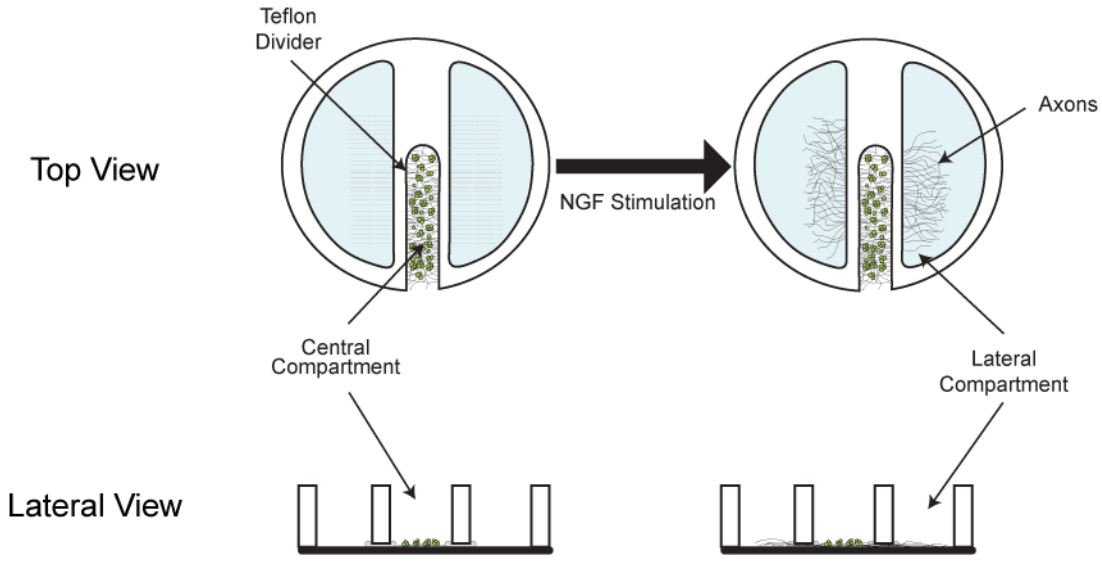

Fig.1.2 Schematic representation of compartmentalised chambers. Sympathetic neurons are cultured in the central compartment, with NGF initially provided to both central and lateral compartments. Although neurons project axons under the Teflon dividers, there is no significant fluid diffusion between chambers, allowing isolation of the subcellular compartments.

More than 50% of neurons generated during SNS development undergo apoptosis (Oppenheim 1991). The neurotrophic hypothesis postulates that this is due to the neurons failing to reach their targets through either poor axonal growth or faulty pathfinding. The neurons that reach the target tissues compete for limiting amounts of trophic factors, ensuring that the number of innervating axons matches the size of the target (**Fig.1.3**). In support of this hypothesis, the *NGF* transcript is expressed in sympathetic targets and the levels of expression correlate with the final density of target innervation (Heumann *et al.* 1984, Shelton and Reichardt 1984).

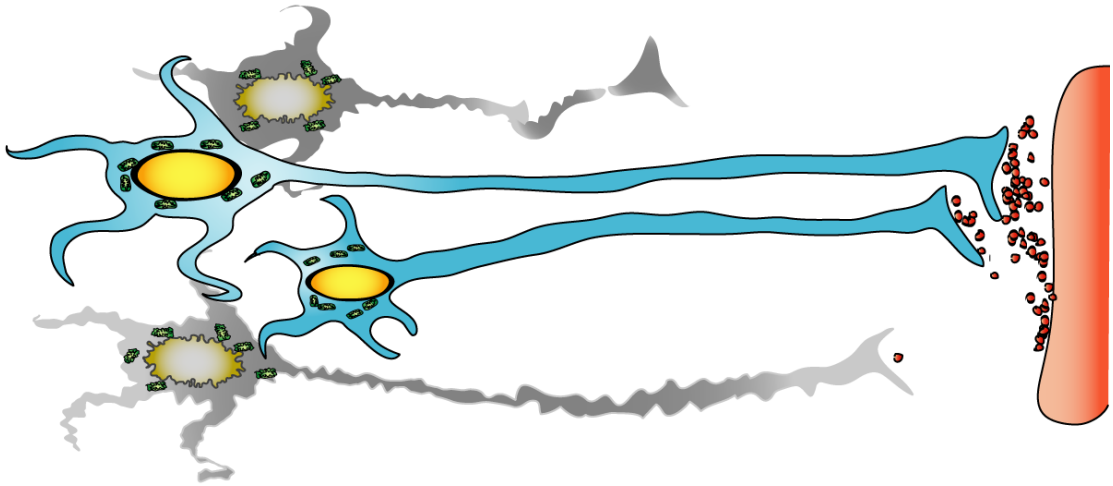

Fig.1.3 The neurotrophic hypothesis A limited supply of target-derived neurotrophin ensures that only neurons that correctly innervate their targets survive, while neurons that fail to reach their targets die through apoptosis. Figure provided by Antonella Riccio.

1.1.3 Neurotrophin signalling in sympathetic neurons

NGF signalling is initiated by the binding of NGF to the tyrosine receptor kinase A (TrkA), a member of the tyrosine receptor kinase family that includes TrkA, TrkB and TrkC. Each receptor has high affinity for specific members of the neurotrophic family; NGF preferentially binds TrkA, BDNF and NT-4/-5 bind TrkB, and NT-3 binds TrkC and with a lesser affinity to TrkA and TrkB

(Zweifel *et al.* 2005). Moreover, all neurotrophins bind to the p75 neurotrophin receptor ($p75^{NTR}$) with approximately equal low affinity (Rodriguez-Tebar *et al.* 1990, Rodriguez-Tebar *et al.* 1992). The Trk receptors consist of a cytoplasmic domain containing tyrosine kinase activity, a single transmembrane domain and an extracellular domain. The extracellular domain includes three leucine rich repeat motifs flanked by two cysteine clusters and two immunoglobin-like (Ig) domains (Huang and Reichardt 2003). The Ig domains are chiefly responsible for the binding of specific neurotrophins (Perez *et al.* 1995).

TrkA was identified as the high affinity receptor for NGF in the early 1990s, (Kaplan *et al.* 1991, Klein *et al.* 1991). NGF application was sufficient to induce TrkA phosphorylation in sensory neurons, in the PC12 cell line (a neural crest-derived cell line that expresses TrkA) and in mouse 3T3 fibroblast cells expressing human *TrkA* cDNA (Kaplan *et al.* 1991, Klein *et al.* 1991). Expression of human TrkA was also sufficient to pull down I^{125} labelled NGF (Kaplan *et al.* 1991, Klein *et al.* 1991). Ablation of the TrkA gene in mice leads to extensive loss of sympathetic neurons in sympathetic ganglia, reduced target innervation, and lethality within one month of birth (Smeyne *et al.* 1994, Fagan *et al.* 1996). The phenotype of the $TrkA^{-/-}$ mouse closely resembles that of $NGF^{-/-}$ mice, highlighting its role as the main functional receptor of NGF.

NGF binding to TrkA induces homodimerisation of the receptor and trans-autophosphorylation of several tyrosine residues within the cytoplasmic domain (Huang and Reichardt 2003). In human cells, TrkA tyrosines (Y) 670, 674, and 675 are essential for the tyrosine kinase activity of the receptor,

while Y490 and Y785 are the major docking sites of effector proteins responsible for mediating downstream signalling (Obermeier *et al.* 1993, Stephens *et al.* 1994, Cunningham *et al.* 1997). Phosphorylated Y490 serves as a docking site for the adaptor proteins Shc and Frs2, which in turn recruit and activate the PI3K and Ras-ERK pathways, and the activation of Akt and the MAPK signalling cascade respectively (Stephens *et al.* 1994, Kao *et al.* 2001, Reichardt 2006). Phospho-Y785 recruits phospholipase C gamma (PLC-γ) causing its activation by the Trk receptor's kinase activity (Obermeier *et al.* 1993, Loeb *et al.* 1994). Activated PLC-γ then hydrolyses the phospholipid $PI(4,5)P_2$, generating diaglycerol (DAG) and inositol triphosphate (IP3), resulting in IP3-dependent release of Ca^{2+} from cytoplasmic stores and DAG-dependent activation of Protein kinase C (PKC) (Reichardt 2006) (**Fig.1.4)**. In axons, these signalling pathways act locally to promote and regulate growth. In *Xenopus* spinal neurons, pharmacological inhibition of the MAPK pathways in axons prevents growth cone steering towards guidance cues Netrin-1 and BDNF (Ming *et al.* 2002). In sympathetic neurons transduced with the TrkB receptor, local application of BDNF to axons rapidly activates the MEK and PI3K pathways in an Shc-dependent manner, and promotes axonal elongation (Atwal *et al.* 2000). Further experiments performed in sensory neurons revealed that NGF-dependent activation of PI3K in growth cones regulates the microtubule plus end binding protein, Adenomatous polyposis coli (APC), which is essential for rapid axonal growth (Zhou *et al.* 2004).

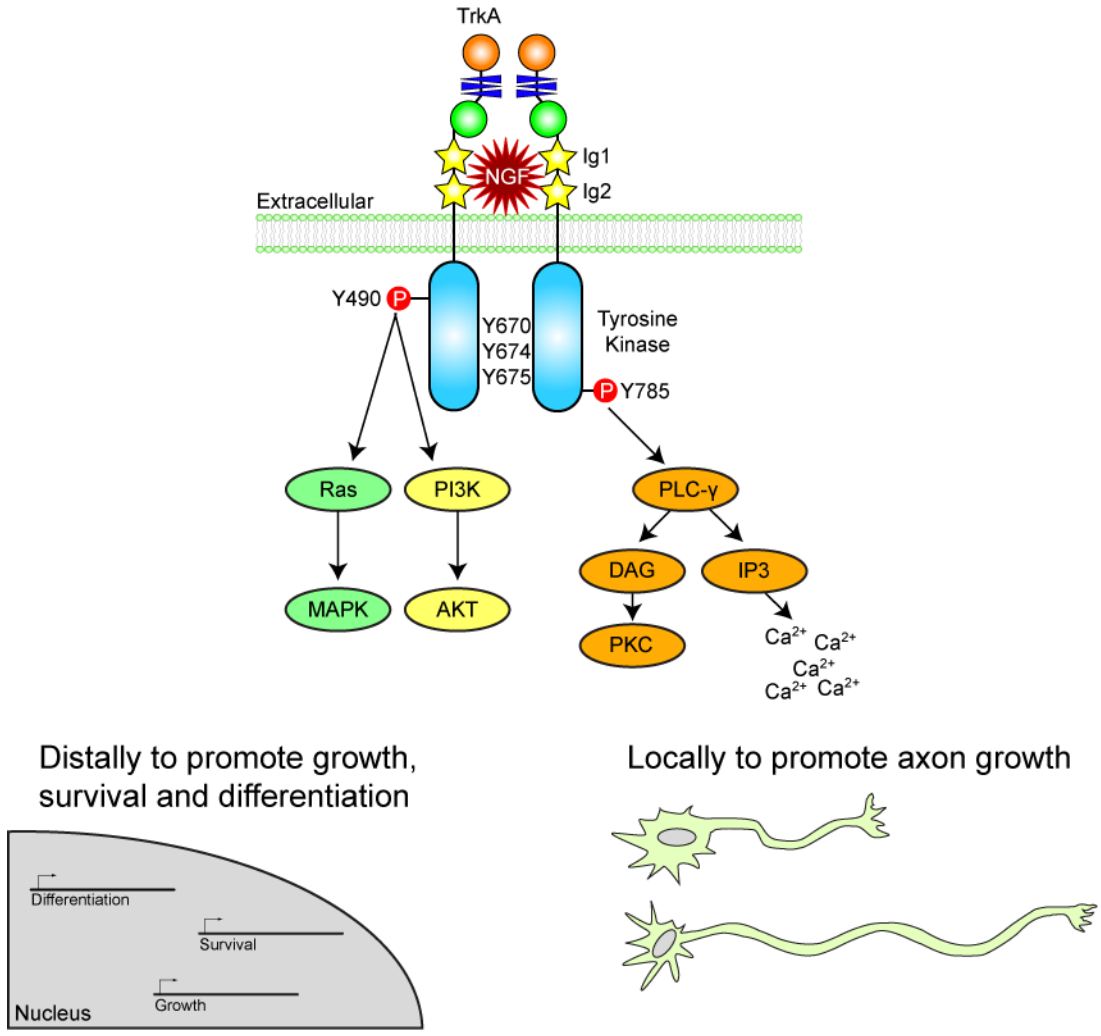

Fig.1.4 NGF-TrkA signalling Illustrative schematic of NGF-bound TrkA homodimers. The immunoglobin-like (Ig) domains are chiefly responsible for NGF recognition. Phosphorylated TrkA activates downstream signalling pathways in axons and cell bodies responsible for axonal outgrowth and survival. The major tyrosine (Y) residues for effector docking and kinase activity are indicated.

In addition to mediating local signalling, NGF binding to TrkA induces the internalisation of ligand-receptor complexes, retrograde trafficking and activation of signalling pathways within the cell body essential for neuronal survival and differentiation (Harrington and Ginty 2013). The mechanism of ligand-receptor internalisation is not fully understood, with *in vitro* evidence supporting two independent mechanisms: clathrin-dependent endocytosis and

Pincher-mediated macropinocytosis (Yamashita and Kuruvilla 2016). Exposure of cultured dorsal root ganglia (DRG) sensory neurons to NGF leads to an increased association of clathrin with the plasma membrane (Howe *et al.* 2001). Conversely, overexpression of Pincher protein in PC12 cells led to a significant increase in the internalisation of NGF-TrkA complexes (Shao *et al.* 2002). However, evidence supporting either of these mechanisms *in vivo* is still lacking.

Recent work has explored how receptor-ligand internalisation is initiated in sympathetic neurons. Bodmer and colleagues demonstrated that NGF-TrkA dependent activation of PLC-γ induces receptor internalisation in a calcineurin dependent manner (Bodmer *et al.* 2011). Calcineurin is a calcium-responsive phosphatase that regulates axonal outgrowth and its conditional deletion in the SNS reduced target field innervation (Graef *et al.* 2003, Bodmer *et al.* 2011, Ascano *et al.* 2012). PLC-γ activation in response to NGF stimulates calcineurin-dependent dephosphorylation of the endocytic GTPase dynamin-1, initiating NGF-TrkA internalisation. This event induces the recruitment of the actin-modifying proteins Rac1 and cofilin, which sever the actin cytoskeleton allowing efficient entry of the receptor-ligand complex into axons and the maturation into retrograde transport competent endosomes (Harrington *et al.* 2011). Alongside receptor-ligand complexes, signalling endosomes contain components of activated Ras-MAPK signalling pathways, pErk1/2, as well as PI3K and PLC-γ (Howe *et al.* 2001). Signalling endosomes are retrogradely transported to cell bodies along microtubules in a dynein-dependent manner (**Fig.1.5**) (Hafezparast *et al.* 2003, Heerssen *et al.* 2004). A model for the initiation of retrograde signalling entails the recruitment

of the microtubule plus-end binding proteins EB1 and EB3 and the cytoplasmic linker protein CLIP170 to the endosome (Moughamian *et al.* 2013). This event leads to the recruitment of the dynein activator protein dynactin, the association of the whole complex with the microtubule network and the initiation of retrograde transport (Moughamian *et al.* 2013).

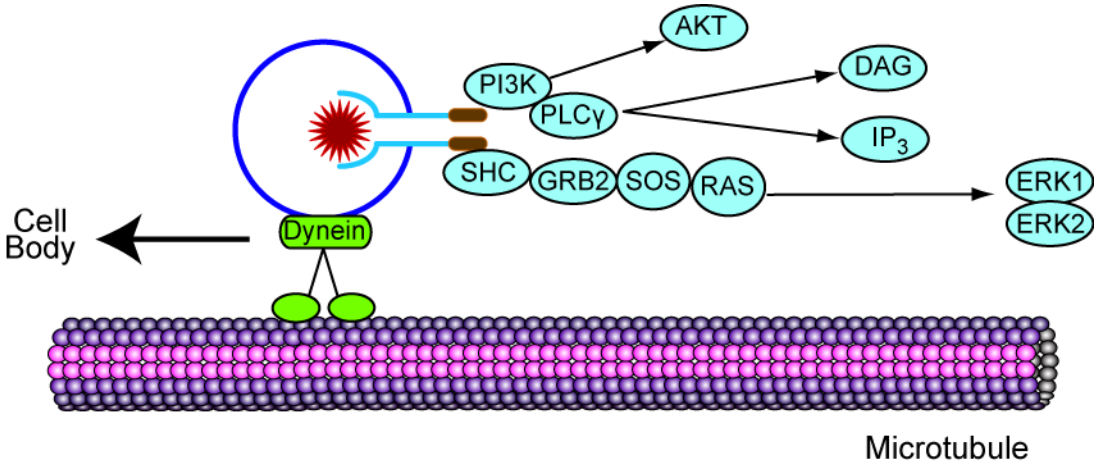

Fig.1.5 The signalling endosome The NGF-TrkA complex, along with downstream signalling components, is internalised as a signalling endosome. The endosome recruits the motor protein dynein, allowing retrograde transport along microtubules to the neuronal cell body. Adapted from (Harrington and Ginty 2013)

Retrograde trafficking of signalling endosomes is critical for sympathetic neuron survival, as attenuation of TrkA phosphorylation in axons or prevention of retrograde trafficking induces apoptosis (Kuruvilla *et al.* 2000, Ye *et al.* 2003). Activation of the Ras-MAPK and PI3K/Akt pathways in cell bodies are necessary for NGF-dependent survival of sympathetic neurons (Bartlett *et al.* 1997, Markus *et al.* 1997, Crowder and Freeman 1998). Pharmacological inhibition of PI3K signalling or expression of a dominant negative form of PI3K in rat sympathetic neurons significantly increased cell death (Bartlett *et al.* 1997, Crowder and Freeman 1998), while in the chick, injection of anti-Ras antibodies induces the loss of 30% of SCG neurons (Markus *et al.* 1997). Dominant negative forms of Akt transduced in sympathetic neurons induced

55% cell death in the presence of NGF, while expression of constitutively activated Akt supported survival even in the absence of NGF (Crowder and Freeman 1998).

These signalling pathways promote survival through the activation of several transcription factors, including the cAMP response element-binding protein (CREB), the myocyte enhancer factor 2D (MEF2D) and the Nuclear factor of activated T-Cells (NFAT), which regulate the expression of genes necessary for neuronal survival and axonal outgrowth (Riccio *et al.* 1997, Graef *et al.* 2003, Pazyra-Murphy *et al.* 2009). Ras activation induces Mek1/2 phosphorylation that, in turn, phosphorylates Erk1/2. The kinases translocate to the nucleus where they phosphorylate and activate the CREB kinase Rsk2, leading to CREB phosphorylation at Ser133 (Ginty *et al.* 1994, Xing *et al.* 1996). CREB activation and the expression of its target genes are necessary and sufficient for supporting survival in central and peripheral neurons (Bonni *et al.* 1999, Riccio *et al.* 1999, Watson *et al.* 1999). Target genes activated following NGF stimulation include anti-apoptopic factors, such as *bcl-2*, and guidance transmembrane proteins, such as *Linx* and other members of the LIG family (Riccio *et al.* 1999, Mandai *et al.* 2009, Pazyra-Murphy *et al.* 2009). Interestingly, expression of the *TrkA* gene is also upregulated, providing a positive feedback loop that may increase neuron sensitivity to NGF and their chances of survival (Deppmann *et al.* 2008).

The binding of neurotrophins to $p75^{NTR}$ also regulates neuronal growth and survival. The $p75^{NTR}$ belongs to the tumour necrosis factor (TNF) superfamily of receptors and contains four cysteine rich motifs in the extracellular domain, a single transmembrane domain and a cytoplasmic domain that includes a

'death' domain. Unlike Trk receptors, $p75^{NTR}$ does not contain intrinsic catalytic activity, and instead interacts with effector proteins, including the Trk receptors, to mediate a broad range of neuronal functions such as promoting survival or apoptosis and axonal growth or inhibition (Reichardt 2006). In neurons that do not express TrkA, such as hippocampal neurons, $p75^{NTR}$ regulates axon outgrowth through interaction with RhoA. In its active state, RhoA stabilises the actin cytoskeleton, preventing axonal elongation. Upon NGF stimulation RhoA activity decreases, promoting neurite outgrowth (Yamashita *et al.* 1999). In the absence of NGF, $p75^{NTR}$ interacts with the RhoA inhibitor, Rho-GDIα, promoting the release and activation of RhoA. Following NGF stimulation, $p75^{NTR}$ no longer inhibits Rho-GDIα, thereby inactivating RhoA and promoting axon growth (Yamashita and Tohyama 2003). Interestingly, $p75^{NTR}$ regulates signalling pathways involved in both cell survival and apoptosis through the activation of the transcription factors NF-κB and c-Jun, respectively (Casaccia-Bonnefil *et al.* 1996, Bamji *et al.* 1998, Hamanoue *et al.* 1999). In the absence of their respective high-affinity Trk receptors, neurotrophins bind $p75^{NTR}$ and activate the Jun kinase pathway (Bamji *et al.* 1998). BDNF supplied to sympathetic neurons, which do not express TrkB, binds to $p75^{NTR}$ and induces apoptosis in a c-Jun dependent manner (Bamji *et al.* 1998). It is possible that $p75^{NTR}$-dependent apoptosis may be a means to prevent ectopic innervation. In further support of this theory, the number of neurons within the SCG is increased by 36% in $BDNF^{-/-}$ transgenic mice compared to control littermates (Bamji *et al.* 1998, Glebova and Ginty 2005).

p75^{NTR} also acts to modulate the Trk receptors' sensitivity and response to neurotrophin. A striking example of this modulation comes from studying the switch between intermediate and final targets of sympathetic neurons, when responsiveness to NGF is increased at the expense of NT-3. When axons grow towards their initial intermediate targets, p75^{NTR} receptor levels are much lower than that of TrkA, ensuring that NT-3 stimulation occurs through TrkA, but by birth p75^{NTR} expression matches TrkA (Wyatt and Davies 1995, Horton *et al.* 1997). Interestingly, binding of NGF to TrkA stimulates *p75^{NTR}* expression, which interacts with TrkA on the cell surface, inhibiting NT-3 binding to TrkA (Horton *et al.* 1997, Mischel *et al.* 2001, Kuruvilla *et al.* 2004). This mechanism provides a feedback loop whereby axons exposed to higher levels of NGF become more responsive to NGF and less to NT-3, allowing the axons to grow past their intermediate NT-3 expressing targets towards their final targets (**Fig.1.6**).

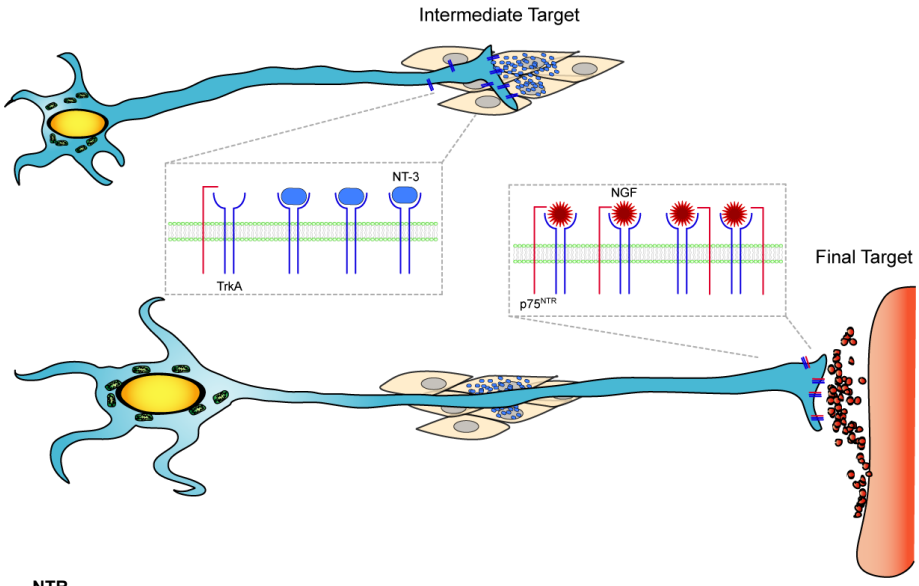

Fig.1.6 p75^{NTR} facilitates the switch between intermediate and final target innervation During initial outgrowth, intermediate targets secrete NT-3 to guide axons. As development progresses, levels of p75NTR expression increase to match those of TrkA. p75NTR interacts with TrkA to prevent NT-3 binding, and facilitate high affinity binding of NGF, thus allowing final target innervation.

1.2 mRNA localisation in neurons

Long-distance innervation of targets implies that neurons are amongst the largest cells in mammals. In rodents, the distance between cell bodies and growth cones can be centimetres or even meters away. For example, the cell bodies of sensory neurons located in DRGs at the top of the spine innervate tissues throughout the body, projecting axons that can be over one metre long in humans, and over 25 metres in blue whales (González and Couve 2014). In addition to their large size, neurons are highly polarised. This is essential for neuronal function, as it allows the localisation of cellular processes to either cell bodies, dendrites or axons. The establishment of cellular polarity is dependent on the expression of proteins in distinct subcellular compartments (Barnes and Polleux 2009). Although protein localisation can be achieved by transporting newly synthesised proteins to dendrites and axons, the complex morphology of neurons presents a unique challenge as the time that it takes to transport a protein from cell bodies to growth cones is often longer than the half-life of the protein. For example, tubulin is anterogradely transported at varying speeds of 0.2 to 1 mm/day but its half-life is only ~48 hrs (Spiegelman *et al.* 1977, Subhojit 2014). Asymmetric localisation of RNA provides a means to overcome these challenges. Dendrites and axons can function with a high degree of autonomy from the cell body, and mRNA can be rapidly translated 'on site' in response to stimuli, providing tight spatiotemporal control (Jung *et al.* 2014). Asymmetric localisation of mRNA provides further advantages over the transport and localisation of protein. For example, a common method for protein targeting relies upon amino acid sequences, such as the nuclear localisation signal. An advantage of mRNA localisation is that it allows protein

localisation without affecting the amino acid sequence (Jung *et al.* 2014). Transport of translationally repressed transcripts prevents ectopic protein expression and bypasses lengthy transport times. It is also energetically cost efficient, as a single mRNA molecule can serve as a template for multiple rounds of translation (Martin and Ephrussi, 2009).

1.2.1 Asymmetric localisation of mRNA is conserved across eukaryotes

The structure of mRNA is highly conserved in eukaryotes, where it consists of a protein coding sequence (Open Reading Frame, ORF) containing motifs that indicate the start and stop of translation (**Fig.1.7**). The ORF is flanked by stretches of untranslated sequence, named the 5' and 3' untranslated regions (UTRs). The 5' end of the nascent mRNA transcript is 'capped' with 7-methylguanosine, which stabilises the mature mRNA and allows ribosome loading. The 3' end is modified with a string of ~200-250 untemplated adenosines, named the polyA tail that is essential for nuclear export, transcript stability and efficient translation (Elkon *et al.* 2013). Both 3' and 5' UTRs regulate overall mRNA functions, as they contain regulatory *cis* elements responsible for all aspects of transcript metabolism, including stability, translational control and localisation (Doyle and Kiebler 2011). In *S. cerevisiae,* 3'UTR polyU elements interact with the polyA tail, increasing transcript stability, while localisation elements (LE) such as the *ß-actin* 'Zipcode' or the *MBP* 'A2RE' element drive axonal localisation of transcripts (Kislauskis *et al.* 1994, Ainger *et al.* 1997, Geisberg *et al.* 2014).

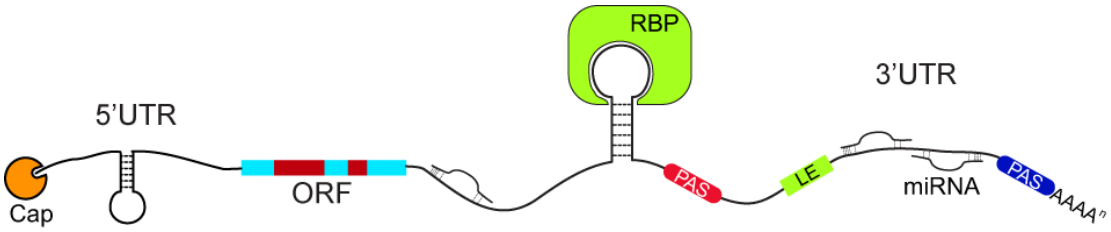

Fig.1.7 Structure of eukaryotic mRNA Regulatory sequences, such as localisation elements (LE) or miRNA binding sites are found throughout the transcript, but are typically enriched in the UTRs. Adapted from (Doyle and Kiebler 2011)

mRNA localisation is an evolutionarily conserved mechanism through which all eukaryotic cells regulate gene expression both spatially and temporally. Thousands of asymmetrically localised mRNA have been identified in eukaryotic cells (Miyashiro *et al.* 1994, Mili *et al.* 2008, Andreassi *et al.* 2010, Zivraj *et al.* 2010, Gumy *et al.* 2011, Cajigas *et al.* 2012, Taliaferro *et al.* 2016). In *S. cerevisiae,* over 30 mRNA transcripts are localised to the growing bud, including *ASH1*, a transcriptional repressor that is involved in regulating mating type switching (Paquin and Chartrand 2008). The localisation of *ASH1* mRNA to the bud depends upon the actin cytoskeleton and is regulated by a *cis* element within the 3'UTR (Long *et al.* 1997, Takizawa *et al.* 1997). Restriction of *ASH1* localisation to the growing bud ensures that the encoded protein is only delivered to the daughter cell, where it prevents mating type switching (Paquin and Chartrand 2008).

In the *Drosophila* embryo, most transcripts show distinct localisation patterns. High-resolution *in-situ* hybridisation of over 3000 mRNAs revealed that over 70% are specifically localised (Lecuyer *et al.* 2007). *Bicoid* is one of the first transcripts that was found to be localised to the anterior pole of the oocyte, where the concentrated expression of Bicoid protein is essential for axis specification (Johnstone and Lasko 2001). *Bicoid* anterior localisation

elements are found within the 3'UTR and their function depends on the primary and secondary structure of the RNA (Macdonald and Struhl 1988).

Similar to *Drosophila*, polar localisation of transcripts in *Xenopus* oocytes is critical for the establishment of embryonic polarity. *Vg1* mRNA is targeted to the vegetal pole by a 340-nucleotide element in its 3'UTR. Local expression of Vg1 protein determines mesoderm and endoderm specification (Mowry and Melton 1992, Thomsen and Melton 1993), whereas ectopic expression of Vg1 protein within the animal hemisphere leads to aberrant induction of mesoderm cells (Dale *et al.* 1993). Thus, mRNA localisation ensures that the protein is not expressed ectopically.

Asymmetrically localised mRNA are commonly detected in mammalian cell types, from fibroblasts to developing and mature neurons (Martin and Ephrussi 2009, Jung *et al.* 2014, Rangaraju *et al.* 2017). One of the earliest identified and best-characterised localised transcripts is *ß-actin*. Compartmentalisation of *ß-actin* transcript was first observed in fibroblasts by Lawrence and Singer in the 1980s and was subsequently detected in the cellular projections of many cell types, including axons and dendrites (Lawrence and Singer 1986, Bassel *et al.* 1998, Leung *et al.* 2006, Mili *et al.* 2008, Andreassi *et al.* 2010, Zivraj *et al.* 2010, Gumy *et al.* 2011, Cajigas *et al.* 2012).

Few cell types are more amenable than neurons to study mRNA localisation, as dendrites and axons are easy to isolate *in vitro* and *in vivo*, allowing the identification of transcripts within. There are numerous examples of axonally and dendritically localised mRNA transcripts that have been identified across a range of species, neuronal types and developmental time

points (Miyashiro *et al.* 1994, Poon *et al.* 2006, Andreassi *et al.* 2010, Zivraj *et al.* 2010, Gumy *et al.* 2011, Cajigas *et al.* 2012, Baleriola *et al.* 2014, Taliaferro *et al.* 2016, Andreassi *et al.* 2017). *Inositol Monophosphatase 1 (IMPA1)* mRNA is enriched in rat sympathetic neuron axons and its expression is necessary for maintaining axonal integrity (Andreassi *et al.* 2010). In retinal ganglion cell (RGC) neurons, the axonal localisation and expression of *ALCAM* is essential for axonal navigation (Thelen *et al.* 2012), and in adult DRG neurons, axonal *Importin ß1* is required for activating response to injury (Perry *et al.* 2012).

1.2.2 Identification of localised transcripts

Transcriptomic screens of neuronal projections across species, time points and cell types have identified thousands of individual mRNAs localised in axons and dendrites, with functions ranging from mitochondrial function to cytoskeletal dynamics, protein synthesis, and signal transduction (Willis *et al.* 2007, Taylor *et al.* 2009, Andreassi *et al.* 2010, Zivraj *et al.* 2010, Gumy *et al.* 2011, Cajigas *et al.* 2012). The transcriptome of axons and dendrites is highly dynamic, changing throughout development and in response to injury. Embryonic and adult sensory neurons have similar numbers of mRNA in axons (2627 and 2924 transcripts respectively) but with very different functions: cytoskeletal and transport related mRNA are enriched in embryonic axons whereas immune response and nociception are found in the adult (Gumy *et al.* 2011). In *Xenopus* RGC, the repertoire of the growth cone transcriptome becomes larger and more diverse as axons grow and project further towards their targets. Interestingly, in *Xenopus* axons, the

transcriptome in growth cones and the axonal shaft differs significantly, suggesting that even within broad subcellular compartments, specific localisation of mRNA could be vital for the establishment of functional domains (Zivraj *et al.* 2010).

Nerve injury also induces a shift of the axonal transcriptome. In cultured rat cortical and hippocampal neurons, the transcriptome of healthy mature axons is enriched for functions related to mitochondrial maintenance, translation and intracellular transport (Taylor *et al.* 2009). However, following axon transection, the composition of the transcriptome changes significantly, with transcripts relating to axon targeting and synaptic function upregulated, suggesting a switch towards neuronal growth and synapse reformation (Taylor *et al.* 2009).

These studies highlight the remarkable scale and dynamic nature of asymmetrically localised mRNA in neurons. The breadth and diversity of transcripts identified so far underline far-reaching biological implications of axonal translation. Correct localisation and local expression of the axonal transcriptome are critical, and this regulation is mediated by elements contained in the mRNA sequence.

1.2.3 Alternative polyadenylation (APA)

Polyadenylation occurs at defined sites within the mRNA transcript, termed poly(A) signals (PAS), which are recognised by the cleavage and polyadenylation machinery. Most PASs are located in the 3'UTRs, though they can occur upstream of the terminal coding exons (Hoque *et al.* 2013). In mammals, the canonical PAS is AAUAAA, which is associated with 42% of mouse 3'UTRs. Alternative variants are also commonly found, such as

AU/GUAAA and UAUAAA (Proudfoot 2011, Hoque *et al.* 2013, Lianoglou *et al.* 2013). In addition, U-rich and GU-rich elements are frequently observed upstream and downstream of the PAS hexamer and it is the combination of these elements that determines the 'strength' of the site (Tian *et al.* 2005, Cheng *et al.* 2006, Tian and Manley 2017). The PAS is recognised by the 3' processing machinery which comprises ~85 proteins arranged into complexes (Shi *et al.* 2009). The cleavage and polyadenylation specificity factor (CPSF) and the cleavage-stimulating factor (CTSF) are two major complexes that recognise the PAS hexamers and downstream elements respectively (Elkon *et al.* 2013). Once associated with the RNA, the complexes initiate cleavage ~10-35nt downstream of the PAS followed by the addition of a stretch of roughly 250 untemplated adenosines to form the polyA tail (**Fig.1.8**) (Tian and Manley 2017).

In humans, 3'UTR length is variable, ranging from a few nucleotides to 8kb (Lianoglou *et al.* 2013). Remarkable variability is observed not only between genes, but also at the level of individual genes, as a gene can produce multiple mRNA isoforms that vary only in the length of their 3'UTR. Variation of the length of the 3'UTR results in exclusion or inclusion of regulatory elements, allowing differential regulation of the mRNA without altering the protein sequence. This mechanism is used to localise mRNA to specific subcellular compartments and to regulate translational efficiency (Sandberg *et al.* 2008, Mayr and Bartel 2009, Andreassi *et al*. 2010, Perry *et al*. 2012).

Advances in transcriptome-wide sequencing have identified multiple PAS within the 3'UTRs of the majority of transcribed genes. Screens carried out in mammalian species (human, rhesus, dog, mouse and rat) and in various

tissues (brain, muscle, testis and whole embryo) revealed that almost 75% of genes undergo alternative polyadenylation, highlighting the potential for differential regulation of gene expression dependent on PAS choice (Derti *et al.* 2012, Shi 2012, Hoque *et al.* 2013).

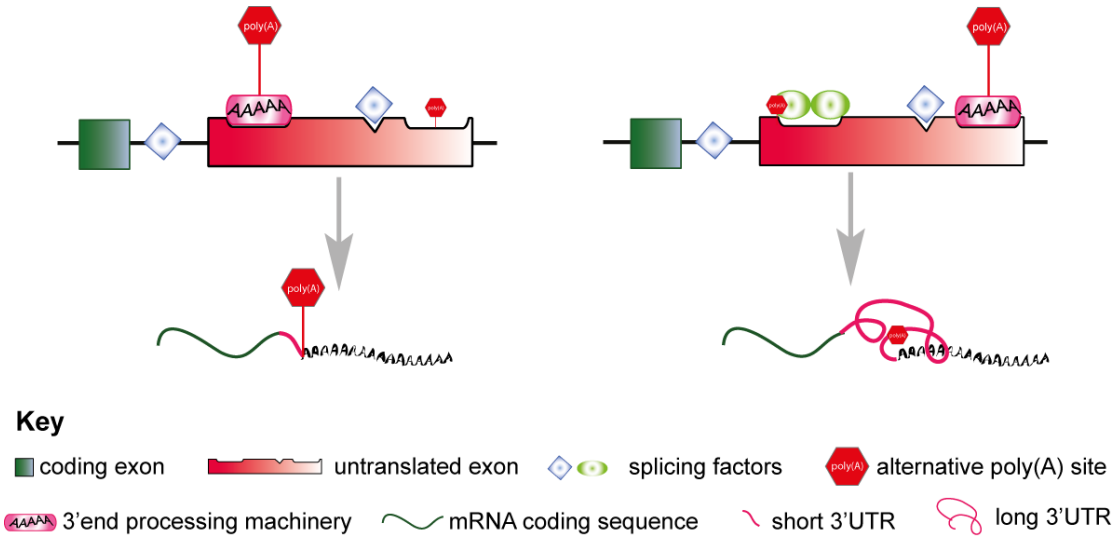

Fig.1.8 Alternative polyadenylation The usage of alternative PAS sites results in different length 3'UTRs. If a distal PAS is selected then a transcript with a long 3'UTR is produced (right diagram), while proximal PAS choice results in a shortened 3'UTR (left diagram). Altering the length of the 3'UTR allows the inclusion or exclusion of regulatory elements, thereby allowing differential regulation of transcripts.

1.2.4 APA regulates mRNA localisation and translation

In neurons, transcripts can be differentially localised to distinct subcellular compartments based on PAS choice and therefore 3'UTR length (An *et al.* 2008, Yudin *et al.* 2008, Andreassi *et al.* 2010, Perry *et al.* 2012, Will *et al.* 2013). In sympathetic neurons, *IMPA1* mRNA is transcribed as multiple isoforms dependent on PAS choice, which differ in subcellular localisation. The short isoform *IMPA1-S* includes a 1.12Kb 3'UTR and is restricted to the cell body. The longest isoform *IMPA1-L* contains an additional 120nt element at the distal end of the 3'UTR that is necessary and sufficient for axonal localisation (Andreassi *et al.* 2010). The expression of *IMPA1* in sympathetic

neuron axons is required for axon integrity, as evidenced by siRNA-mediated knockdown. Importantly, expression of the axonally targeted *IMPA1-L,* but not the coding sequence alone, was sufficient to rescue axon degeneration.

Finally, *Importin β1* mRNA is localised in sensory neuron axons where it is translated in response to nerve lesion (Hanz *et al.* 2003). *Importin β1* is expressed as a short and a long isoform bearing a 134nt 3'UTR and 1148nt 3'UTR, respectively (Perry *et al.* 2012). Similar to *IMPA1*, the longer 3'UTR guides localisation and translation in axons. In response to injury, the newly synthesised Importin-ß1 protein binds to Importin-α1, forming a complex with cargo proteins bearing a nuclear localisation signal (NLS) that are retrogradely transported to cell bodies. Importin-α1/ß1 complexes enter the nucleus where they trigger the expression of genes required for axonal regeneration in response to injury (Michaelevski *et al.* 2010, Perry *et al.* 2012, Tasdemir-Yilmaz and Segal 2016). Local translation of *Importin β1* expressing the long 3'UTR is essential for efficient retrograde signalling in response to injury and decreased injury-dependent changes of the transcriptome was observed in transgenic mice lacking this isoform (Perry *et al.* 2012).

These examples highlight how APA generates 3'UTR isoforms that are localised in different cellular compartments. In most cases shorter isoforms are restricted to the cell body while the long isoforms are targeted to dendrites and axons, however alternative scenarios are possible. A recent study comparing 3'UTR isoform usage in neurite projections of two neuronal cell lines and in axons of mouse cortical neurons did not find a clear link between 3'UTR length and peripheral enrichment (Taliaferro *et al.* 2016). However, recent work from our laboratory revealed a clear enrichment of longer 3'UTRs

in sympathetic neuron axons, relative to cell bodies, suggesting that the relationship between 3'UTR length and localisation may be cell type specific (Andreassi *et al.* 2017).

In addition to regulating localisation of transcripts within cells, APA regulates gene expression across different tissues and developmental stages. Several studies found that tissues preferentially express certain 3'UTR isoforms. For example, neurons are enriched with isoforms expressing longer 3'UTRs, whereas the testes and muscles, as well as cells undergoing rapid proliferation such as activated murine CD4+ T-lymphocytes, preferentially utilise proximal PASs (Zhang *et al.* 2005, Sandberg *et al.* 2008, Derti *et al.* 2012, Lianoglou *et al.* 2013). Ubiquitously expressed genes are also more likely to express different 3'UTR isoforms in specific tissues, indicating that APA may provide a mechanism for tissue-specific regulation of gene expression (Lianoglou *et al.* 2013, Tian and Manley 2017).

The preferential expression of long 3'UTRs in the nervous system may indicate elevated post-transcriptional regulation of gene expression (Glock *et al.* 2017). Longer 3'UTRs provide a greater scope for post-transcriptional control, allowing the inclusion of additional elements responsible for localisation and translational control (Flavell *et al.* 2008, Sandberg *et al.* 2008, Mayr and Bartel 2009, Hurt *et al.* 2013). Additionally, alternative longer 3'UTRs tend to have a higher AU content, which promotes the binding of regulatory proteins or RNA species by reducing the formation of secondary structures in the UTR (Ji *et al.* 2009). More than half of conserved mammalian miRNA binding sites are located in the 3'UTR, and longer 3'UTRs contain 30% more conserved miRNA binding sites than their shorter isoforms (Ji *et al.*

2009, Tian and Manley 2017). Thus, the expression of specific 3'UTRs determines the inclusion of miRNA binding sites, impacting on translational efficiency and mRNA stability.

The effect of 3'UTR length on protein output has been studied both at the level of individual transcripts and, more recently, genome-wide. Using luciferase reporter constructs fused to long or short 3'UTRs of five candidate genes (*Cnn3, E4300 Gtf2e2, Hip2 and Rab1*) Sandberg *et al.* observed that for all candidates, the longer 3'UTR isoform resulted in lower luciferase activity in activated human T cells (Sandberg *et al.* 2008). Similar results were obtained for the long and short 3'UTRs of *IMP-1, Cyclin D2* and *DICER1.* When transfected into 16 different cell lines, the shorter isoform always produced more luciferase, ranging from 1.6 to 42 fold higher expression (Mayr and Bartel 2009). These studies suggest that 3'UTR length has a significant influence on translational efficiency. Several studies have addressed the potential correlation between 3'UTR length and translational efficiency at the level of the transcriptome (Spies *et al.* 2013, Gruber *et al.* 2014, Floor and Doudna 2016). Two studies have combined 3'end RNA sequencing with polysome profiling to analyse the translational profile of transcript isoforms. In HEK-293T cells, 3'UTR length was inversely correlated with translational efficiency, whereas in mouse 3T3 cells elements located within the 5'UTR and ORF were more associated with translation (Spies *et al.* 2013, Floor and Doudna 2016). In activated T-cells, 3'end sequencing to identify PAS choice was combined with quantitative mass spectrometry to analyse protein levels. Interestingly, this study observed no correlation between shortening of 3'UTRs and protein output (Gruber *et al.* 2014).

The expression of specific 3'UTRs changes during tissue development. During mouse embryonic development, 3'UTR length increases globally along with developmental time (Ji *et al.* 2009). Similarly, in cultured embryonic stem cells and in the myoblastic cell line C2C12, differentiation correlated with global lengthening of 3'UTRs (Ji *et al.* 2009, Shepard *et al.* 2011). Extracellular stimuli also induce changes in PAS choice and 3'UTR isoform expression. In cortical neurons for example, synaptic activity leads to the activation of the transcription factor MEF2, a key regulator of gene expression necessary for mediating synaptic plasticity (Flavell *et al.* 2006). Interestingly, a large subset of MEF2-dependent genes expressed following neuronal activity use a proximal PAS, resulting in shortening of the 3'UTR (Flavell *et al.* 2008). This switch in PAS choice may be required for the dendritic expression of these genes. In the immune system, activation of CD4+ T lymphocytes is central to mounting an effective immune response, and induces a sharp rise in cell proliferation. Interestingly, the immune response correlates with 3'UTR shortening of more than 150 genes, including genes involved in regulation of proliferation, such as *Bcl-2* and *Creb1* (Sandberg *et al.* 2008, Gruber *et al.* 2014). Importantly, in cancer cells, a global choice of proximal PAS results in the expression in shorter 3'UTRs, generating isoforms of specific proto-oncogenes that may undergo less regulated translation (Mayr and Bartel 2009).

1.2.5 RNA binding proteins and mRNA localisation

The nascent mRNA interacts with a range of RNA binding proteins (RBPs) such as splicing factors, polyadenylation complexes and transport proteins that ensure appropriate localisation and translation (Sephton and Yu 2015). In

addition to RBPs, a number of associated RNA species regulate mRNA translation and stability. These regulatory factors target *cis*-elements located throughout the whole transcript but typically enriched in the 5' and 3'UTRs. The elements' length ranges from a few nucleotides to a kilobase, and allows the recruitment of *trans*-acting factors by direct interaction with the mRNA primary nucleotide sequence and through the formation of secondary structures (Jambhekar and DeRisi 2007).

The *Zipcode* is located within the 3'UTR of *ß-actin* mRNA and is one of the best-characterised elements that drives peripheral localisation of a transcript (Kislauskis *et al.* 1994). This 54nt element is both necessary and sufficient for the transport of mRNA to the lamellipodia of fibroblasts as well as to axons and dendrites (Kislauskis *et al.* 1994, Eom *et al.* 2003, Farina *et al.* 2003, Willis *et al.* 2011). In sympathetic neurons, *IMPA1* and *cytochrome c oxidase 4* (*Cox4*) are localised in axons via 120nt and 38nt elements respectively, located within their 3'UTRs (Andreassi *et al.* 2010, Aschrafi *et al.* 2010). Localisation elements provide binding sites for a host of RBPs that in the case of the *Zipcode* for example, include the ubiquitously expressed Zipcode Binding Protein 1 (ZBP1) (Ross *et al.* 1997, Eom *et al.* 2003). The element responsible for *Cox4*'s axonal localisation was identified nearly a decade ago, however the RBPs responsible for transcript localisation were discovered only recently. Kar and colleagues used the 38nt *Cox4* localisation element as a 'bait' to pull-down associated proteins in sympathetic neurons. Over 50 proteins were found associated with the localisation element, including fused in sarcoma (FUS) and Y-box-protein 1 (YB-1). Further validation confirmed a direct interaction of these proteins with the 38nt element, and siRNA

knockdown of FUS and YB-1 led to a reduction in axonal *Cox4* mRNA (Kar *et al.* 2017). This study may provide the basis for further identification of RBPs mediating subcellular localisation.

An additional level of post-transcriptional regulation is provided by RBPs expression. In sensory neurons, the levels of ZBP1 represents the limiting factor of *ß-actin* localisation in axons (Donnelly *et al.* 2011). Though many localisation elements are conserved across cell types, there are exceptions. *Neuritin* mRNA is targeted to central and peripheral neuron axons, however the localisation depends on distinct elements, located within the 3'UTR and 5'UTR, respectively (Willis *et al.* 2007, Taylor *et al.* 2009, Merianda *et al.* 2013). Thus, both the expression of alternative 3'UTR isoforms and differential expression of RBPs allow cell type specific regulation of mRNA localisation.

1.2.6 RNA binding proteins and translational regulation

Extensive work has been performed on the RBPs that interact with *cis* elements located in the 3'UTR of localised transcripts. Several element families have been identified, defined by their nucleotide content, which promote the binding of RBPs responsible for translational regulation. The adenylate uridylate (AU-rich) elements (AREs) are regulatory elements responsible for mRNA stability and translational regulation. The prototypical ARE motif AUUUA can be of variable length due to the repetition of uracil-rich regions (Matoulkova *et al.* 2012). ARE elements are recognised by the ARE-binding proteins (ARE-BPs) and can act either by stabilising the transcripts and enabling translation, or by actively inhibiting protein synthesis. ARE-BPs

finely tune the expression of target mRNAs by acting either cooperatively or antagonistically. The AU-binding factor 1 (AUF1) and the Hu-antigen R (HuR) are among the best-studied ARE-BPs that bind to the transcription factor *ATF3* mRNA (Pan *et al.* 2005). In unstimulated conditions, ATF3 protein levels are low, but they rapidly increase following cellular stresses, such as injury, exposure to toxins and oxygen deprivation (Chen *et al.* 1996, Hai *et al.* 1999). In unstimulated conditions, binding of AUF1 to *ATF3* prevents translation, but in response to stress, AUF1 is displaced, allowing HuR to bind *ATF3*. This event enhances *ATF3*'s half-life and increases protein levels (Pan *et al.* 2005). AUF1 and HuR can also cooperate to repress translation and destabilise transcripts. Both HuR and AUF1 bind AREs located in the 3'UTR of $p16^{INK4}$ mRNA. Rather than antagonising the action of one another, HuR and AUF1 cooperate to destabilise the transcript through recruitment of the RNA-induced silencing complex (Chang *et al.* 2010).

Several RBPs act as translational regulators in dendrites and axons. One of the best-studied regulators of mRNA translation is the RBP fragile x mental retardation protein (FMRP). The main role of FMRP in the nervous system is to transport multiple mRNA transcripts to axons and dendrites and to regulate their translation (Antar *et al.* 2005). How target transcripts are recognised by FMRP remains unclear, with evidence supporting both its binding to secondary structures formed by G-quartet stem loops and through direct interaction of FMRP with the primary transcript sequence (Darnell *et al.* 2001, Darnell *et al.* 2011, Ascano *et al.* 2012). The Cytoplasmic polyadenylation element binding protein (CPEB1) binds elements within the 3'UTR of transcripts, such as *ß-catenin* (Kundel *et al.* 2009). In growth cones of

hippocampal neurons, NT-3 stimulation results in phosphorylation of CPEB1, an event shown to be required for the release of CPEB1-mediated translational repression (Mendez *et al.* 2000, Kundel *et al.* 2009). The phosphorylation of CPEB1 is required for increased translation of axonal *ß-catenin,* allowing axonal branching in response to NT-3 (Kundel *et al.* 2009). Finally, ZBP1 also represses *ß-actin* translation during its transport to axons and dendrites (Huttelmaier *et al.* 2005).

1.2.7 RNA granules

mRNA transport and metabolism is regulated through the binding of *trans* acting factors that are assembled into large ribonucleoprotein complexes (RNPs) known as granules, which are heterogeneous in size and composition (Kiebler and Bassell 2006). It is essential that mRNA translation is tightly regulated during transport, preventing ectopic or premature expression of the encoded protein. The granules form in the nucleus, either co- or immediately post-transcriptionally (Sephton and Yu 2015). In neurons, several types of granules have been identified that differ in their protein and RNA components, and functions (Kiebler and Bassell 2006). Transport granules are primarily involved in the transport, translational regulation and storage of mRNA (Kiebler and Bassell 2006). They are typically associated with cytoskeletal motors and are highly dynamic (Zhang *et al.* 2001). Protein components of transport granules include translational repressors, such as FMRP and CPEB, and protein involved in transcript localisation, such as ZBP1 (Huang *et al.* 2003, Antar *et al.* 2004, Elvira *et al.* 2006). Stress granules are generated in eukaryotic cells during periods of cellular stress, including chemical exposure, heat shock and UV irradiation (Anderson and Kedersha 2008). They

sequester and translationally repress mRNA that are not required for the stress response (Wolozin 2012). Processing bodies are both sites of short-term translational repression and mRNA degradation (Anderson and Kedersha 2006). As such, they tend to contain components of the miRNA processing machinery, including Argonaute-2 (Ago2) (Sen and Blau 2005).

Additionally, the orchestrated transport of groups of functionally related mRNAs by RBPs may coordinate the expression of functionally related genes. The RBP splicing factor poly-glutamine rich (SFPQ) has a number of functions including splicing and transcriptional regulation and is highly expressed in the developing mouse brain (Chanas-Sacre *et al.* 1999, Emili *et al.* 2002, Dong *et al.* 2007). A recent study showed that, in sensory neurons, SFPQ may also act as a hub for the axonal transport of several mRNA transcripts, including *LaminB2, bcl-w* and *IMPA1*, promoting neurotrophin-dependent survival (**Fig.1.9**) (Cosker *et al.* 2016). siRNA-mediated knockdown of SFPQ prevented neurotrophin-dependent axonal targeting of these mRNAs and local translation. Moreover, SFPQ knockdown induced axon degeneration, similar to the loss of *LaminB2, bcl-w* and *IMPA1* (Andreassi *et al.* 2010, Yoon *et al.* 2012, Cosker *et al.* 2013, Cosker *et al.* 2016). The assembly of functionally related mRNAs around RBP hubs provides an additional mechanism used by neurons to coordinate local gene expression.

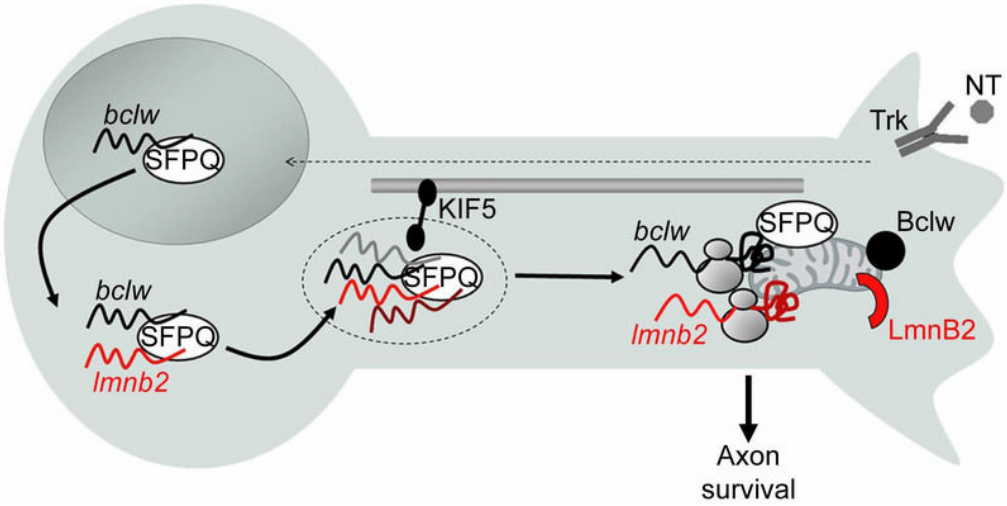

Fig.1.9 SFPQ regulates the transport of mRNA required for axon viability In response to neurotrophin (NT) stimulation, SFPQ binds several mRNA, including *bclw, lmnb2* and *IMPA1,* acting as a molecular 'hub' to regulate their transport to axons. The local translation of these target mRNAs is required for axonal maintenance and survival. Taken from Cosker *et al.* 2016.

1.2.8 miRNA regulation of mRNA translation and stability

It is increasingly apparent that the regulation of mRNA does not depend exclusively on the recruitment of certain RBPs, but on a complex interplay between RBPs, noncoding RNA (ncRNA) and the mRNA itself. miRNAs are small 20-22nt transcripts that regulate gene expression post-transcriptionally. They typically function through translational repression and destabilisation of target mRNAs (Bartel 2009). The biogenesis of miRNA is a multistep process that starts with the transcription of a primary miRNA (pri-miRNA) containing hairpin secondary structures. The pri-miRNA is cleaved by the Drosha-DGCR8 processing complex, generating a ~70nt intermediate precursor (the pre-miRNA). Following nuclear export, pre-miRNA is further cleaved by the cytoplasmic RNase DICER, generating the final mature miRNAs duplexes (Fineberg *et al.* 2009, Iyengar *et al.* 2014). Mature miRNAs are recognised by the Argonaute (Ago)-containing RNA induced silencing complex (RISC). The miRNA guides the RISC complex to the mRNA sequence, inhibiting the

expression of the target. miRNA binding sites are localised throughout the mRNA transcript, but are found more frequently in the 3'UTRs (Lewis *et al.* 2005, Nielsen *et al.* 2007, Bartel 2009). Importantly, binding of miRNAs to target sites does not require a perfect homology, as it relies on the 7-8 bases located at the most 5' end of the miRNA (Ha and Kim 2014). The limited target homology allows individual miRNA to target hundreds of different transcripts, enabling coordinated regulation of gene expression (Im and Kenny 2012). For example, miR-1 and miR-124 are preferentially expressed in muscle and brain tissue, respectively (Lagos-Quintana *et al.* 2002). In HeLa cells, expression of miR-1 and miR-124 inhibits 96 and 174 mRNAs, respectively. mRNAs downregulated by miR-124 were generally found at lower levels in the brain that other tissues (Lim *et al.* 2005).

In the nervous system, miRNAs regulate a variety of processes, ranging from neuronal development to synaptic plasticity (Krichevsky *et al.* 2003, Sempere *et al.* 2004, Kosik 2006). During the early phases of neurogenesis, the neuronal cell population is established through initial over-proliferation followed by apoptosis of roughly 50% of neurons (Oppenheim 1991). miRNAs control both neural progenitor proliferation and the apoptopic events that refine neuron number (Iyengar *et al.* 2014). For example during neuronal differentiation, the miRNA miR-29b is upregulated and targets multiple members of the pro-apoptopic gene family BH3, preventing their translation and supressing apoptosis (Kole *et al.* 2011).

miRNAs also provide a means of local regulation of gene expression, which is essential for axonal and dendritic functions. A study by Natera-Naranjo *et al* identified 140 miRNAs in sympathetic neuron axons (Natera-

Naranjo *et al.* 2010). Interestingly, several miRNAs were significantly enriched in axons compared to cell bodies, indicating a selective transport and potential axon-specific functions for these transcripts. Bioinformatics analysis revealed that miRNA targets were enriched for neuronal signalling and mRNA transport and translation (Natera-Naranjo *et al.* 2010). The selective peripheral enrichment of about 30 miRNA has also been observed in other model systems, such as cortical, hippocampal and sensory neurons (Pichardo-Casas *et al.* 2012, Hancock *et al.* 2014, Sasaki *et al.* 2014). miR134 is one of the first miRNAs identified in dendrites of hippocampal neurons and is a negative regulator of spine maturation by preventing activity-dependent translation of the actin cytoskeletal regulator Limk1 (Schratt *et al.* 2006), (Fiore *et al.* 2009). miR-9 is enriched in cortical neuron axons where it regulates axon growth and branching, at least in part through inhibiting *Map1b* translation (Dajas-Bailador *et al.* 2012).

Recent studies have demonstrated that extracellular stimuli can impact upon miRNAs functions in axons. In sensory neurons, NGF stimulation leads to the dissociation of *Map1b* and *calmodulin* mRNAs from repressive granules containing miRNA-181d, allowing their translation and subsequent axonal outgrowth (Wang *et al.* 2015). Extrinsic signals have also been shown to affect the levels of miRNAs in axons. A short pulse of BDNF decreases miR-9 levels in axons, increasing MAP1B protein and axonal outgrowth. However, longer exposure to BDNF results in increased miR-9 levels and axonal branching (Dajas-Bailador *et al.* 2012).

Despite these recent discoveries, the targets of most localised miRNAs remain unknown. The limited homology required for the binding of miRNA to

transcripts makes it difficult to predict their targets *in silico*. Moreover, how miRNAs are targeted and localised to neuronal projections is still not fully understood. Two non-exclusive mechanisms have been proposed. The first relies on the transport of mature miRNAs, either alongside their targets or in association with intermediate RBPs (Lugli *et al.* 2008). In sensory neurons for example, the localisation of miR-181d in axons depends on the expression of FMRP, and knockdown of FMRP decreases axonal, but not cell body levels of miR-181d (Wang *et al.* 2015). The second mechanism relies on the transport and subsequent maturation of the pre-miRNA, rather than the mature miRNA. In support of this hypothesis, several studies have now identified peripherally localised pre-miRNA (Lugli *et al.* 2008, Saba *et al.* 2012, Bicker *et al.* 2013). For example, the pre-miR134 is found in dendrites of hippocampal neurons bound to DHX36, which is a RBP that prevents premature processing of the transcript (Bicker *et al.* 2013, Sambandan *et al.* 2017). Accordingly, components of the processing machinery, such as DICER, are expressed in dendritic spines (Lugli *et al.* 2005). The Schuman laboratory recently provided further support for this model using an inducible probe system that consists of a fluorophore-tagged pre-miRNA backbone capable of detecting miRNA maturation. They observed that precursor miRNAs are cleaved to produce mature miRNA products within dendrites in an activity dependent manner (Sambandan *et al.* 2017). This mechanism allows the fine-tuning of translational control, through miRNA in a precise and highly localised manner.

1.2.9 Local translation in response to extracellular stimuli

Though now recognised as an important aspect of neuronal biology, there was initial controversy over whether localised translation occurred outside the soma. There was a firmly established dogma that all axonal proteins were synthesised in the soma, and then transported to the axon (Alvarez *et al.* 2000). This was based on early electron microscopy work failing to identify polyribosomes within axons, and subsequent work failing to identify ribosomal RNA in isolated axoplasm (Lasek *et al.* 1973, Palay and Palade 1955). However, more recent work has provided strong support for the occurrence of axonal translation. The first evidence of local protein synthesis within growing axons came in the 1960s. These early studies showed that vertebrate and invertebrate axons severed from the cell body incorporated heavy-labelled leucine into the newly synthesised proteins and were capable of synthesising protein *de novo* (Koenig 1967, Giuditta *et al.* 1968). Following these pioneering studies, experiments performed on severed axons further strengthened this hypothesis (Van Minnen *et al*. 1997, Campbell and Holt 2001, Ming *et al*. 2002). For example, Van Minnen and colleagues demonstrated that exogenous mRNA injected into the transected axons of cultured *L. stagnalis* neurons was translated within two hours of injection. There is now a large body of work demonstrating the importance of intra-axonal translation during development, following injury and in synaptic function. As a result local translation is now recognised as a major regulator of axonal function, and in particular, responses to extracellular cues.

Growth cones rapidly respond to guidance molecules by steering axons towards attractive cues, such as netrin-1 and BDNF, and away from repulsive

cues, such as semaphorin 3A and Slit2. Importantly, steering occurs even when axons are severed from the cell bodies (Campbell and Holt 2001, Ming *et al.* 2002, Wu *et al.* 2005). Though this could be mediated by proteins already present in axons, exposure of severed axons to translational inhibitors abolishes their capacity to steer towards these cues (Campbell and Holt 2001, Ming *et al.* 2002, Wu *et al.* 2005, Leung *et al.* 2006, Piper *et al.* 2006, Hengst *et al.* 2009). Local translation of cytoskeletal components is necessary for growth cone turning. In cultured *Xenopus* spinal and RGC neurons, application of a BDNF or Netrin-1 gradient results in rapid transport of *ß-actin* mRNA to the side of the growth cone closest to the highest concentrations of the gradient, where it is rapidly translated, generating a local, high concentration of nascent actin monomers. The translated *ß-actin* creates a point of nucleation for cytoskeletal remodelling, allowing growth cone turning (**Fig.1.10**) (Leung *et al.* 2006, Yao *et al.* 2006). Asymmetric localisation of *ß-actin* mRNA is controlled with remarkable specificity. Application of NT-3 coated beads to cultured sensory neurons results in an accumulation of *ß-actin* mRNA within 5µm of the bead's point of application (Willis *et al.* 2007).

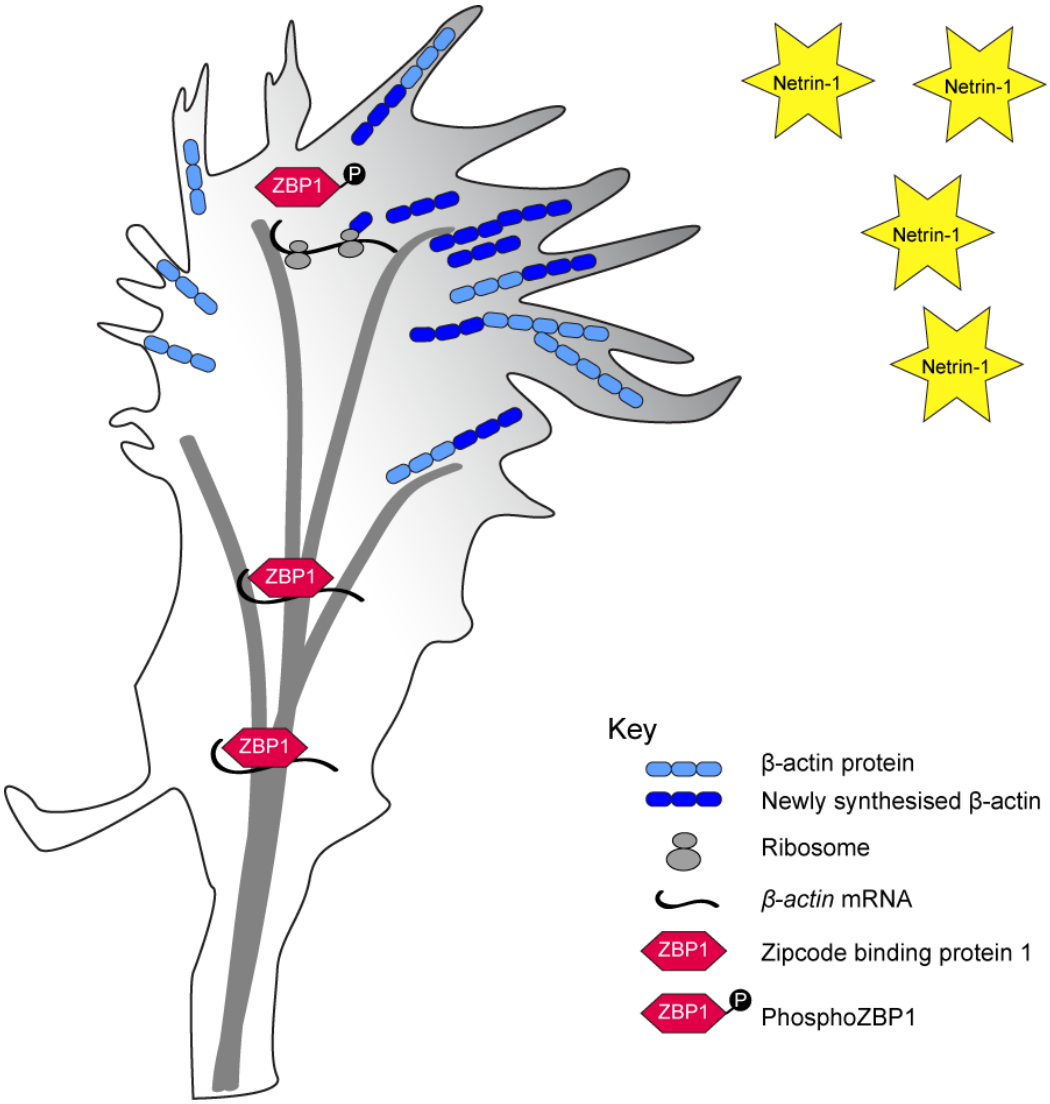

Fig.1.10 Local translation facilitates growth cone turning. ZBP1 binds *ß-actin* mRNA in the soma and mediates its transport to the axonal growth cone. In response to a guidance cue (Netrin-1), Zbp1 is phosphorylated, releasing its translational repression of *ß-actin* and allowing local synthesis of ß-actin protein. The newly synthesised ß-actin is incorporated into the cytoskeleton and facilitates growth cone turning. Adapted from (Welshhans and Bassell 2011)

In addition to axon steering, local translation of mRNA also impacts on growth cone stability, axon growth, synaptic functions and injury response (Aakalu *et al.* 2001, Zheng *et al.* 2001, Andreassi *et al.* 2010, Jung *et al.* 2014). Jeffrey Twiss and colleagues demonstrated that the ability of sensory neuron axons to regenerate *in vitro* following crush injury is dependent upon translation (Twiss *et al.* 2000). Zheng and colleagues showed that axons

contain mRNA encoding *ß-actin* and *neurofilament* as well as the ribosomal proteins L4, 17 and 29 and other components of the translational machinery. In severed axons, exposure to cyclohexamide caused growth cone collapse, suggesting that a maintained translation of actin is necessary for maintaining growth following injury (Zheng *et al.* 2001). Stimulus induced local translation is also required for axonal growth and viability. NGF stimulation of sympathetic neurons is required for the axonal translation of *IMPA1,* an event required for maintaining axonal integrity (Andreassi *et al.* 2010). Additionally, NGF stimulation on sensory neurons leads to local translation of *PAR3* in axons, a key regulator of NGF induced axon growth (Hengst *et al.* 2009).

Interestingly, several mRNA encoding transcription factors have been detected in axons. The activating transcription factor 4 (*Atf4*) mRNA is translated in axons of mouse forebrain neurons following $Aß_{1-42}$ application, and *CREB* is translated in sensory neuron axons in response to NGF (Cox *et al.* 2008, Baleriola *et al.* 2014). Local translation of transcription factors may also elicit a rapid nuclear response following injury. Transection of sensory neuron axons leads to the local translation of *signal transducer and activation 3* (STAT3). The protein is retrogradely trafficked to the nucleus where it activates expression of genes necessary for cell survival and injury response (Ben-Yaakov *et al.* 2012). A possible explanation for these unusual observations is that axonal translation of a transcription factor may allow the expression of specific genes, although whether axonally derived transcription factors are “marked” and recognised in the nucleus remains unclear.

The examples given above are for specific mRNA, however it is known that extracellular stimuli lead to large changes in levels of translation. One of the

mechanisms responsible for stimulus-induced translation is the relief of repression mediated by RBPs. BDNF stimulation leads to the phosphorylation of Zbp1, inducing a conformational change that results in the release of *ß-actin* mRNA and its translation (Huttelmaier *et al.* 2005). FMRP's activity as a translational repressor within dendrites is regulated by neuronal activity; acute mGluR activation leads to dephosphorylation of FMRP, its ubiquitination and subsequent degradation (Nalavadi *et al.* 2012). This results in the release of associated transcripts and derepression of translation.

An alternative mechanism by which extracellular stimuli may induce translation is through the release of the translational machinery itself. In commissural and hippocampal neurons, the surface receptor for netrin-1 Deleted in Colorectal Cancer (DCC) co-localises with various components of the translation machinery in axons, including the eukaryotic initiation factor 4E (eIF4E) and various ribosomal subunits. In its unbound state, DCC sequesters these components, preventing the initiation of translation. Upon Netrin-1 stimulation, DCC's repression of the translational machinery is lifted triggering local translation (Tcherkezian *et al.* 2010). Although there are examples of mechanisms of translational control following stimuli, how specific mRNA are selected for translation, whereas others are held repressed, is still unknown.

Protein levels are not necessarily linked to the abundance of the transcript, and may depend more heavily on the rate of mRNA translation (Schwanhausser *et al.* 2011). The advent of techniques such as ribosomal profiling has allowed the identification of mRNA associated with ribosomes, thereby providing an accurate measure of the cellular 'translatome' (Ingolia *et al.* 2009). The technique can also be coupled with translating ribosome affinity

purification (TRAP), which allows cell-type specific assessment of the translatome (Shigeoka *et al*. 2016, Glock *et al.* 2017). TRAP utilises the expression of a tagged ribosomal subunit to pull down translating ribosomes, and the transgene can be driven by a cell-type specific promoter (Heiman *et al.* 2008). Pulldown followed by ribosome profiling allows the identification of ribosome bound mRNA, providing a snapshot of the cells translatome. TRAP has been recently used in axons of mouse RGC neurons to capture ribosomes at four developmental stages (Shigeoka *et al.* 2016). The study showed that axonal translation occurs from early development to adulthood with remarkable changes of the functional classes of translated mRNA, which shift from axonal growth towards synaptic function and cell survival. When the translatome was compared to the axonal transcriptome at corresponding developmental stages, a large proportion of mRNA was found not to be translated and held in a translationally repressed state (Zivraj *et al.* 2010). Although a significant fraction of the transcripts was found in the translatome at later developmental stages, the function of the translationally repressed axonal mRNA is unknown.

1.2.10 Coding-independent functions of 3'UTRs

Recent evidence suggests that 3'UTRs may play a broader role in the regulation of gene expression by acting as molecular scaffolding for protein complexes and/or by modulating the action of miRNA (Jenny *et al.* 2006, Berkovits and Mayr 2015, Valluy *et al.* 2015, Chao and Vogel 2016).

Translation of the localised *Oskar* mRNA is necessary for the establishment of morphogen gradients and spatial patterning of the oocyte

(Ephrussi and Lehmann 1992). In these experiments, knockout of the gene prevented the expression of Oskar protein, however low-level expression of the *Oskar* 3'UTR remained (Ephrussi *et al.* 1991, Kim-Ha *et al.* 1991). Interestingly, a subsequent knockout line that fully abolished *Oskar* expression resulted in early arrest of oogenesis and the complete failure of egg production, suggesting that 3'UTR expression in the absence of the ORF was sufficient to promote oocyte development (Jenny *et al.* 2006). In support of this hypothesis, expression of the *Oskar* 3'UTR alone rescued early oogenesis arrest (Jenny *et al.* 2006). A recent study indicated that the 3'UTR of *Oskar* may alter the distribution of the translational regulator Bruno, mediating its spatiotemporal activation during oogenesis (Kanke *et al.* 2015).

The potential role of 3'UTRs in regulating protein expression *in trans* has been recently demonstrated in prokaryotes. In *Salmonella enterica*, the *CpxP* gene is a major component of the bacterial stress response to conditions such as excessive pH or salt concentrations (Hunke *et al.* 2012). These stresses can cause misfolding of extracytoplasmic proteins and the role of CpxP protein is to target misfolded proteins to the proteasomal machinery (Isaac *et al.* 2005). Interestingly, the 3'UTR of the *CpxP* transcript is cleaved and acts to inhibit the translation of proteins that may be damaged by the persisting stress (Chao and Vogel 2016).

Distinct functions of transcripts and encoded proteins have also been observed in mammalian neurons. Expression of an alternative isoform of the *ubiquitin-protein ligase E3A* (*ube3a*) mRNA regulates dendritic spine growth and elaboration in a coding independent manner. Ube3a is part of the protein degradation pathway, necessary for experience-dependent development of

neuronal connectivity. Loss of this gene is linked to Angelmans syndrome, a neurodevelopment disorder resulting in learning difficulties, speech defects and characteristic behavioural traits such as a happy demeanour, reduced attention span and restlessness (Kishino *et al.* 1997, Matsuura *et al.* 1997, Bird 2014). In mouse hippocampal neurons, three isoforms of *ube3a* are detected; Isoform 2 and 3 share a common 3'UTR and encode a full-length active protein, whereas isoform 1 utilises a proximal PAS that results in the exclusion of the two 3' exons and the translation of a truncated, catalytically inactive protein (Valluy *et al.* 2015). Despite not being translated into a functioning protein, knockdown of *Ube3a1* increases dendritic growth and complexity. Similar to *Oskar*, the 3'UTR alone is sufficient to rescue the phenotype by sequestering miRNAs that repress dendritic translation of the key regulator of dendritic spine development Limk1 (Schratt *et al.* 2006, Valluy *et al.* 2015). Though relatively few examples have been described so far, the repertoire of mammalian mRNA with coding independent functions will likely grow in the future, as they provide a means of diversifying gene functions without expanding the transcriptome.

mRNA transcripts may also influence post-translational regulation of their encoded proteins. CD47 is a cell surface molecule that acts as a marker of 'self' preventing phagocytosis (Oldenborg *et al.* 2000). *CD47* encodes two mRNA isoforms that bear different 3'UTRs due to APA (Lianoglou *et al.* 2013). The two isoforms are localised near the perinuclear endoplasmic reticulum (ER), yet reporter constructs revealed that proteins derived from the long isoform are localised to the cell surface, while the protein encoded from the short isoform remained at the ER. The long 3'UTR of *CD47* mRNA acts as a

molecular scaffold that recruits the RBP HuR, SET1 and RAC1. This event ensures that following translation, CD47 is immediately complexed with SET1 and RAC1 and localised to the cell surface (Berkovits and Mayr 2015).

Interestingly, in tissues of many species, 3'UTRs are expressed independently of their coding sequences (Mercer *et al.* 2011). This phenomenon was demonstrated in mouse dopaminergic and serotonergic neurons (Kocabas *et al.* 2015). It is still unclear what is the function of the 3'UTRs expressed independently of their ORFs, though the authors speculate that they may act to regulate protein expression (Kocabas *et al.* 2015). These studies indicate that the ability of 3'UTRs to function in *trans* is not restricted to a small number of transcripts and may represent a widespread phenomenon with fundamental biological implications.

1.3 3'end RNAseq of axonally enriched mRNA isoforms

A number of studies have analysed the transcriptome of axons compared to cell bodies. Genome-wide sequencing has been performed in several vertebrate species including mouse, rat and *Xenopus,* and across neuronal subtypes (Andreassi *et al.* 2010, Zivraj *et al.* 2010, Gumy *et al.* 2011). We now have an understanding of how the axonal transcriptome changes during development, and in response to injury (Taylor *et al.* 2009, Zivraj *et al.* 2010, Ben-Yaakov *et al.* 2012). However, these screens focused on the coding sequence of the transcript and as a result, there is limited information on the differential usage of 3'UTR isoforms of axonal transcripts.

We recently performed a 3'end seq to identify differential 3'UTR usage and abundance of mRNA enriched in axons of sympathetic neurons (Andreassi *et*

al. 2017). We found that in axons, the most abundant transcript was Tumour protein 53 inducible nuclear protein 2 (Tp53inp2). Importantly, this finding correlated with a previous screen performed in our lab under similar conditions that revealed that *Tp53inp2* is highly abundant and enriched in axons relative to cell bodies (**Fig.1.11**) (Andreassi *et al.* 2010).

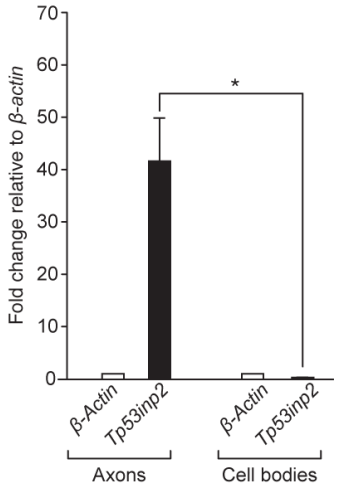

Fig.1.11 *Tp53inp2* is highly enriched in sympathetic neuron axons RT-qPCR analysis on mRNA isolated from rat sympathetic neuron axons or cell bodies revealed a striking enrichment of *Tp53inp2* mRNA in axons. Adapted from (Andreassi *et al.* 2010)

Interestingly, the peripheral localisation of *Tp53inp2* mRNA is not restricted to the axons of sympathetic neurons. Several studies utilising a variety of techniques, species and cell types (both neuronal and non-neuronal) have identified *Tp53inp2* in cellular projections (**Table 1.1**).

Subcellular Compartment	Cell Type	Species	Method	Reference
Axons	SCG Neurons	Rat	RNAseq	(Andreassi *et al.* 2017)
Axons	SCG Neurons	Rat	SAGE	(Andreassi *et al.* 2010)
Axons	RGC Neurons	Mouse Xenopus	Microarray	(Zivraj *et al.* 2010)
Axons	DRG Neurons	Mouse	Microarray	(Gumy *et al.* 2011)
Pseudopodia	Fibroblasts	Mouse	Microarray	(Mili *et al.* 2008)
Neurite	CAD Cell line	Mouse	RNAseq	(Taliaferro *et al.* 2016)
Dendrites	Hippocampal Neuropil	Rat	RNAseq	(Cajigas *et al.* 2012)

Table 1.1 Transcriptome screens identifying *Tp53inp2* in cellular projections. CAD =cath.-a-differentiated, SAGE= Serial analysis of gene expression

1.3.1 *Tp53inp2*, the most abundant mRNA in axons of sympathetic neurons

Tp53inp2, also known as diabetes and obesity regulator (DOR), is a gene that shares partial identity (32%) with *Tp53inp1* (Nowak *et al.* 2005, Bennetts *et al.* 2007). *Tp53inp2* is highly conserved across mammals, with sequence orthologues that are identified across a broad range of metazoans and a similarity between human and rodents greater than 70% (Bennetts *et al.* 2007, Sancho *et al.* 2012). In rat, *Tp53inp2* is located on chromosome 3 and its 4 exons span ~8Kb, which includes a 666nt ORF, a 249nt 5'UTR and a large 3'UTR of 3.1Kb. The coding sequence encodes an unstructured 221 amino acid protein with a nuclear localisation signal (R-R-X-X) at its C-terminus (Bennetts *et al.* 2007).

Tp53inp2 mRNA shows a restricted spatial pattern of expression during mouse embryogenesis (**Fig.1.12**). Between E9.5 and E12.5, the mRNA is expressed in the developing nervous system, including major components of the sympathetic nervous system such as the sympathetic chain ganglia (Bennetts *et al.* 2006, Bennetts *et al.* 2007). The restricted expression of *Tp53inp2* mRNA in the developing nervous system, and the projections of differentiated neurons matches what was observed in our screen and strongly points towards a role in neuronal development. As development reaches adulthood, the expression pattern of *Tp53inp2* changes. In adult mice, skeletal and cardiac muscle show significantly higher levels of mRNA expression relative to other tissues, such as the brain, the liver and lungs, with protein levels showing a similar trend (Sala *et al.* 2014).

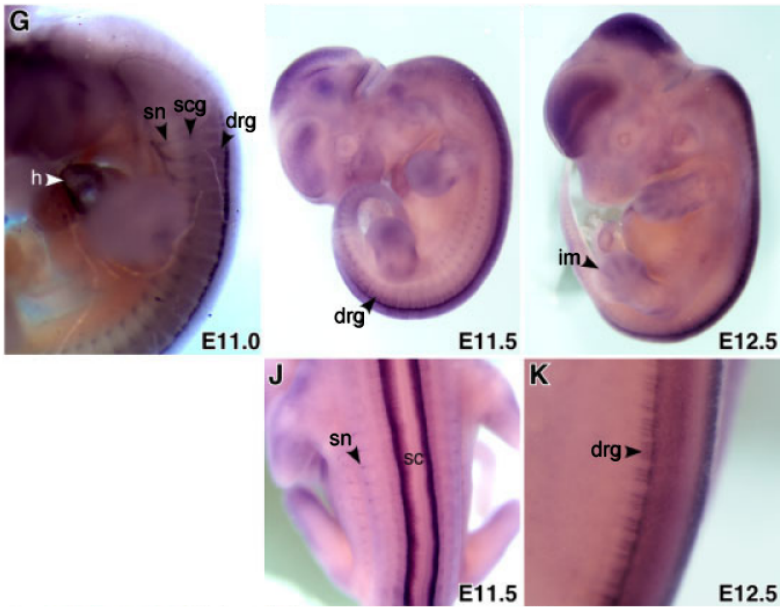

Fig.1.12 *Tp53inp2* mRNA expression in development. Mouse embryo whole mount *in situ* hybridisation staining for *Tp53inp2* mRNA at different developmental stages (indicated). The expression of *Tp53inp2* is tightly restricted to the ganglia and neuronal projections of the developing nervous system. Sn, spinal nerve; scg, superior cervical ganglia; drg, dorsal root ganglia; im, interdigital mesenchyme. Adapted from Bennetts *et al.* 2007.

Immunofluorescence studies performed in various cell lines (HEK-293, HeLa, C2C12) and in mouse skeletal muscle have shown that Tp53inp2 shuttles between the nucleus and the cytoplasm (Baumgartner *et al.* 2007, Nowak *et al.* 2009, Mauvezin *et al.* 2012, Sala *et al.* 2014). Nucleolar localisation was demonstrated in HeLa and MCF-7 cells (Xu *et al.* 2016). It should be noted however, that most studies were performed using overexpressed, tagged *Tp53inp2* constructs expressing only the ORF. Tp53inp2 has been described as a co-activator of transcriptional activity in the nucleus and as a regulator of autophagy in the cytoplasm. Autophagy involves the degradation and recycling of cytosolic components within double-membrane vesicles known as autophagosomes (Kaur and Debnath 2015). Though autophagy increases following cellular stresses, cells utilise low levels of autophagy in basal conditions to maintain homeostasis (Hu *et al.* 2017). For

example in skeletal muscle, autophagy is finely balanced to maintain muscle mass, and diseases associated with excessive autophagy often coincide with muscle loss (Masiero *et al.* 2009, Sala and Zorzano 2015).

Yeast two-hybrid screens and co-immunoprecipitation following Tp53inp2 overexpression in HeLa cells demonstrated that the protein interacts with key regulators of autophagy, including LC3, VMP1, GABARAP and GABRAP-like2 (Nowak *et al.* 2009). The authors proposed that Tp53inp2 protein may act as a scaffold to recruit these key factors and assist formation of the autophagosome. In support of this hypothesis, *Tp53inp2* overexpression in HeLa cells led to autophagosome formation and increased proteolytic activity, whereas the opposite effect was observed in C2C12 cells lacking *Tp53inp2* (Mauvezin *et al.* 2010). Transgenic mice overexpressing the coding sequence of *Tp53inp2* in skeletal muscle showed increased proteolysis and reduced muscle mass, compared to wildtype littermates, while a skeletal muscle-specific knockout displayed muscular hypertrophy (Sala *et al.* 2014). These findings suggest that in muscle tissue, Tp53inp2 regulates basal autophagy and maintains cellular homeostasis.

Tp53inp2 also functions as a co-activator of nuclear receptor-mediated transcription (Sala and Zorzano 2015). Overexpressed Tp53inp2 interacts with a variety of nuclear receptors, such as thyroid hormone receptor α1, mammalian glucocorticoid receptor and vitamin D receptor (Baumgartner *et al.* 2007, Sancho *et al.* 2012). Luciferase assays performed in HeLa cells indicate that Tp53inp2 increases transcription of their targets (Baumgartner *et al.* 2007). However, microarray analysis of mouse skeletal muscle cells either lacking or overexpressing Tp53inp2 revealed only subtle changes in gene

expression (Sala *et al.* 2014). Additionally, recent work performed in HeLa cells suggests that endogenous Tp53inp2 contributes to the recruitment of the polymerase I transcription machinery (polI) to the promoters of ribosomal DNA (rDNA) (Xu *et al.* 2016). Ribosome biogenesis is a fundamental process for cell growth and proliferation that requires the transcription of ribosomal RNA precursors from rDNA in a polI dependent manner (Xu *et al.* 2016). Chromatin immunoprecipitation (ChIP) assay found that endogenous Tp53inp2 is associated with the rDNA promoter in HeLa cells, acting to recruit and stabilise the polI complex (Xu *et al.* 2016).

The majority of work performed on *Tp53inp2* thus far has utilised overexpressed *Tp53inp2* constructs lacking the untranslated regions. The 3'UTR of *Tp53inp2* is very long (3121nt), accounting for ~75% of the transcript's length. Given the importance of 3'UTRs in the regulation of gene expression, the influence of the 3'UTR on *Tp53inp2*'s overall regulation and function could be of the utmost importance. However, limited work has been done to explore the function of the endogenous *Tp53inp2* transcript in primary cells, such as sympathetic neurons.

Aims

The aim of my work is to understand the regulation and function of *Tp53inp2*, a transcript localised and highly enriched in the axons of sympathetic neurons. Previous studies have identified *Tp53inp2* mRNA in neuronal projections, and its expression is spatiotemporally restricted to the developing nervous system. However, a role for *Tp53inp2* mRNA during neuronal development and the role of the 3'UTR is unknown.

The main questions that I have addressed during my graduate research are:

1. Is *Tp53inp2* mRNA translated in sympathetic neuron axons?
2. Does *Tp53inp2* mRNA play a role in the development of the sympathetic nervous system?
3. Does*Tp53inp2* mRNA regulate NGF-TrkA signalling?

2. Results

2.1 Tp53inp2's translation is repressed in sympathetic neurons

2.1.1 *Tp53inp2* transcript is enriched in sympathetic neuron axons

To investigate differential 3'UTR usage and transcript abundance, Dr. Catia Andreassi in our laboratory previously performed a 3'end RNAseq screen (Andreassi *et al.* 2017). Sympathetic neurons dissociated from P0.5 rat SCG were cultured in compartmentalised chambers, and mRNA isolated from axons and cell bodies. Samples were subjected to two rounds of poly(A) linear amplification before sequencing to ensure detection of lowly expressed transcripts. Bioinformatics analysis of the 3'end-seq data was performed by our collaborators Raphaëlle Luisier and Nick Luscombe (Francis Crick Institute, London) and resulted in identification of 6410 transcripts in axons. The most abundant transcript and one of the most highly enriched relative to the cell body was *Tp53inp2,* accounting for nearly one third of the axonal sequencing reads (**Table 2.1**).

GeneID	GeneSymbol	Cell Body Log2 Read Count (Average)	Axon Log2 Read Count (Average)	Axon:Cell Body Ratio
ENRNOT00000055310	Tp53inp2	9.091	18.150	1.997
ENRNOT00000015034	Trak2-202	6.627	15.205	2.294
ENRNOT00000014939	Trak2-201	6.627	15.204	2.294
ENRNOT00000030919	Fth1	9.292	14.888	1.602
ENRNOT00000071069	Nefm	12.422	13.547	1.091

Table 2.1 Identification of transcript abundance in axons of sympathetic neurons Shown are the top 5 most abundant transcripts identified by 3'end RNAseq performed on mRNA isolated from the axons of cultured P0.5 sympathetic neurons. Values are expressed as Log_2-read counts from the average of two biological replicates and as a ratio between Axon and Cell Body Log_2-read counts. GeneID provided for Ensembl Rn6.

Strikingly, despite *Tp53inp2* mRNA's abundance in axons, a functional role of *Tp53inp2* in the nervous system had yet to be described. Hence, I decided to further characterise the role of Tp52inp2 in neurons.

2.1.2 Tp53inp2 protein is not expressed in sympathetic neurons

In order to investigate the potential function of *Tp53inp2*, I first attempted to detect the endogenous protein by western blotting using cultured sympathetic neurons dissected from SCG of P0/P1 rats. Unfortunately, SCG neurons are not amenable to transfection by lipid-based methods, and are not suitable for electroporation, which makes it difficult to perform genetic manipulations. Thus, to aid in the validation of the antibodies used for the detection of Tp53inp2 protein, I used PC12 cells. PC12 cells are a model system alternative to sympathetic neurons that are particularly attractive as they can be transfected at a reasonably high efficiency. PC12 cells derive from the same neural crest progenitors that give rise to sympathetic neurons and retains the ability to differentiate into a neuron-like state in response to NGF stimulation (Greene and Tischler 1976).

Using a variety of both commercially available and lab-generated antibodies, Dr. Marife Cano, a previous post-doc in the lab, and I were unable to detect endogenous Tp53inp2 protein in sympathetic neurons or in PC12 cells **(Fig.2.1 and 2)**. This result was not due to the inability of the antibodies to recognise Tp53inp2 protein *per se*, as it reliably detected Tp53inp2 protein when cells were transfected with vectors containing the ORF of *Tp53inp2* (**Fig.2.1A**). In PC12 cells, this was demonstrated through the generation of both C-terminal Flag tagged (**Fig.2.1A**) and N-terminal Myc tagged (**Fig.2.2**)

constructs containing the rat coding sequence of Tp53inp2 expressed under the control of the CMV promoter (**Fig.2.1A and 2.2**). In SCG neurons, infection with adenoviral vectors expressing the ORF of Tp53inp2 allows a robust detection of Tp53inp2 protein (**Fig.2.1B).** Additionally, Tp53inp2 expression was inhibited when PC12 cells were co-transfected with siRNA targeting *Tp53inp2* mRNA*,* demonstrating the specificity of the antibodies (**Fig.2.1A, C**). siRNA induced a robust knockdown of mRNA levels of endogenous *Tp53inp2* in PC12 cells, yet no difference in banding pattern was observed for any of the antibodies tested.

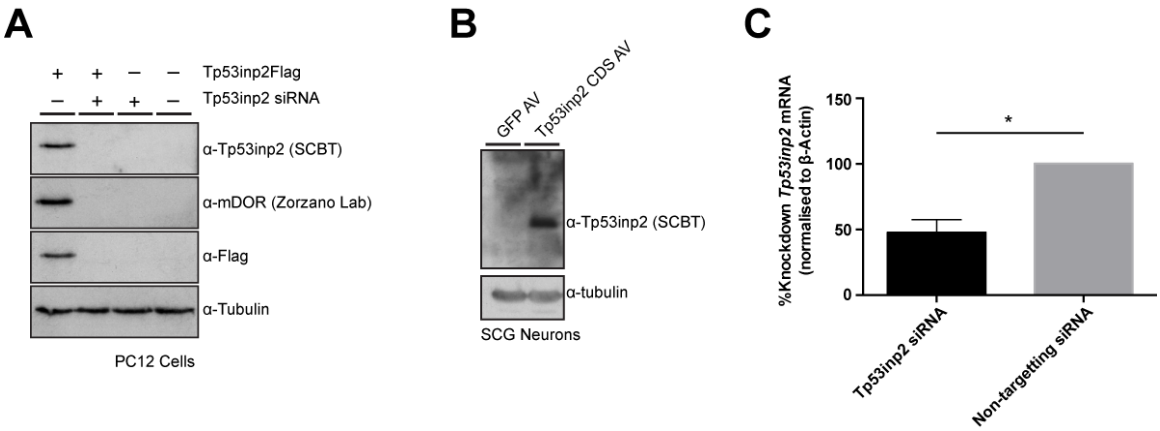

Fig.2.1 Endogenous Tp53inp2 protein is not detectable in sympathetic neurons or PC12 cells using commercial antibodies (**A**) PC12 cells were transfected with plasmids expressing either C-terminal Flag tagged *Tp53inp2* CDS or empty vector control and siRNA targeting *Tp53inp2* mRNA or non-targeting control, as indicated. Protein lysates were separated by SDS-PAGE followed by immunoblotting with the indicated antibodies. mDOR is a Tp53inp2 antibody generated in Zorzano Lab (Sala *et al.* 2014). Tubulin was used as a loading control. (**B**) Sympathetic neurons cultured *in vitro* were infected with adenovirus expressing either *Tp53inp2* CDS or GFP. Cells were cultured for a further 48 hours before lysis and protein separation by SDS-PAGE. Immunoblotting performed with Tp53inp2 and tubulin antibodies. (**C**) *Tp53inp2* mRNA expression in PC12 cells transfected with siRNA targeting *Tp53inp2* or a non-targeting control was analysed by RT-qPCR. Values are normalised to *ß-Actin* mRNA and expressed as % knockdown relative to controls. Data presented as average ±s.e.m. n=3 independent experiments. * = P<0.05, unpaired t test with Welch's correction.

Similarly, antibodies generated in our laboratory isolated from the serum of rabbits immunised with a synthetic peptide of the N-terminal region (N26) or full-length (Ig26) Tp53inp2 specifically detected the overexpressed Tp53inp2

in PC12 cells. However, we were unable to detect the endogenous Tp53inp2 protein in PC12 cells or sympathetic neurons (**Fig.2.2A,B**). Although *Tp53inp2* mRNA is very abundant and highly enriched in axons, the protein was not found when compartmentalised chambers were used to analyse cell bodies and axons (**Fig.2.2A**).

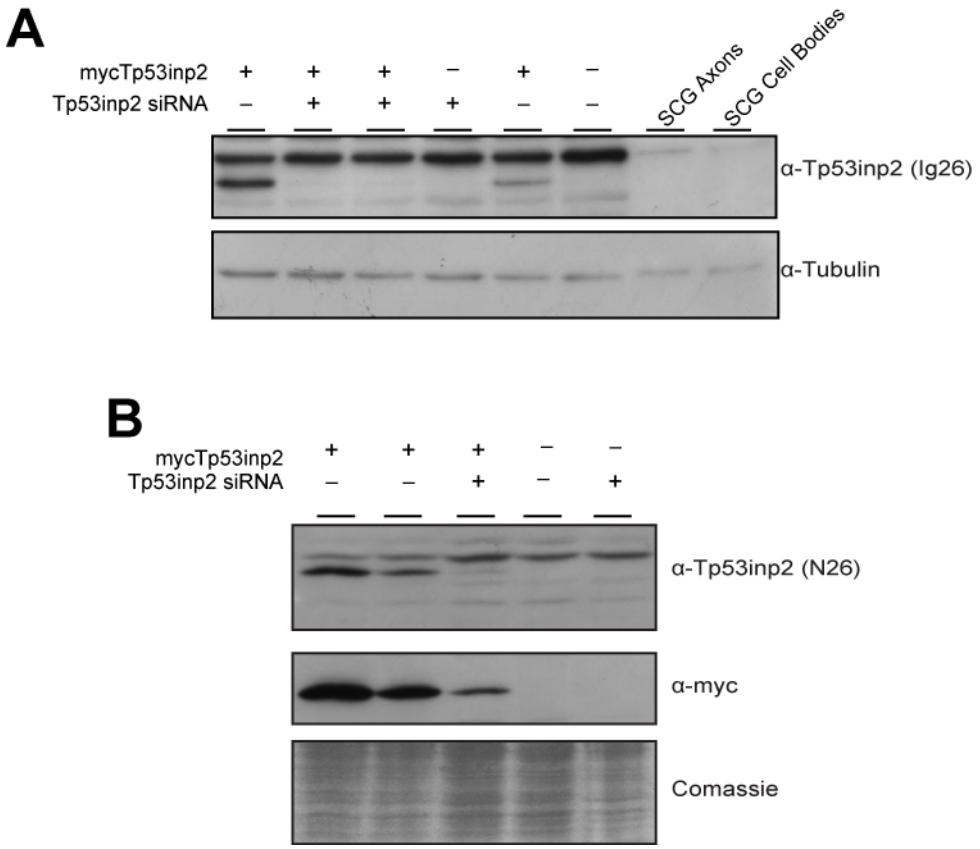

Fig.2.2 Endogenous Tp53inp2 protein is not detectable in Sympathetic neurons or PC12 cells using lab generated antibodies (**A**) PC12 cells were transfected with plasmids expressing either N-terminal Myc tagged *Tp53inp2* CDS or empty vector control, and siRNA targeting *Tp53inp2* mRNA or non-targeting control, as indicated. Lysates from axons and cell bodies of sympathetic neurons cultured in compartmentalised chambers were run on the same gel. Protein lysates were separated by SDS-PAGE followed by immunoblotting with lab-generated antibody targeting full length Tp53inp2 (Ig26) and tubulin antibody. (**B**) PC12 cells were transfected with plasmids and siRNA as indicated. Immunoblotting was performed with lab-generated antibody targeting Tp53inp2 N-Terminal (N26) and Myc antibody. Comassie stain was performed to show equal loading of protein lysates. Experiments performed by Marife Cano (Riccio Lab)

Long-term exposure of PC12 cells to NGF did not increase *Tp53inp2* translation even after 13 days of stimulation, at which point the cells are fully

differentiated into a neuron-like phenotype (**Fig.2.3**). Thus, we concluded that *Tp53inp2* is not translated in both PC12 cell and sympathetic neurons and NGF stimulation does not induce *Tp53inp2* translation.

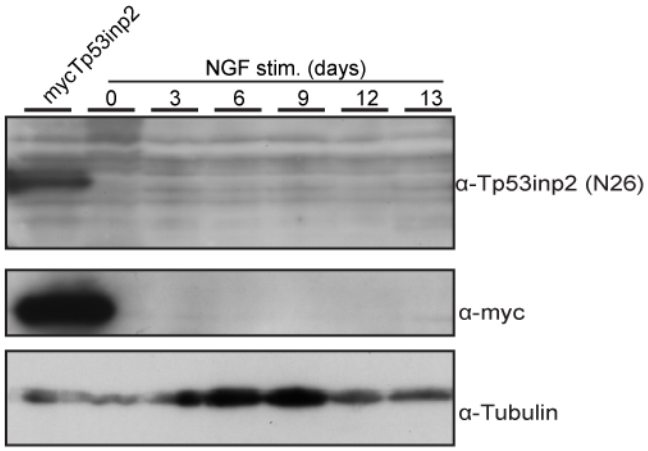

Fig.2.3 NGF stimulation does not induce Tp53inp2 translation in PC12 cells. PC12 cells stimulated with 50 ng/ml NGF for indicated number of days. PC12 cells transfected with mycTp53inp2 were included as a positive control. Lysates were separated by SDS-PAGE and immunoblotted using Tp53inp2 (n26), Myc and tubulin antibodies. Experiment performed by Marife Cano (Riccio Lab)

Due to the lack of detectable protein despite the abundance of mRNA, I reasoned that endogenous Tp53inp2 might be synthesised and rapidly degraded, whereas overexpressed constructs are translated at a much higher level that overcomes degradation. To test this hypothesis, the cellular proteasome machinery was blocked by exposing PC12 cells differentiated with NGF to the proteasome inhibitor MG132. MG132 inhibits the proteasome by reducing the degradation of ubiquitin-conjugated proteins (Lee and Goldberg 1998). In differentiated PC12 cells transfected with Myc-tagged Tp53inp2, the levels of the ectopically expressed protein were increased, demonstrating that the inhibitor efficiently blocks the proteasome machinery (**Fig.2.4A**). However, when PC12 cells were transfected with a control vector (CMV-Myc), no detectable Tp53inp2 was observed following exposure to

MG132 (**Fig.2.4A**). This finding suggests that the lack of endogenous Tp53inp2 detection was not due to rapid degradation. Similarly, in sympathetic neurons, MG132 did not increase the levels of Tp53Inp2 protein (**Fig.2.4B**). Thus, I concluded that Tp53inp2 protein in sympathetic neurons is not subjected to rapid degradation by the ubiquitin-mediated proteasomal machinery.

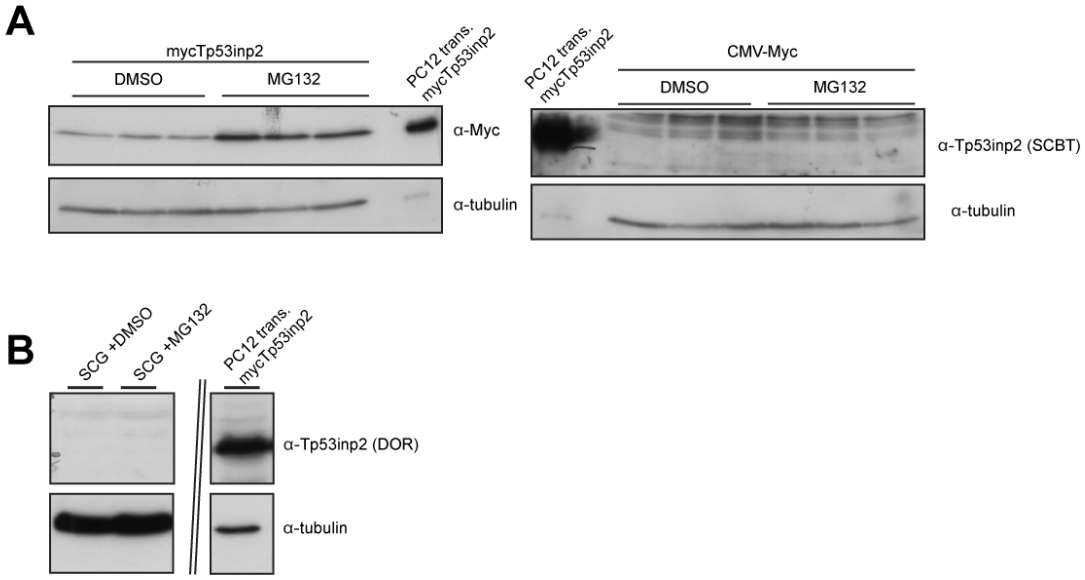

Fig.2.4 Tp53inp2 is not being rapidly degraded by the proteasomal machinery (**A)** PC12 cells were transfected with either mycTp53inp2 or an empty vector. Cells were then cultured in the presence of the proteasomal inhibitor MG132 (10μM) or DMSO for 8 h. Cell lysates were separated by SDS-PAGE and immunoblotted with the indicated antibodies. DMSO treated PC12 transfected with mycTp53inp2 included as positive control. (**B**) Sympathetic neurons were treated with MG132 (10 μM) or DMSO as a control. After 8 h, samples were lysed and separated by SDS-PAGE and immunoblotted with indicated antibodies. Double-diagonal lines indicate samples run on same gel but not adjacent. Experiment performed by Marife Cano (Riccio Lab)

Recently published data from the Zorzano group indicated that Tp53inp2 protein is expressed in muscle tissue and in a number of cell lines (Sala *et al.* 2014). I used their homemade antibody (labelled as mDOR) to further study Tp53inp2 in sympathetic neurons. The antibody detected the transfected Tp53inp2 protein in both HEK293 and PC12 cells, but not the endogenous protein in cell lines or sympathetic neurons (**Fig.2.1A, 2.4B**). I next

investigated Tp53inp2 levels in mammalian tissues obtained from neonatal rats, including cardiac muscle, skeletal muscle and brain. There was no detectable Tp53inp2 protein in the cardiac or skeletal muscle, though total protein levels in the skeletal muscle were also lower (**Fig.2.5**). Interestingly, a band was visible in the brain lysates at a molecular weight lower than expected. As previously observed, endogenous Tp53inp2 protein was not detected in lysates of sympathetic neurons (**Fig.2.5**).

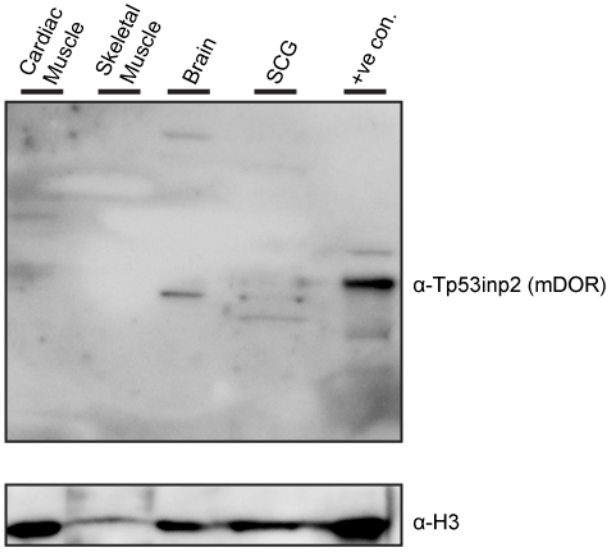

Fig.2.5 Tp53inp2 protein is not detected in sympathetic neurons. Tissue (indicated) collected from P0 rat, lysed and separated by SDS-PAGE. HEK293 cells transfected with plasmid expressing Tp53inp2CDS lysate included as a positive control. Immunoblotting performed with Tp53inp2 antibody generated in Zorzano lab and Histone H3 as loading control.

Though it is possible to detect exogenous Tp53inp2 using vectors expressing the coding region alone, the endogenous Tp53inp2 was not found in sympathetic neurons or PC12 cells using the same antibodies, despite a range of stimuli and stresses applied to the cells. Together, these results indicate that neurons do not express Tp53inp2 at detectable levels. Alternatively, the protein may be present at extremely low levels below the threshold of sensitivity of all antibodies tested.

2.1.3 Targeted mass spectrometry of Tp53inp2 in sympathetic neurons

Next, in collaboration with Dr. Marco Gaspari (University of Catanzaro, Italy), we attempted to identify endogenous Tp53inp2 protein in sympathetic neurons using mass spectrometry. For this technique, I isolated proteins from either the distal axons or the cell bodies of sympathetic neurons. To increase the amount of material I could obtain, and therefore the chance of identifying endogenous Tp53inp2 protein, I opted for axonal transection of explants, rather than Campenot chambers. In this system, sympathetic ganglia were grown *in vitro* as tissue explants for 7 days in the presence of NGF, which promotes extensive axon outgrowth (**Fig.2.6**). The cluster of cell bodies in the ganglia explant was surgically excised from the distal axons using a scalpel, and axons and cell bodies were collected from several explants (~50) and analysed by mass spectrometry.

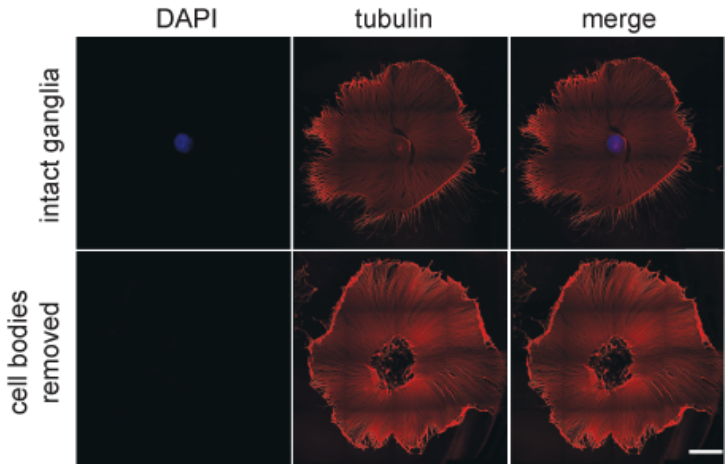

Fig.2.6 Preparation of sympathetic neurons for targeted mass spectrometry. Sympathetic ganglia explants were cultured in the presence of NGF for 7 days to allow extensive axonal outgrowth and cell bodies were surgically removed. Tubulin immunostaining of representative SCG explants before (*Top*) or after (*Bottom*) the removal of cell bodies. Nuclei were stained with DAPI. Scale bar = 200 µm.

To ensure the highest chance of detecting endogenous Tp53inp2 protein, I opted for a targeted mass-spectrometry approach. PC12 cells were transfected with a Myc-tagged Tp53inp2 vector and cultured for 48 hours. The cells were lysed and a Myc antibody conjugated to protein A beads was used to immunoprecipitate Tp53inp2 protein from the sample. The immunoprecipitated samples were subjected to on-bead trypsin digestion and the resulting peptides were sent for mass-spectrometry analysis. The detection of the peptides and their fragments provides a molecular fingerprint that allowed an accurate and sensitive detection of endogenous Tp53inp2. In the immunoprecipitated samples, two Tp53inp2 peptides with a mass to charge ratio (m/z) of 420 and 507 were found. The peptides were fragmented by the spectrometer into fragments with m/z 343, 530, 601 672 and m/z 560, 642, 688, 670, 851 respectively (**Fig.2.7**).

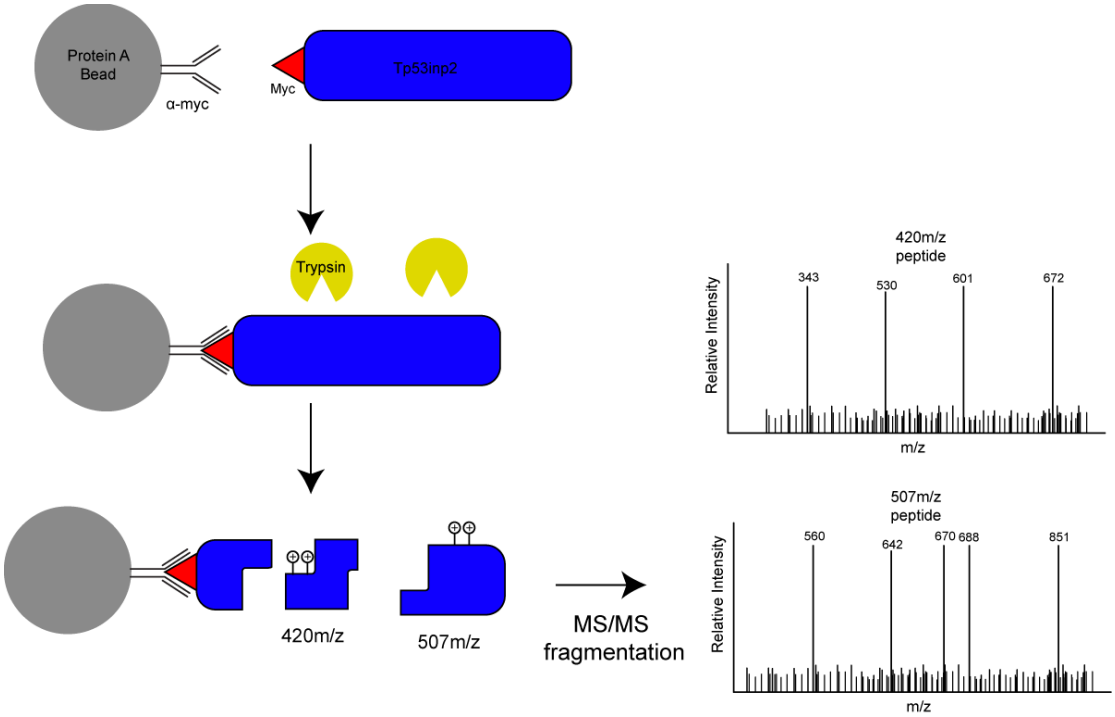

Fig.2.7 Illustrative schematic of identification of Tp53inp2 mass spectrometry targeted 'fingerprint'. Myc-tagged Tp53inp2 was immunoprecipitated from lysates of PC12 cells before being subjected to trypsinisation. Two double-charged peptide fragments of 420m/z and 507m/z were produced. These were further fragmented by tandem mass-spec (MS/MS), yielding single-charged fragments of indicated size.

When the immunoprecipitated samples were analysed, we observed a clear signal for all 4 fragments of 420m/z, which co-eluted at the same retention time of 7.3 minutes (**Fig.2.8A**). Similarly, all 5 fragments of the second peptide co-eluted at the retention time of 25.1 minutes (**Fig.2.8B**). In the axon sample however, we did not detect two fragments co-eluting at exactly the same retention time, which is the requisite to establish the presence of a certain protein. In the cell bodies sample we found Tp53inp2 protein, albeit at the detection limit of the spectrophotometer (**Fig.2.8A**). Three fragments of the 420m/z peptide co-eluted at the same retention time of 6.9 minutes. Though this differs slightly from the immunoprecipitated sample (7.1 minutes), a small deviation in retention time between two separately run samples is expected. For the second peptide, there are two fragments co-eluting at 23.4 minutes, again at the limit of detection of the spectrophotometer (**Fig.2.8B**).

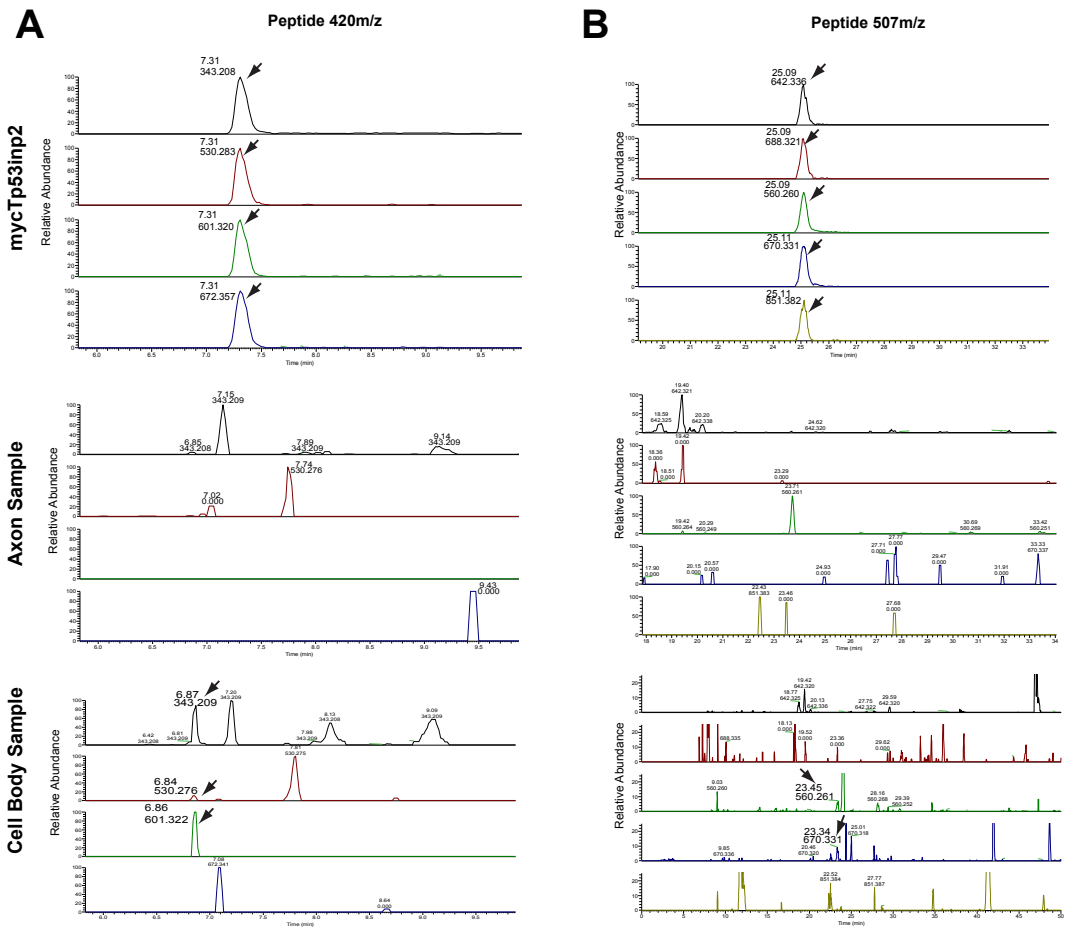

Fig.2.8 Targeted MS does not detect Tp53inp2 in axons of sympathetic neurons. Traces of targeted mass-spectrometry analysis for Tp53inp2 protein in sympathetic neuron axon or cell body samples immunoprecipitated with mycTp53inp2 antibody. (**A**) represents 420m/z peptide ALHHAAAPMPAR and (**B**) represents 507m/z HQGSFIYQPCQR. For each panel, the traces represent the fragments detected from the peptide precursor. Arrows indicate identified peptide fragments in each sample. Values above each peak are retention time (Top) and m/z (bottom), some values removed for clarity.

It should be noted that sympathetic cervical ganglia contain a variety of different cell types in addition to neurons, including glial cells, macrophages and fibroblasts (Roufa *et al.* 1986, Schreiber *et al.* 2002). Cytosine arabinoside (AraC), which is a potent anti-proliferative drug, was added to the culture medium; however, the explants provide a protected environment for a small population on non-neuronal cells that may persist within the tissue. Thus, I cannot exclude that the low levels of Tp53inp2 protein detected in this sample may derive from non-neuronal cells. Despite the presence of low

levels of Tp53inp2 protein in the cell bodies there was no detectable Tp53inp2 protein in axons. The mass-spectrometry analysis detected a large number of proteins overall: 2702 proteins in the cell bodies and 1628 in axons. Within the axon sample, we observed proteins known to be locally translated, such as IMPA1 and the actin regulatory protein Cofilin (Piper *et al.* 2006, Andreassi *et al.* 2010).

Taken together, these results indicate that Tp53inp2 is present in the cell bodies of SCG at extremely low levels and is not detectable in axons. I therefore concluded that despite the high levels of *Tp53inp2* mRNA present in axons, the transcript is not translated.

2.1.4 *Tp53inp2* mRNA is not translated in sympathetic neurons

To further investigate *Tp53inp2* mRNA translation in sympathetic neurons, I used polysomal fractionation. This technique is based on the principle that translating mRNA is preferentially bound to polysomes for translational elongation, whereas non translated mRNAs are either associated with the assembling components of a single 80s mature ribosome (monosome) or are not bound to the ribosomal machinery (free RNA) (Del Prete *et al.* 2007). The state of ribosomal loading confers specific densities to the RNA that can then be fractionated using a sucrose gradient. Free RNA has the lowest density so will remain in the lightest fractions of the gradient. This is followed by the monosomally bound RNA and then polysomal, with higher levels of ribosomal loading conferring increasingly higher density.

Sympathetic neurons were enzymatically dissociated and cultured with NGF for 7 days. At this point, neurons were treated with 0.1 mg/ml

cyclohexamide, a translational inhibitor that immobilises the ribosomes onto the mRNA. This allows accurate measurement of the current levels of translation. Neurons were lysed and the ribosome bound RNA was separated using ultracentrifugation on a sucrose gradient ranging from 15% to 40%. Fractions of increasing sucrose density were collected, with the low percentage fractions corresponding to free RNA and monosomes and the higher percentage to the polysomes (**Fig.2.9**).

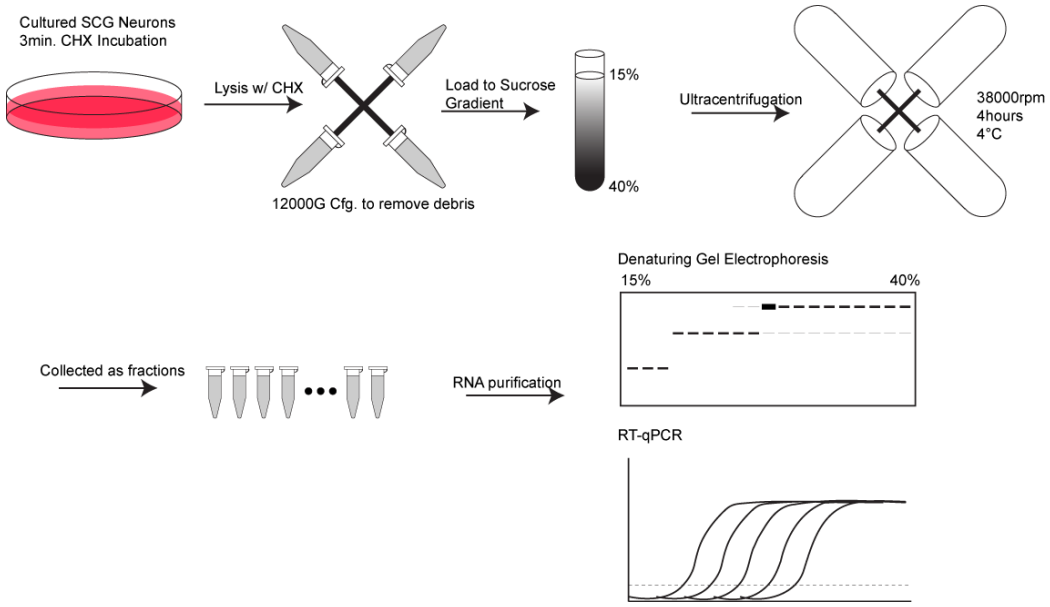

Fig.2.9 Illustrative schematic of polysomal fractionation technique. Sympathetic neurons were cultured for 7 days prior to treatment with the translational inhibitor cyclohexamide (CHX). Samples were loaded onto a progressive 15-40% sucrose gradient and ultracentrifuged to separate mRNA according to density. Fractions of increasing sucrose percentage were sequentially collected and RNA purified and analysed by denaturing gel electrophoresis and RT-qPCR. Adapted from (Del Prete *et al.* 2007)

RNA was purified from the fractions by phenol:chloroform extraction and divided into two samples, one of which was used to assess the quality of fractionation by denaturing gel electrophoresis. The free RNA fractions (low percentage) are characterised by the absence of the 18s and 28s rRNA. The polysome bound fractions are defined by the increase abundance of the 28s rRNA, relative to the 18s rRNA (**Fig.2.10**).

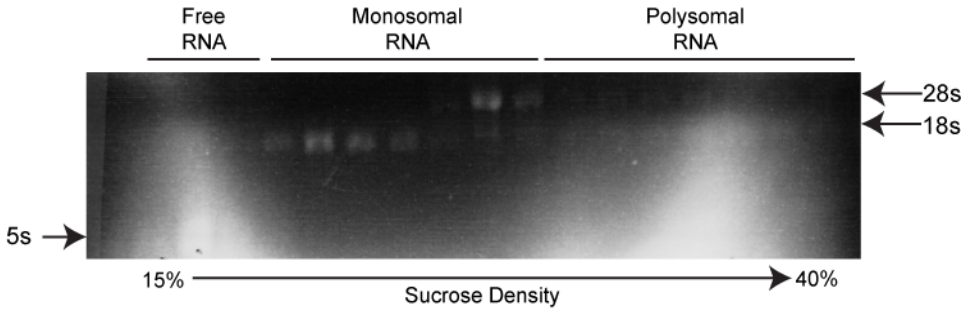

Fig.2.10 RNA separated by polysome fractionation. Fractions of ribosome-bound RNA from sucrose gradient were run on a denaturing agarose gel to assess quality of fractionation. Different height bands represent 5S, 18s or 28s ribosomal RNA (rRNA), which allow the distinction between free, monosomal and polysomal fractions.

Once the quality of the fractionation was confirmed, the remaining RNA was reverse transcribed and RNA levels analysed by RT-qPCR. To normalise for RNA lost during the extraction and reverse transcription process, a known quantity of *in vitro* transcribed RNA was added to all fractions and measured by RT-qPCR. In order to account for differences in overall levels of RNA between experimental repeats, the RNA present in each fraction was quantified as a percentage of total RNA detected. To achieve this, the relative RNA levels for all fractions were combined to obtain total RNA, and each fraction was expressed as a percentage of the total. As a positive control, I used *β-actin*, which is known to be translated in neurons. I observed that the majority of *β-actin* mRNA (~62%) was found in the polysomal fractions, whereas the non-coding RNA TERC, a key component of the telomerase complex, was almost exclusively (~90%) detected in the free and monosomal fractions (**Fig.2.11A, B**). When *Tp53inp2* mRNA levels were measured, the majority (~68%) of RNA was found within the free and monosomal fractions of the gradient, compared to *β-actin* (**Fig.2.11C, D**). Although most *Tp53inp2* mRNA was not translated, detectable levels of *Tp53inp2* mRNA were found within the polysomal fractions. This indicates that some translation is

occurring, which is consistent with the presence of Tp53inp2 protein in cell body samples analysed by mass spectrometry.

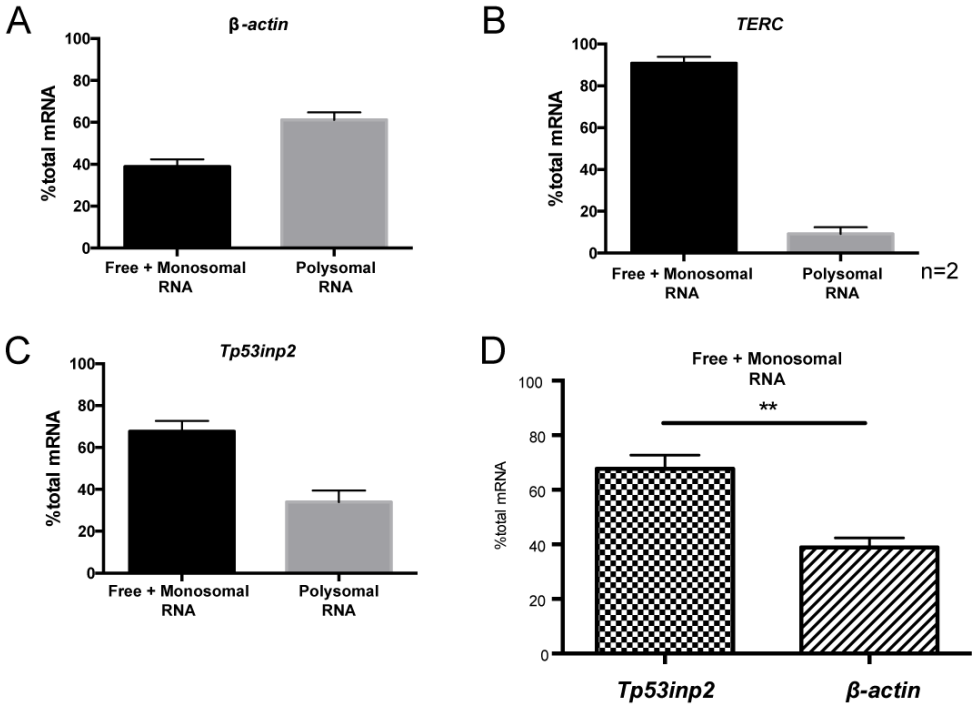

Fig.2.11 The majority of *Tp53inp2* is not actively translated in sympathetic neurons. Sympathetic neurons were cultured *in vitro* and lysed under translational inhibition of cyclohexamide (0.1mg/ml). mRNA was separated by polysome fractionation and mRNA levels were analysed by RT-qPCR. The polysomal profiles of *ß-actin* (**A**), *TERC* (**B**) and *Tp53inp2* (**C**) mRNA are shown, along with comparison between free + monosomal profiles of *Tp53inp2* and *ß-actin* (**D**). *ß-actin* and *TERC* were used as positive and negative controls, respectively. Data presented as averages ±s.e.m. N=3 independent experiments except where indicated. ** = P<0.001 unpaired T-Test

Taken together, these data indicate that despite being the most abundant mRNA in sympathetic neuron axons, *Tp53inp2* is held in a tightly translationally repressed state and suggest that the function of the transcript may be independent from its coding functions.

2.1.5 The 3'UTR of *Tp53inp2* represses translation

The elements responsible for regulating mRNA metabolism can be located anywhere along the length of the transcript; however, most regulatory elements are found within the UTRs (Sandberg *et al.* 2008, Andreassi and Riccio 2009, Mayr and Bartel 2009, Andreassi *et al.* 2010, Perry *et al.* 2012). Because the Tp53inp2 protein was easily detected when only the coding sequence was expressed, I hypothesised that the UTRs of *Tp53inp2* may contain elements responsible for maintaining the transcript in a translationally repressed state.

The nature of the linear amplification performed prior to the RNAseq analysis allowed the identification of 3'UTR isoform usage. The oligo(dT) dependent amplification results in an accumulation of sequencing reads within the last 500nt of the transcript (**Fig.2.12A**), allowing the study of isoform usage in a manner similar to the traditional Poly(A)-Seq (Shepard *et al.* 2011). A marked increase in the relative levels of read coverage is expected to occur at the boundary of alternative polyadenylation sites **(Fig.2.12B**).

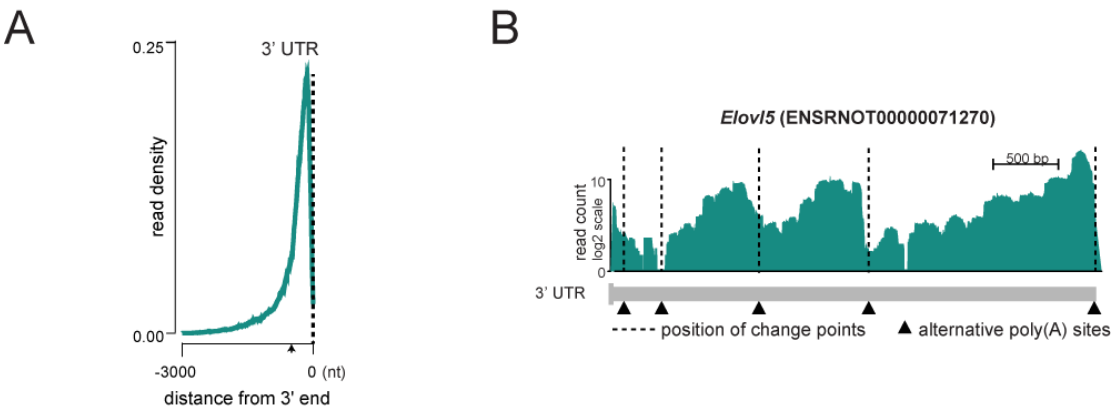

Fig.2.12 3'endSeq allows the identification of 3'UTR isoforms in sympathetic neurons. (**A**) Accumulation of reads at the 3' end of transcript. The read density (number of reads per nucleotide divided by the total number of reads) of 4,975 transcripts between 2000 and 3000 nts long is shown. Dashed line indicates the 3' end. Arrowhead indicates 500nt from 3' end of UTR (**B**) Identification of novel 3' ends in the longest 3'UTR of *Elovl5*. Potential 3' ends were identified by segmenting sudden transitions in read depth.

In both axons and cell bodies, a 3121nt 3'UTR isoform of *Tp53inp2* was readily detected (**Fig.2.13**). Importantly, the canonical PAS AATAAA is found in close proximity (21nt) of the 3' end of the isoform. This would allow efficient binding of the polyadenylation machinery and generation of a mature mRNA transcript, providing support of a *bone fide* isoform. The 3.1Kb isoform is considerably above the average length for 3'UTRs identified by the RNAseq screen (~2Kb). Interestingly, longer 3'UTRs have been shown to be associated with increased translational repression (Sandberg *et al.* 2008, Mayr and Bartel 2009, Floor and Doudna 2016).

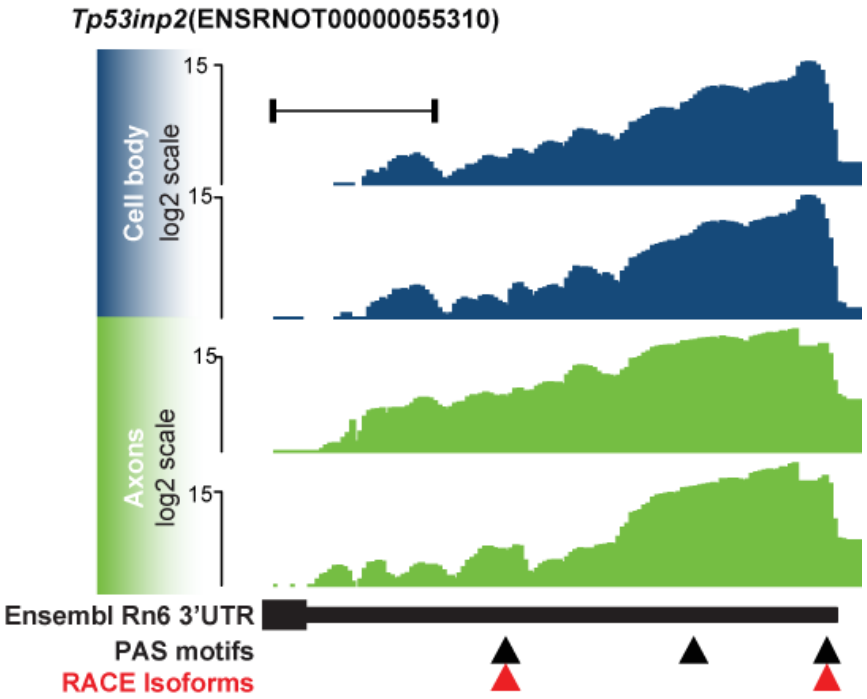

Fig.2.13 Read coverage of *Tp53inp2* 3'UTR from 3'end RNAseq screen. Ensembl Rn6 genome browser view of *Tp53inp2*'s 3'UTR with log2 scale read coverage for sympathetic neuron axon and cell body RNA. 3'UTR sequence was checked for the 12 canonical and non-canonical PAS sequences (black arrowheads) from PolyA_db (Lee *et al.* 2007). Isoforms identified by RACE analysis are indicated by red arrowheads. The two traces for each compartment are technical repeats. Scale bar = 1000bp

Next, we used Rapid Amplification of cDNA Ends (RACE) to confirm that the *Tp53inp2* isoform containing the 3.1Kb 3'UTR is expressed in sympathetic neurons. In this technique, the 3'UTRs of the gene of interest are specifically amplified, allowing the detection of different isoforms (**Fig.2.14**). In the RACE analysis, we also detected a shorter 3'UTR isoform (**Fig.2.14B**). This isoform was ~1.2Kb in length, with a canonical AATAAA polyadenylation signal within 21 nucleotides of the end of the isoform. Because this isoform was not detected in the 3'end RNAseq data, it is likely that it is present at a very low abundance.

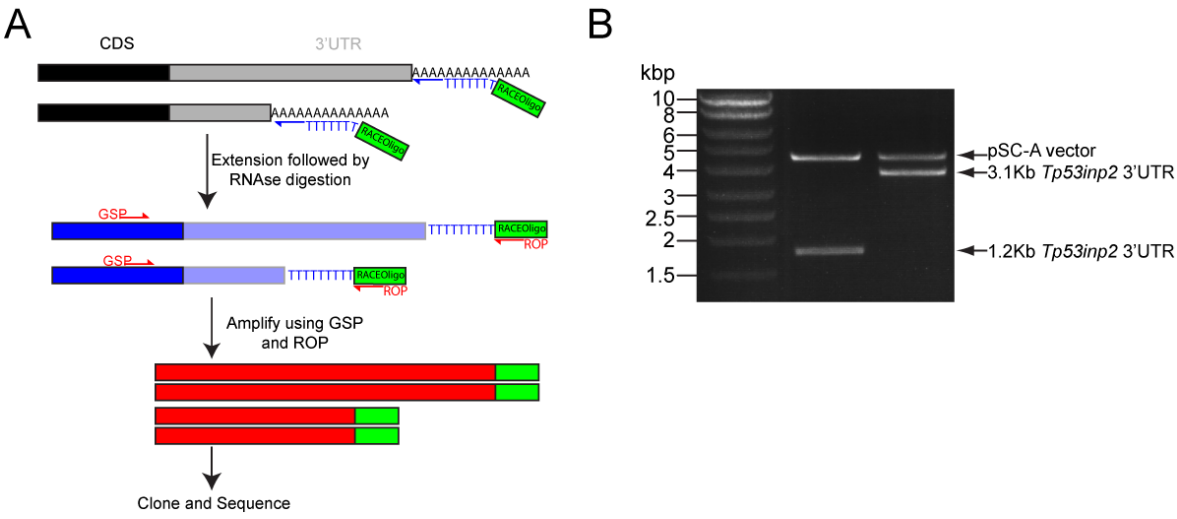

Fig.2.14 3'RACE to identify 3'UTR isoforms in sympathetic neurons (**A**) Schematic representation of 3'RACE technique. 3' Rapid Amplification of cDNA Ends (RACE) allows the identification of different 3'UTR isoforms of the gene of interest. Modified oligo(dT) primers ligated with a RACE oligo are used to initiate first strand extension of 3'UTRs. Gene-specific primer (GSP) and RACE oligo primers (ROP) are used to amplify 3'UTRs sequences prior to blunt end cloning into plasmid vectors and sequencing. (**B**) Restriction digests of clones obtained from RACE PCR performed on sympathetic neuron RNA. The GSP annealing in the CDS of *Tp53inp2* and the inclusion of the primers and adapters results in the increased length of the digestion product.

To investigate the impact that *Tp53inp2* 3'UTR has on translation, I generated GFP reporter constructs by PCR amplifying the full length 3'UTR and the shorter ~1.2Kb isoform identified by the RACE. In addition, I generated a truncated isoform of ~2.2Kb**.** This was included because the

difference in length between the two identified isoforms was close to 2Kb. The intermediate isoform was generated to narrow down the location of potential regulatory elements. The UTR isoforms were cloned at the 3' end of the coding region of destabilised, myristoylated EGFP (dEGFP) reporter (Aakalu *et al.* 2001). The Ensembl annotated 5'UTR of *Tp53inp2* was cloned at the 5'end (**Fig.2.15A**). The wildtype GFP protein is very stable, with a half-life of over 24 hours, making it unsuitable for measuring sensitive changes in gene expression (Corish and Tyler-Smith 1999). The dEGFP protein has a greatly reduced half-life of around 2hours, allowing much more sensitive detection of changes in translational efficiency (Li *et al.* 1998).

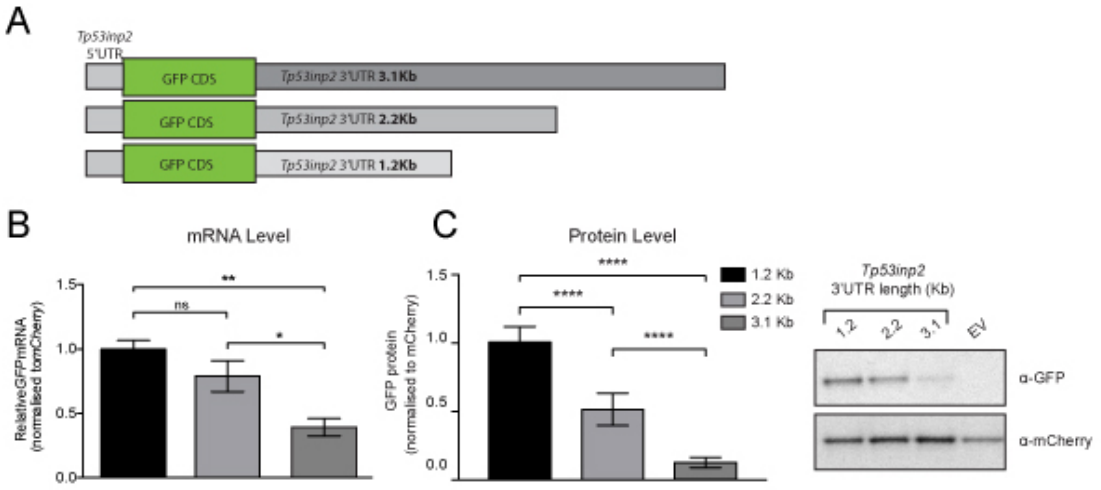

Fig.2.15 The 3'UTR of *Tp53inp2* represses translation. (**A**) Schematic representation of GFP-*Tp53inp2* 3' UTR fusion constructs. PC12 cells transfected with the UTR fusions constructs or empty vector control (EV), and a plasmid expressing mCherry to account for transfection efficiency, were lysed and protein and mRNA levels analysed. For mRNA analyses (**B**), *GFP* mRNA levels were measured by RT-qPCR and normalized to *mCherry* mRNA. Protein levels (**C**) were measured by immunoblotting with GFP antibody and normalized to mCherry as a loading control. Densitometry analysis was performed in imageJ. Data were further normalized to the mean GFP level of the 1.2Kb construct (Left). Representative image of western blotting (right). Values presented as averages ±s.e.m. N=5 independent experiments n.s. = not significant *=P>0.05 **=P>0.01 ****=P>0.0001 One-way ANOVA

PC12 cells were transfected with the different vectors, and after 48 hours, samples were collected and subjected to western blotting and RT-qPCR

analyses. All vectors were efficiently transcribed, though there were some differences in the expression levels of one vector (**Fig.2.15B**). However, increasingly longer 3'UTR led to a dramatic reduction of GFP protein levels, when compared to the 1.2Kb isoform (**Fig.2.15C**), indicating the presence of elements within the full-length 3'UTR of *Tp53inp2* that act to maintain it translationally repressed.

I next investigated whether the translational inhibition was limited to neurons or extended to other cell types. When human embryonic kidney cells HEK293 were analysed, I obtained similar results (**Fig.2.16B**), suggesting that the mechanism by which the long *Tp53inp2* 3'UTR regulates translation may be shared with other mammalian cell types.

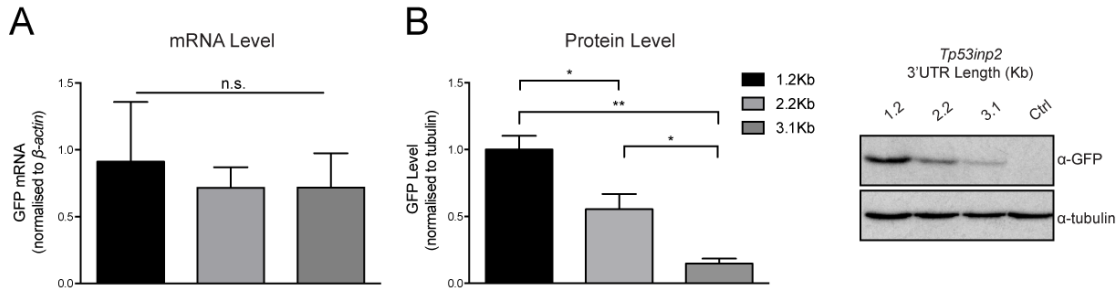

Fig.2.16 The 3'UTR of *Tp53inp2* represses translation in a non-neuronal specific manner. HEK293 cells were transfected with the UTR fusions constructs or empty vector control, and protein and mRNA levels were analysed. (**B**) GFP mRNA was measured by RT-qPCR and normalized to *ß-actin* mRNA. Proteins (**C**) were measured by immunoblotting with GFP antibody and normalized to tubulin as a loading control. Densitometry analysis was performed in imageJ. Data was further normalized to the mean GFP level of the 1.2Kb construct (Left). Representative image of western blotting (right). Values presented as averages ±s.e.m. N=3 independent experiments n.s.= not significant *=P>0.05 **=P>0.01 One-way ANOVA

These data indicate that regulatory elements that tightly repress translation are present within the isoform of *Tp53inp2* expressing the long 3'UTR. Translational efficiency correlates with the length of the 3'UTR, suggesting that repressive elements may be located in the more distal regions.

2.1.6 Summary

I identified *Tp53inp2* as the most abundant and enriched RNA in the axons of sympathetic neurons. Interestingly, despite its abundance, the endogenous Tp53inp2 protein was not detectable by western blot. Using mass spectrometry, trace amounts of Tp53inp2 protein was detected in cell bodies, with none detected in axons. Polysome-fractionation revealed that *Tp53inp2* mRNA was enriched in monosomal fractions, suggesting most transcripts are not actively translated. The addition of full-length *Tp53inp2* UTRs to a GFP ORF abolished protein translation. Taken together, these findings indicate that despite its high levels in, *Tp53inp2* is not translated in sympathetic neuron axons.

2.2 *Tp53inp2* mRNA is essential for the development of the sympathetic nervous system

2.2.1 *Tp53inp2* is necessary for axon growth *in vivo*

Tp53inp2 expression's is spatially restricted to the nervous system during embryogenesis (Bennetts *et al.* 2007). Furthermore, we have shown that *Tp53inp2* mRNA is extremely abundant in the axons of sympathetic neurons *in vitro.* I therefore hypothesised that *Tp53inp2* may play a key role during neurodevelopment, and that this role may be associated with NGF signalling. We first studied the expression pattern of *Tp53inp2* in mouse using *in situ* hybridisation (ISH) performed on cryo-sections of tissue isolated at various developmental time points (**Fig.2.17**). With this technique, labelled anti-sense RNA probes were used to assess the localisation and the abundance of endogenous *Tp53inp2* mRNA. We observed that *Tp53inp2* is expressed in neurons of the SCG at early stages of neurodevelopment (E14.5 and P0.5) and decreases as the animals mature into adulthood (**Fig.2.17**). Importantly, *Tp53inp2* expression is highest when sympathetic neurons are most sensitive to NGF stimulation for growth, differentiation and survival (Glebova and Ginty 2005). Taken together, the spatiotemporal expression of *Tp53inp2* strongly supports the hypothesis that is playing a key role in neurodevelopment.

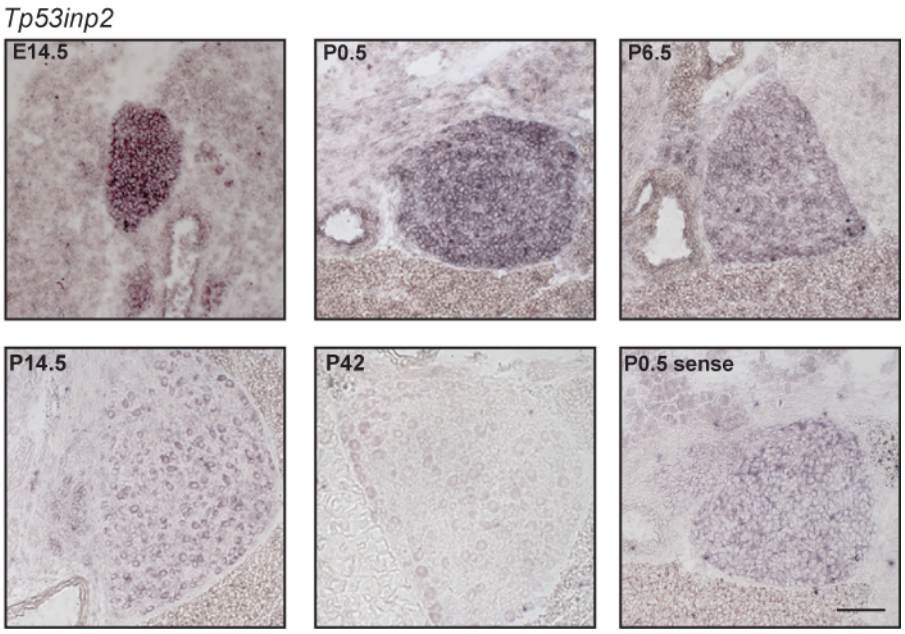

Fig.2.17 *Tp53inp2*'s expression is temporally linked to the developing nervous system Mouse tissues were collected at indicated developmental time points (E=embryonic P= postnatal). The tissues were subjected to *in situ* hybridisation using a digoxigenin-labelled antisense probe targeting *Tp53inp2* mRNA. P0.5 sense probe included as negative control for background staining. Scale bar = 100 μm Experiment performed by Chantal Bodkin-Clarke (Prof. Kuruvilla laboratory).

We next generated a SNS-conditional *Tp53inp2* knockout mouse (CKO) in collaboration with the Kuruvilla lab (Johns Hopkins University, Baltimore MD USA). The CKO model was generated by creating transgenic mice with exons 2 and 3 of the *Tp53inp2* gene flanked by loxP sites (Tp53inp2$^{fl/fl}$). The mice were crossed with a transgenic mouse expressing the Cre-recombinase under the control of the Tyrosine hydroxylase (TH) promoter (**Fig.2.18A**). TH expression is restricted to catecholaminergic neurons and the crossing induced *Tp53inp2* deletion in sympathetic neurons (*TH-Cre;Tp53inp2*$^{fl/fl}$). The *TH-Cre* mouse line has been previously demonstrated to mediate specific and efficient deletion of floxed *Wnt5a* in the sympathetic nervous system (Ryu *et al.* 2013). Due to the lack of detectable Tp53inp2 protein in wildtype sympathetic neurons, the efficiency of the Cre induced knockdown was

established by RT-qPCR. Sympathetic neurons were collected from P0.5 *TH-Cre:Tp53inp2*$^{fl/fl}$ and *Tp53inp2*$^{fl/fl}$ mice and the levels of *Tp53inp2* mRNA was measured. In *TH-Cre:Tp53inp2*$^{fl/fl}$ SCG neurons, there was a greater than 90% reduction of detectable *Tp53inp2* mRNA, compared to *Tp53inp2*$^{fl/fl}$ control (**Fig.2.18B**), demonstrating that this model system is a suitable for studying the role of *Tp53inp2* in sympathetic neurons.

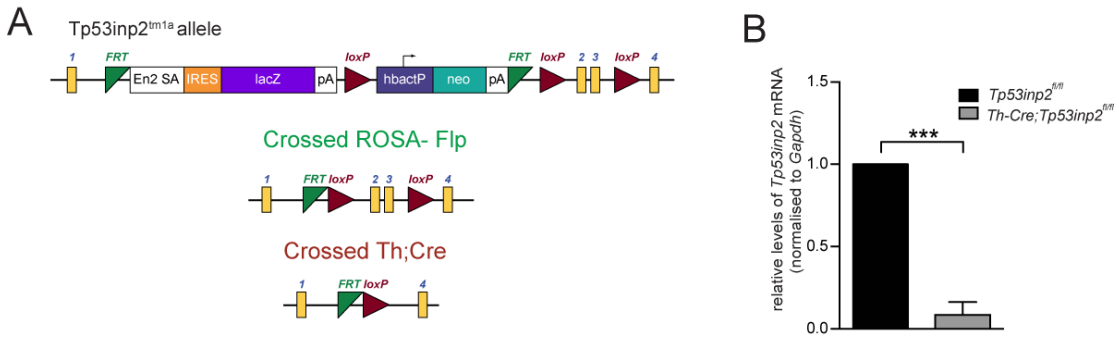

Fig.2.18 Generation of *TH-Cre;Tp53inp2*$^{fl/fl}$ conditional knockout mouse (**A**) Schematic representation of vectors used for the generation of transgenic *Tp53inp2*$^{fl/fl}$ and *Th-Cre;Tp53inp2*$^{fl/fl}$ mice. ROSA-Flp=ubiquitously-expressing Flippase (**B**) Sympathetic neurons were collected from P0.5 *Tp53inp2*$^{fl/fl}$ and *Th-Cre;Tp53inp2*$^{fl/fl}$ mice and levels of *Tp53inp2* mRNA expression were analysed by RT-qPCR. Values are normalized to GAPDH and presented as fold change relative to *Tp53inp2*$^{fl/fl}$. Data are presented as average ±s.e.m. N=3 mice per genotype *** = P<0.001 unpaired T-test. Experiment performed by Chantal Bodkin-Clarke (Kuruvilla Lab).

Given the high levels of *Tp53inp2* expression at a stage when sympathetic neurons are undergoing axonal growth and establishing NGF-dependent cell survival, we investigated whether *TH-Cre;Tp53inp2*$^{fl/fl}$ mice displayed abnormalities of neuronal survival or target organ innervation. We first studied whether loss of *Tp53inp2* impacted on survival of sympathetic neurons by performing Nissl stain on cryo-sectioned tissue obtained from *TH-Cre;Tp53inp2*$^{fl/fl}$ and *Tp53inp2*$^{fl/fl}$ mice at various developmental time points (**Fig.2.19**). Nissl staining relies on the incorporation of cresyl violet dye into

the DNA and into concentrated RNA at the endoplasmic reticulum. Neurons contain high levels of endoplasmic reticulum relative to other cell types, allowing their identification based on morphology and intensity of cytoplasmic staining (Kádár *et al.* 2009). In the SCG of *TH-Cre;Tp53inp2*$^{fl/fl}$ mice, a significant reduction in the number of neurons was observed at P0.5 and P21, compared to control littermates (**Fig.2.19**). These findings indicate that *Tp53inp2* expression is necessary for promoting neuronal survival.

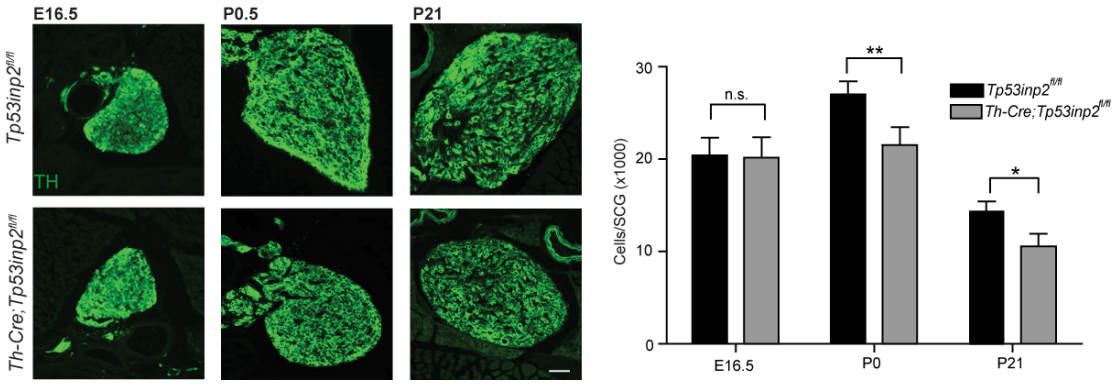

Fig.2.19 *Tp53inp2* KO results in neuronal loss in mouse SCG *in vivo.* SCG were collected from *Tp53inp2*$^{fl/fl}$ and *Th-Cre;Tp53inp2*$^{fl/fl}$ mice at the indicated time points. The SCG were cryosectioned and stained using a tyrosine hydroxylase antibody (TH, **left panels**). (**Right panel**) tissue sections were Nissl stained and cells with characteristic neuronal morphology were counted. Scale bar 200µm. Data are presented as averages ± s.e.m. N=3 mice per genotype *P<0.05, **P<0.01, n.s. not significant, unpaired *t* test. Experiment performed by Chantal Bodkin-Clarke (Kuruvilla Lab).

To investigate whether defects in target derived innervation and abnormal NGF signalling may cause neuronal death in mice lacking *Tp53inp2*, we analysed axonal innervation of the heart, a key target of the SNS. Sympathetic innervation of the heart of E16.5 *TH-Cre;Tp53inp2*$^{fl/fl}$ and *TH-Tp53inp2*$^{fl/fl}$ mice was studied using whole mount TH immunostaining (**Fig.2.20**). We observed that both innervation density and axonal branching were significantly reduced in *TH-Cre;Tp53inp2*$^{fl/fl}$ tissue, relative to control littermates.

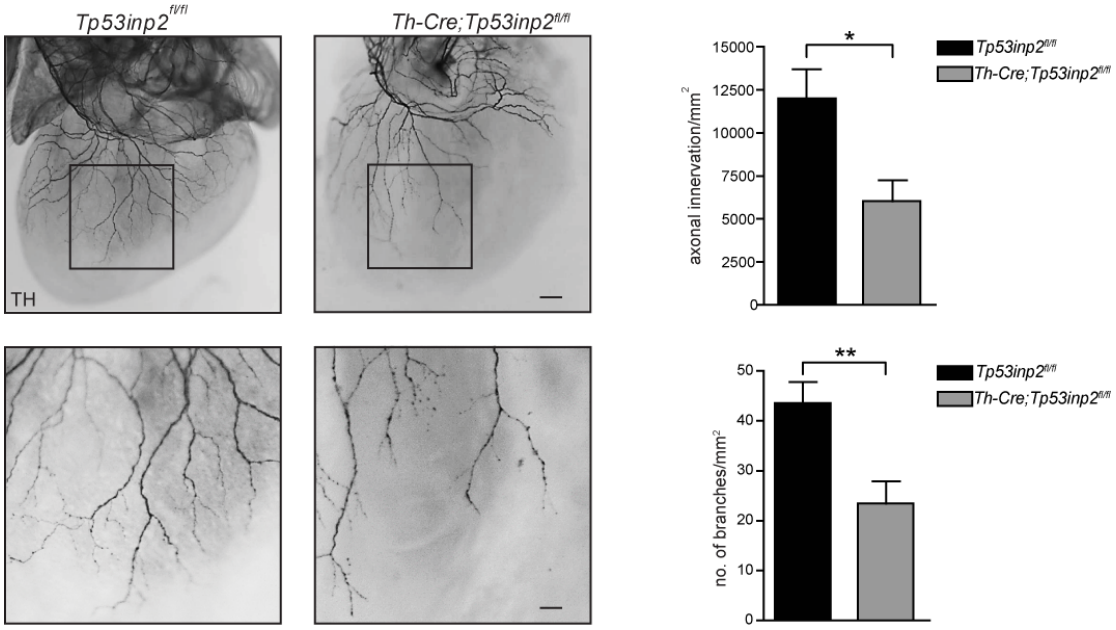

Fig.2.20 *Tp53inp2* KO results in reduced innervation of targets of sympathetic nervous system. Hearts collected from E16.5 *Tp53inp2*$^{fl/fl}$ and *TH-Cre;Tp53inp2*$^{fl/fl}$ mice were subjected to whole mount immunostaining for Tyrosine Hydroxylase (TH) to visualise sympathetic neuron axons. Scale bar 100 µm and 400 µm for magnified images. Innervation density and axonal branching quantified for n=8 mice per genotype. Total innervation was measured as area covered by TH-positive axon fibres. The branch points were counted as the number of axon terminal endpoints. Data as averages ±s.e.m. *P<0.05 **P<0.001 Unpaired T-test Experiment performed by Chantal Bodkin-Clarke (Kuruvilla Lab).

Importantly, the reduced innervation detected at E16.5 precedes the loss of neurons at P0 and P7. Taken together, these data indicate that that *Tp53inp2* expression is required for efficient axon growth. Moreover, sympathetic neuron loss is likely due to incorrect target organ innervation and lack of NGF stimulation resulting in cell death.

2.2.2 *Tp53inp2's* role in axon growth is independent of its translation

To further investigate the role of *Tp53inp2* in regulating axon growth, sympathetic neurons were harvested from P0/P1 *Tp53inp2*$^{fl/fl}$ mice and grown in compartmentalised chambers. Once axonal projections reached the lateral compartments, NGF stimulation was withdrawn from the cell bodies and maintained in the axons to ensure outgrowth. Compartmentalised chambers

also allow measurement of the growth rate of axons, as they extend unidirectionally. Cell bodies were infected with adenovirus expressing either Cre to abolish *Tp53inp2* expression, or LacZ, as a control. Adenoviral expression of Cre was very efficient and we observed ~90% reduction of *Tp53inp2* mRNA relative to LacZ infected controls (**Fig.2.21A**). Upon loss of *Tp53inp2*, axonal growth rate was significantly reduced (~75%) compared to LacZ infected controls (**Fig.21B**). These findings resemble the phenotype observed *in vivo* and further support the hypothesis that *Tp53inp2* expression promotes axon growth.

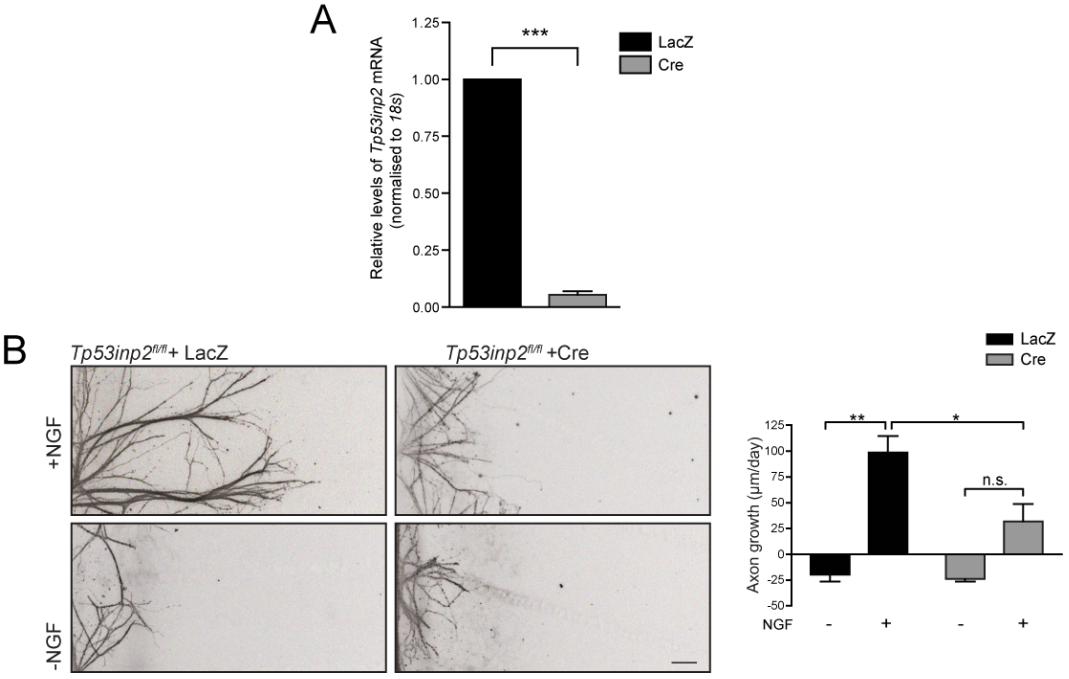

Fig.2.21 *Tp53inp2* deletion *in vitro* attenuates axonal outgrowth. (**A**) *Tp53inp2*$^{fl/fl}$ sympathetic neurons were infected with adenoviruses (AVs) expressing Cre or LacZ (control). Levels of *Tp53inp2* mRNA were quantified by RT-qPCR, normalized to 18s rRNA and expressed as fold change relative to control. N=3 ***P<0.001 unpaired T-test with Welch's correction. (**B**) Sympathetic neurons from P0.5 *Tp53inp2fl/fl* mice were cultured in compartmentalised chambers and infected with AVs expressing either Cre or LacZ in the presence or absence of NGF. (**Left**) Representative images of axons immunostained with anti-tubulin, scale bar = 100 µm. (**Right**) Quantification of axon extension per day, as measured at 24-hour intervals for 72 hours. Data presented as average ± s.e.m. N=3 independent experiments (>70 axons traced per condition) n.s. = not significant *=P<0.05 **= P<0.01 one-way ANOVA. Experiment performed by Chantal Bodkin-Clarke (Kuruvilla Lab).

Importantly, the *in vitro* axon growth defect was observed at the same developmental time point (P0/1) as when high levels of *Tp53inp2* mRNA were detected in axons, but no detectable protein. As the expression of *Tp53inp2* is required for robust axon growth, I hypothesised that the role of *Tp53inp2* mRNA may be independent of translation, and that the mRNA may have an essential coding-independent function in promoting neuronal development.

To investigate whether *Tp53inp2* mRNA may act independently of translation, I generated two constructs to rescue the axon growth defect observed *in vitro*. One vector expressed the full sequence of *Tp53inp2* including the 5' UTR and the complete 3'UTRs (3.1Kb isoform), and was named *WT-Tp53inp2* (**Fig.2.22D**). The second vector (named *ATGNull-Tp53inp2*) expressed a form of *Tp53inp2* mRNA that was made not translatable (**Fig.2.22D**) by deleting an adenosine from the ATG start codon that generated a point mutation in the translational start site. To further ensure that translation was not initiated downstream of the canonical translational start site (TSS), all adenosines of in-frame ATG codons were also mutated to cytosines. The sequences were cloned into the AdEasy Adenoviral vector system (He *et al.* 1998). Briefly, the gene of interest was cloned into an intermediate 'shuttle' vector containing the CMV promoter. The gene and promoter region are then transferred into a large plasmid containing the adenoviral genome through means of homologous recombination. The plasmid was transfected into the HEK293 cells, which result in the production of mature, infectious adenovirus particles expressing the gene of interest. The shuttle constructs were transfected into PC12 cells, and the levels of Tp53inp2 protein and mRNA were analysed by western blotting and RT-

qPCR. Both constructs produced similar high levels of *Tp53inp2* mRNA, relative to the empty vector control (**Fig.2.22B**). Importantly, western blotting using a Tp53inp2 antibody did not detect Tp53inp2 protein in cell lysates transfected with either *WT-Tp53inp2* or *ATGNull-Tp53inp2* (**Fig.2.22A**). The lack of detection in cells infected with *WT-Tp53inp2* was not surprising, as I have previously shown that the full-length UTRs of *Tp53inp2* present in these constructs inhibits translation (**Fig.2.15**). Thus, both rescue constructs are transcribed at similar levels but not translated.

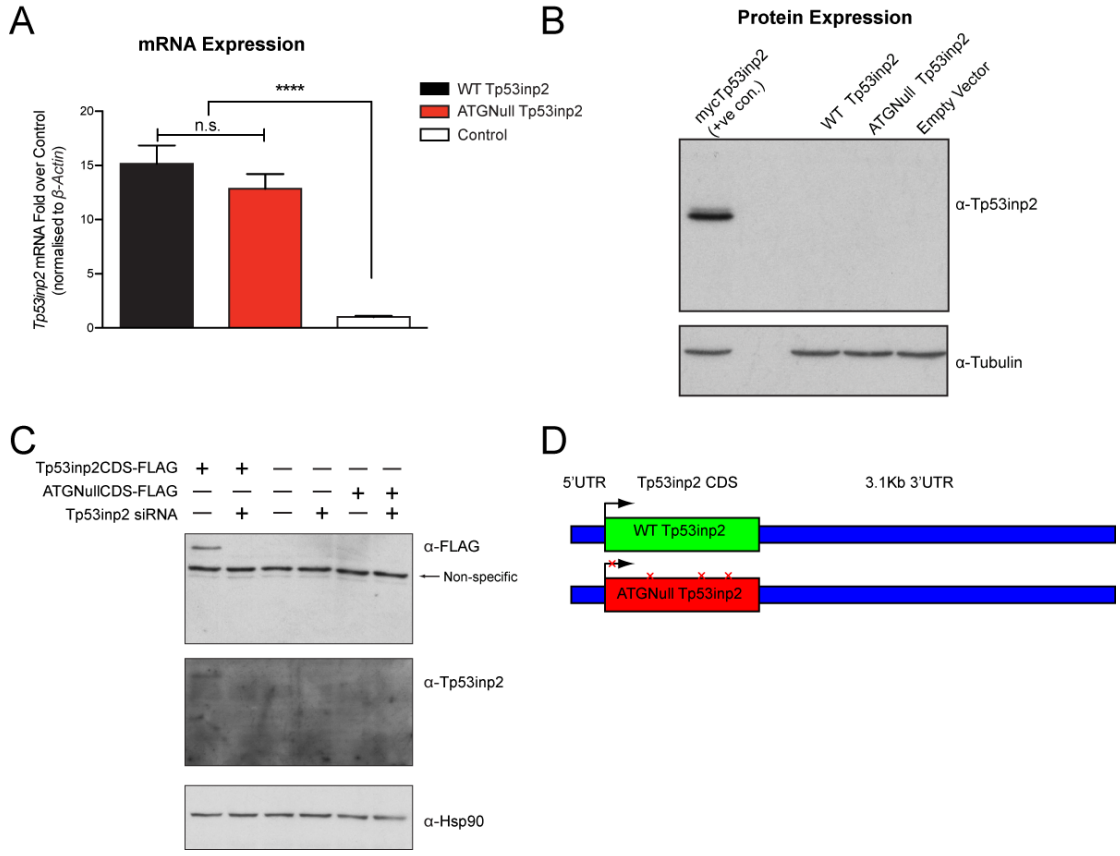

Fig.2.22 Validation of *Tp53inp2* rescue constructs. (**A**) RNA isolated from PC12 cells transfected with wild type (WT), ATGNull or empty vector control were analysed by RT-qPCR (n=5) and (**B**) western blotting (n=3). *Tp53inp2* mRNA was normalized by *ß-actin* and presented as fold over control. Values are average ±s.e.m. n.s. = not significant ****P<0.0001 One-way ANOVA (**C**) Western blotting of PC12 cells transfected with plasmids expressing either C-terminal Flag tagged *Tp53inp2* CDS, C-Terminal Flag tagged ATGNull CDS or empty vector control and siRNA targeting *Tp53inp2* mRNA or non-targeting control, as indicated. (N=3). (**D**) Schematic representation of *Tp53inp2* constructs, red crosses indicate mutated ATG codons.

I further proved that the ATGNull coding sequence was not producing a protein fragment by generating C-terminal Flag-tagged constructs that contained the wildtype and mutant *Tp53inp2* ORFs but lacked the 5' and 3' UTRs. When the wildtype construct was transfected in PC12 cells, a band of the expected size was detected using both the flag and Tp53inp2 antibodies (**Fig.2.22C,** upper band). The antibodies specifically recognised Tp53inp2 protein, as transfection of *Tp53inp2* siRNA completely abolished the signal. Importantly, in cells transfected with the *ATGNull-Tp53inp2* construct, the protein was not detected by either antibody, indicating that even in the absence of the 3'UTR this modified sequence is not translated into protein (**Fig.2.22C**). Next, I purified high titre adenoviral vectors that were used to obtain high expression levels of the rescue constructs in sympathetic neurons. To this end, the viral plasmids were transfected in HEK293 cells to produce mature adenoviruses (AVs), followed by multiple passages of the viruses through HEK293 cells to generate high titres of the viral particles. The AVs were subsequently purified using a caesium chloride gradient to generate concentrated AV stocks. To assess whether *WT-Tp53inp2* and *ATGNull-Tp53inp2* constructs can rescue defects of axon growth induced by *Tp53inp2* loss, I employed the experimental set-up described in **Fig.2.21**. Sympathetic neurons were plated within the central compartment of compartmentalised chambers and axon outgrowth was stimulated by adding NGF to the lateral compartments. Neurons were infected with AVs expressing either Cre, which abolished *Tp53inp2* expression, or a control virus expressing GFP. The Cre-infected neurons were further infected either with the *WT-Tp53inp2, the ATGNull-Tp53inp2* rescue constructs, or neither, to control for Cre efficiency.

Neurons were cultured for 48 hours to ensure sufficient expression of the constructs and complete ablation of endogenous *Tp53inp2* and axon growth was measured every 24 hours for 3 days (**Fig.2.23**).

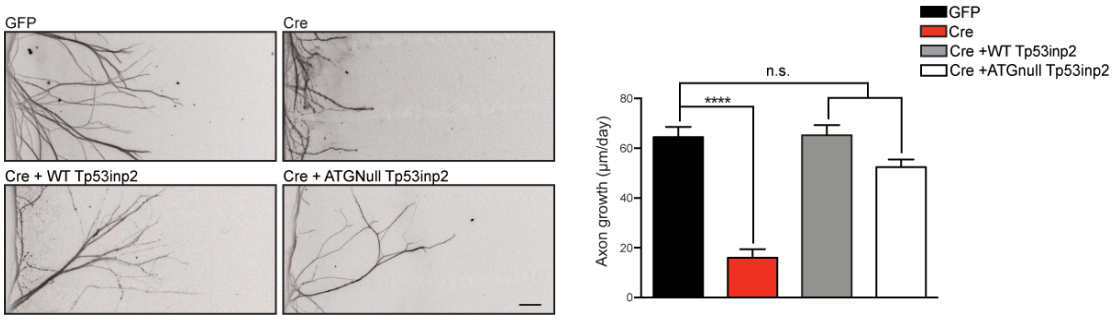

Fig.2.23 *Tp53inp2* regulates axon growth in a coding-independent manner. Sympathetic neurons from *Tp53inp2fl/fl* mice were cultured in compartmentalised chambers and infected with AVs expressing Cre or GFP. Cre infected neurons were simultaneously infected with WT-Tp53inp2, ATGNull-Tp53inp2 or neither. (**Left**) Representative images of axons immunostained with anti-tubulin, scale bar = 100 µm. (**Right**) Quantification of axonal outgrowth per day, measured at 24-hour intervals for 72 hours. Data presented as average ± s.e.m. N=3 independent experiments (>50 axons traced per condition) n.s. = not significant ****=P<0.0001 one-way ANOVA.

As previously observed, loss of *Tp53inp2* resulted in a 75% reduction of axonal outgrowth, relative to control. Strikingly, expression of both *WT-Tp53inp2* and *ATGNull-Tp53inp2* constructs was sufficient to recover the growth defects caused by the loss of *Tp53inp2* (**Fig.2.23**). The ability of the *ATGNull* construct to rescue axonal growth is of particular importance, as it indicates that the role of *Tp53inp2* mRNA in sympathetic neurons is independent of its protein coding capacity.

2.2.3 Summary

Taken together, these findings indicate that *Tp53inp2* plays a critical role during neurodevelopment. *Tp53inp2* is expressed in sympathetic neurons at a developmental time point when they are heavily reliant on NGF signalling for survival and growth. My data suggests that the role of *Tp53inp2* may be linked to NGF signalling. Using a combination of *in vivo* and *vitro* approaches, we show that *Tp53inp2* expression in sympathetic neurons is required for promoting axon growth. When *Tp53inp2* is lost *in vivo*, neurons are unable to extend axons and innervate their target tissues and undergo cell death. Importantly, a construct expressing a non-translatable *Tp53inp2* mRNA rescued the axonal outgrowth defects, supporting the hypothesis that at least in sympathetic neurons, *Tp53inp2* mRNA acts in a coding-independent manner.

2.3 *Tp53inp2* mRNA interacts with TrkA in axons to modulate NGF/TrkA signalling

2.3.1 *Tp53inp2* mRNA is associated with TrkA

I next sought to investigate how *Tp53inp2* RNA regulates axon growth in sympathetic neurons. NGF supports cell survival and growth by binding to the TrkA receptor, which induces homodimerisation and autophosphorylation of the receptor. Receptor-ligand complexes are internalised within signalling endosomes that retrogradely transported to cell bodies (Ascano *et al.* 2012). NGF stimulation of the TrkA receptor is essential for cell survival and growth during development. Recent work has shown that 3UTRs may act as scaffolding for proteins, aiding in the formation and localisation of protein complexes. For example, the 3'UTR of *CD47* mRNA recruits SET to the plasma membrane, where they subsequently form a complex with the CD47 protein (Berkovits and Mayr 2015). I hypothesised that the *Tp53inp2* transcript may interact with the NGF/TrkA complex, thereby enhancing the complex's growth and survival-promoting functions.

To investigate if *Tp53inp2* mRNA binds to TrkA, I used the RNA-immunoprecipitation (RIP) technique, which allows the identification of RNA-protein interactions by immunoprecipitation of the protein of interest and subsequent RT-qPCR to identify RNA associated directly with that protein or protein-complex (Gilbert and Svejstrup 2006). I used a Trk antibody to immunoprecipitate TrkA from lysates of cultured sympathetic neurons, and associated mRNA were analysed by RT-qPCR. Because no known interaction has been identified between TrkA and an mRNA so far, the RNA binding protein HuD was used as a positive control for the RIP technique. I observed

a ~2.5 fold enrichment of *Tp53inp2* mRNA in the Trk pulldown versus control IgG (**Fig.2.24A**). To further prove the specificity of the interaction, I studied the association of TrkA with *IMPA1,* an mRNA that is very abundant in sympathetic neuron axons (Andreassi *et al.* 2010). *IMPA1* was not immunoprecipitated by Trk, though there was a strong enrichment when RIP was performed using an antibody for the known interactor HuD (**Fig.2.24B**) (Andreassi *et al.* 2017). Interestingly, *Tp53inp2* was also immunoprecipitated with HuD (**Fig.2.24B**)**.** HuD is a neuronal-specific member of the ELAV-like protein RBP family that regulates many aspects of mRNA metabolism including transport, stability and translation (Ross *et al.* 1997, Perrone-Bizzozero and Bird 2013). HuD may therefore be important for the localisation and translational repression of *Tp53inp2* in neurons, but further work is required to explore this hypothesis.

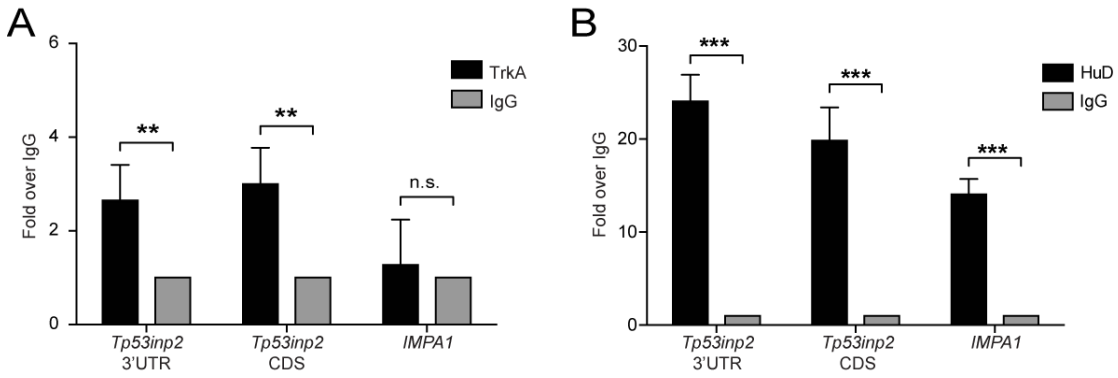

Fig.2.24 *Tp53inp2* interacts with the TrkA complex RNA Immunoprecipitation performed on rat sympathetic neuron lysate using antibodies for Trk (**A**), HuD (**B**) or normal IgG. Levels of mRNA were analysed by RT-qPCR and normalised by levels of total input. Data presented as fold over IgG. N=4 independent experiments, data presented as averages ±s.e.m. Unpaired T-Test n.s. = not significant **P<0.01 ***P<0.001

I next investigated whether the interaction between the TrkA protein complex and *Tp53inp2* mRNA was occurring specifically in axons. Due to the amount of material required for the RIP technique, compartmentalised

chambers were unsuitable. Therefore, I chose to use single molecule RNA fluorescent *in situ* hybridisation (smFISH) coupled with protein immunofluorescence. This technique allows the visualisation RNA-protein co-localisation and has been used previously to demonstrate axonal colocalisation of nucleolin protein and *importin ß1* mRNA in sensory neurons (Perry *et al.* 2016). I utilised the Stellaris probe system, which uses multiple (>25) fluorescently labelled oligos that 'tile' the transcript of interest to provide single molecule resolution (**Fig.2.25A**). The detection of fluorescence signals relies on the binding of most probes to the same mRNA transcript, which minimises off-target effects. Probes were generated targeting *Tp53inp2* mRNA, and the specificity was demonstrated by electroporating siRNA for *Tp53inp2* in sympathetic neurons (**Fig.2.25B**). The marked reduction of signal in the *Tp53inp2* knockdown samples demonstrates that the probes specifically target *Tp53inp2* mRNA.

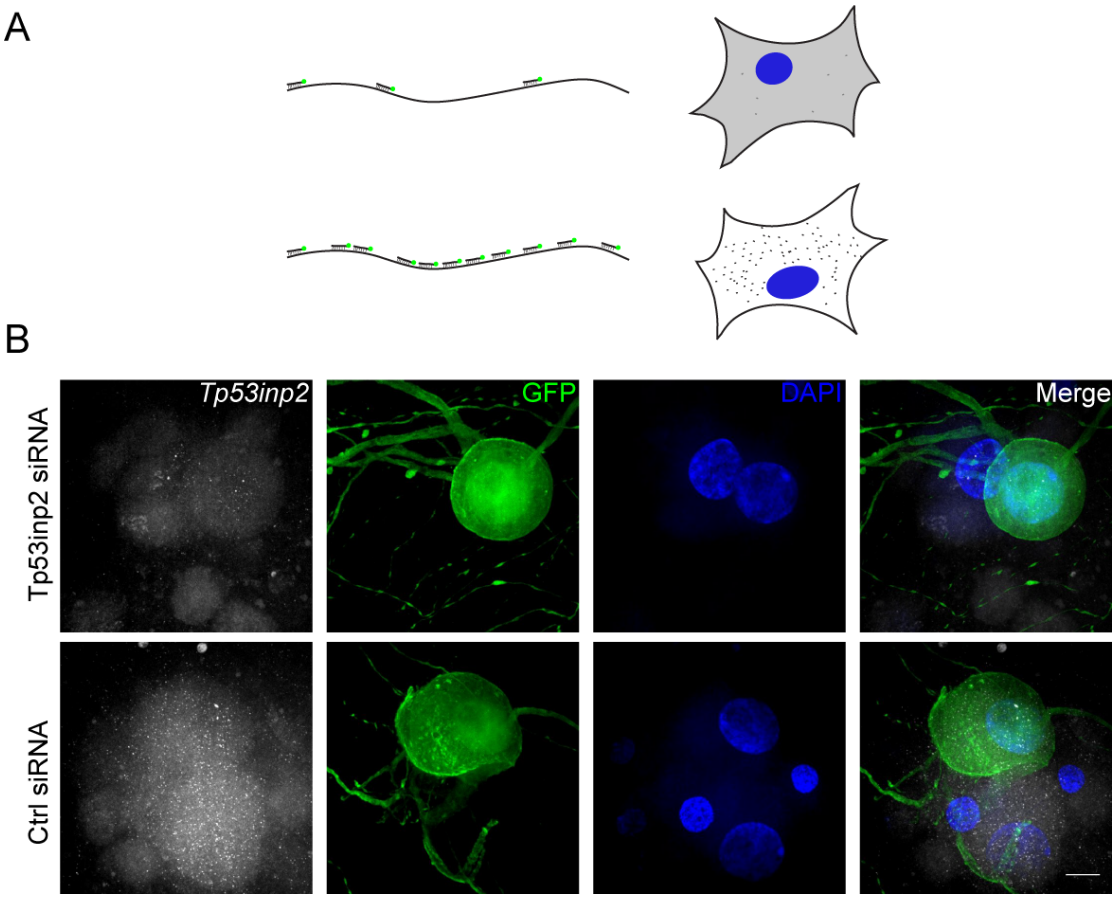

Fig.2.25 smFISH accurately detects *Tp53inp2* in sympathetic neurons A) Illustrative schematic of the principle of Stellaris smFISH. Multiple labelled probes binding to the target transcript provides punctate staining with minimal background **B)** smFISH for endogenous *Tp53inp2* in cultured sympathetic neurons. Neurons were electroporated with siRNA targeting *Tp53inp2* or non-targeting control, with a plasmid expressing GFP. Scale bar 10μm

To investigate *Tp53inp2*-TrkA interaction in axons, I coupled FISH staining with immunofluorescence using a TrkA antibody on cultured sympathetic rat neurons. As *IMPA1* does not interact with TrkA (**Fig.2.24B**), *IMPA1* FISH was used as a negative control. Sympathetic neurons were cultured *in vitro* for 7 days before performing the staining, imaging and quantitative analysis of overlapping RNA FISH and protein immunofluorescence within axons (**Fig.2.26**). Though there is an observable level of overlap between *Tp53inp2* and TrkA (~10%), it is not significantly higher than between *IMPA1* and TrkA. This suggests that this technique is not sufficiently sensitive to detect an

interaction between *Tp53inp2* and TrkA within axons, above the levels of experimental noise.

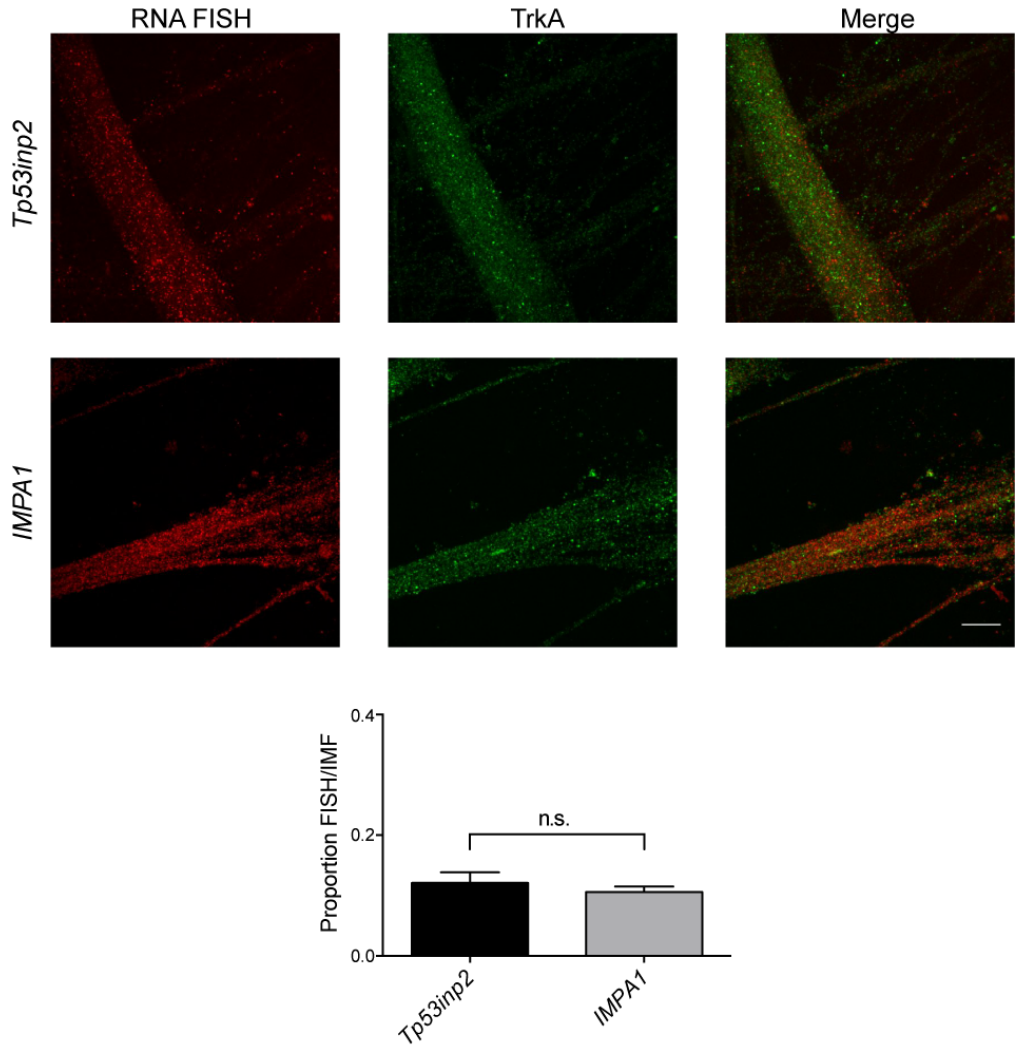

Fig.2.26 CoImmunoFISH for *Tp53inp2* and TrkA in sympathetic neurons Representative images of sympathetic neuron axons subjected to RNA FISH and TrkA immunostaining. Maximal Z-projections of image stacks are shown. Scale bar 10µm. (**Lower Panel**) Quantification of colocalisation of FISH and Immunofluorescence (IMF) performed using JACoP plugin for ImageJ. Value presented as total of RNA FISH signal that overlaps with protein IMF signal. >40 images from 3 independent experiments analysed. Data presented as average ±s.e.m n.s = not significant. Unpaired T-Test

2.3.2 *Tp53inp2* modulates local TrkA signalling

Having established a potential interaction between *Tp53inp2* mRNA and TrkA, I next investigated the function of the complex. Based on the axonal growth defect observed both *in vivo* and *in vitro*, I hypothesised that the loss

of *Tp53inp2* results in an inability of the NGF/TrkA complex to correctly initiate downstream signalling cascades.

Upon internalisation and phosphorylation, the NGF/TrkA complex acts both locally in the axons, and within the cell body following retrograde trafficking. Seminal work from Campenot (1977) demonstrated this local signalling response by observing that NGF applied locally to axons alone is sufficient to maintain axonal outgrowth, while NGF supplied directly to only the cell body is not. Phosphorylation of TrkA leads to the activation of multiple signalling pathways: PLC-γ, MAPK and PI3K. These pathways lead to the propagation of signals for cell survival, axonal outgrowth and differentiation (Ascano *et al.* 2012). Given the enrichment of *Tp53inp2* mRNA in axons, we focused on the local axonal signalling of the NGF/TrkA endosome. Sympathetic ganglia from Tp53inp2$^{fl/fl}$ P0/1 mice were plated as explant tissue and cultured for 7 days before infection with AV expressing either Cre or LacZ. NGF was withdrawn from the growth media for 36 hours, and the anti-apoptopic agent Boc-D-FMK provided to prevent premature cell death following NGF deprivation. The neurons were restimulated with NGF to induce phosphorylation of TrkA and its downstream effectors, or left without NGF as a control. To investigate axonal signalling, cell body tissue was surgically removed and the axons lysed and analysed by western blot. In the LacZ infected control, there is a significant increase in the phosphorylation of TrkA, ERK and AKT, demonstrating a robust activation of the local NGF signalling pathway (**Fig.2.27**). However, in Cre infected neurons, the increased phosphorylation was lost for all observed components. These data indicate that the interaction of *Tp53inp2* mRNA with the TrkA receptor is required in axons for the local

activation of the TrkA signalling pathway. Loss of *Tp53inp2* results in decreased TrkA phosphorylation, and dampened activation of downstream signalling components.

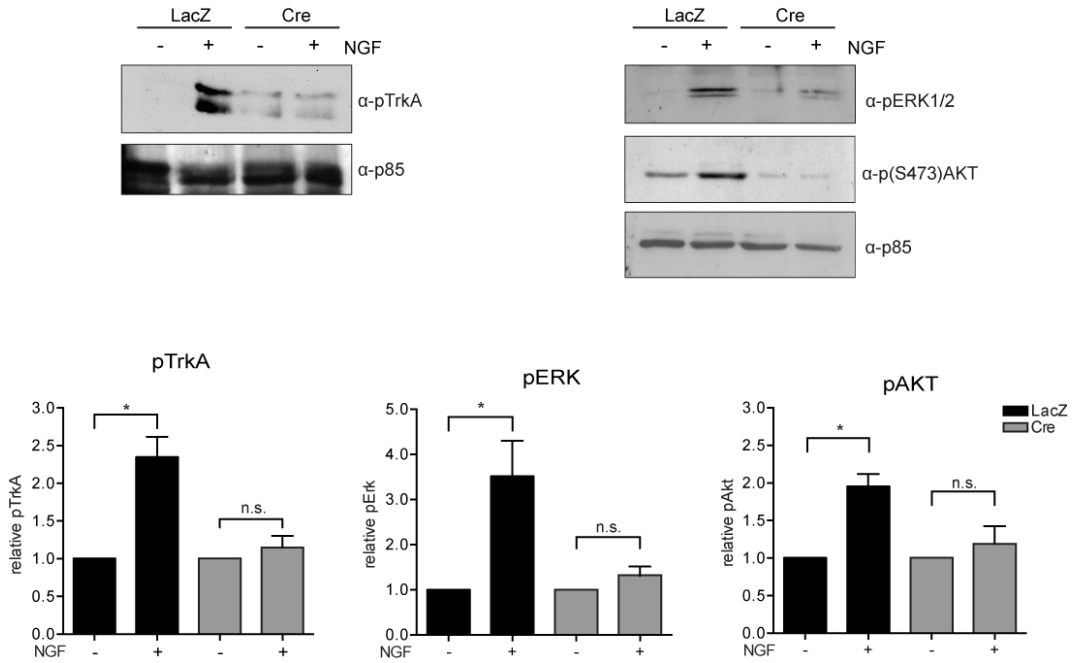

Fig.2.27 *Tp53inp2* mediates local TrkA signalling Western blotting of axonal lysates from cultured *Tp53inp2*$^{fl/fl}$ SCG explants infected with AV expressing either Cre or LacZ. Explants were deprived of NGF for 36 hours, cell bodies were mechanically severed from axons, and isolated axons stimulated with NGF for 30 minutes, or left untreated. Axon lysates were subjected to immunoprecipitation with a P-tyrosine antibody followed by immunoblotting for TrkA to detect pTrkA. The lysate supernatants were immunoblotted for pErk1/2, pAkt and p85 as a loading control. (**Lower panel**) Densitometry of pTrkA, pErk1/2, and pAkt levels. Values were first normalized to p85 levels. Results are average ±s.e.m and expressed relative to no neurotrophin conditions for LacZ and Cre-expressing neurons. N=4 independent experiments *P<0.05, n.s. not significant, Unpaired t test. Experiment performed by Emily Scott-Solomon (Kuruvilla Lab)

2.3.3 Summary

In sympathetic neurons, *Tp53inp2* mRNA directly interacts with the TrkA complex. This interaction is essential for the NGF-dependent activation of the TrkA receptor, and the subsequent activation of downstream signalling pathways within axons. Therefore, *Tp53inp2* has a novel role as a non-coding mRNA responsible for NGF-TrkA mediated axon growth and neuronal survival.

3. Discussion

In order to thrive, neurons must be capable of responding rapidly to extracellular stimuli and must adapt to changing environmental conditions. This is achieved by modulating gene expression at several levels, from transcription, to mRNA localisation and translation. Many transcripts are asymmetrically localised in neurons, allowing accurate spatiotemporal changes in gene expression. This is essential for most neuronal functions including synaptic plasticity, axon growth, guidance and integrity, and nerve regeneration after injury (Leung *et al.* 2006, Andreassi *et al.* 2010, Ben-Yaakov *et al.* 2012). The physiological importance of post-transcriptional regulation of RNA in neurons is exemplified by the growing repertoire of neurological disorders associated with mutations in regulators of RNA transport, stability and translation (Wang *et al.* 2016).

APA-based regulation of 3'UTR length represents a key mechanism by which mRNA is regulated. A number of studies centred on the role of APA at a cellular level have shown striking differences in 3'UTR length between proliferative and differentiated cells, and between tissues (Sandberg *et al.* 2008, Mayr and Bartel 2009, Lianoglou *et al.* 2013). However, the extent to which APA occurs in subcellular compartments, and the role that it plays in this context is largely unknown. The 3'end seq screen performed in our laboratory revealed that axonal transcripts typically expressed multiple isoforms originating from alternative PAS choice. Moreover, we found that axonal transcripts typically possess 3'UTRs longer than those found in the cell body (Andreassi *et al.* 2017), suggesting a more complex regulation of transcripts targeted to axons.

Tp53inp2 mRNA provides a striking example of this regulation, as it is characterised by an unusually long 3'UTR that represses translation and may confer a novel, non-coding function to the transcript. *Tp53inp2* is a recently characterised gene highly conserved across mammalian species (Nowak *et al.* 2005, Bennetts *et al.* 2007). During mouse development, the expression of *Tp53inp2* mRNA is restricted to the nervous system (**Fig.1.12**) (Bennetts *et al.* 2007) and at later embryonic stages the transcript is expressed in sympathetic neurons (**Fig.2.17**). *Tp53inp2* mRNA is enriched in axons and several other screens investigating subcellular localisation of RNA have found that the transcript is targeted to cellular protrusions (Mili *et al.* 2008, Andreassi *et al.* 2010, Zivraj *et al.* 2010, Gumy *et al.* 2011, Cajigas *et al.* 2012, Taliaferro *et al.* 2016). Although the spatial and temporal expression of *Tp53inp2* indicates a potential role in neuronal development, its functions have been mostly investigated in adult skeletal muscle and transformed cell lines. In these systems, *Tp53inp2* acts as a regulator of autophagy and within the nucleus, as a co-activator of transcription (Nowak *et al.* 2009, Mauvezin *et al.* 2010, Sala *et al.* 2014, Xu *et al.* 2016).

Tp53inp2 is not translated in sympathetic neuron axons

Tp53inp2 mRNA possesses all features of a protein coding mRNA (spliced exons, a polyA tail, and a translatable open reading frame), however despite its abundance in axons, three distinct technical approaches (western blotting, MS and Polysome Fractionation) failed to detect Tp53inp2 protein. The inability to detect a protein by one or more antibody-based techniques does not necessarily mean that the protein is not present, as many antibodies

detect overexpressed, but not endogenous proteins (**Fig.2.1, 2.2, 2.5**). However, even the more sensitive targeted MS technique failed to detect Tp53inp2 protein in sympathetic neuron axons, although it was identified at very low levels in cell bodies (**Fig.2.8**). These samples were prepared from ganglia explants that may contain non-neuronal cells, therefore it is possible that the Tp53inp2 detected derived from cells other than sympathetic neurons. Samples obtained from dissociated neuronal cultures would provide a much cleaner system to analyse Tp53inp2 expression, and would allow greater confidence regarding its neuronal derivation. Even if the Tp53inp2 protein detected in cell bodies originates from neurons, these findings highlight two points. Firstly, if *Tp53inp2* is translated in the cell bodies, it is at a very low level. Secondly and importantly, it demonstrates that targeted MS can detect endogenous Tp53inp2. Protein identification by MS is technically challenging, and the number of proteins identified from within a complex sample is estimated to be as low as 50% (McHugh and Arthur 2008, Wang and Wilson 2013). The low-level identification within cell bodies provides a positive control for the axonal sample and strongly indicates that Tp53inp2 protein is indeed absent from axons. Thus, axonal *Tp53inp2* mRNA either is not being translated, or it is axonally translated and rapidly trafficked back to the cell body.

A recent study suggested that Tp53inp2 protein recruits the PolI machinery to the promoters of rDNA in HeLa cells (Xu *et al.* 2016). The axonal localisation of transcription factor mRNAs may allow specific changes in gene expression in response to stimuli applied distal to the cell bodies (Cox *et al.* 2008, Ben-Yaakov *et al.* 2012, Ji and Jaffrey 2012, Baleriola *et al.* 2014). One

such factor is *Stat3* that in response to axonal injury, is translated in sensory axons and trafficked back to the nucleus, where it activates the transcription of genes required for nerve regeneration (Ben-Yaakov *et al.* 2012). In all of the aforementioned studies, both the mRNA and protein were identified in axons. If *Tp53inp2* is translated in axons and retrogradely transported to cell bodies, inhibition of retrograde transport should lead to an accumulation of axonal Tp53inp2 protein detectable by MS. However, my data indicate that translation of *Tp53inp2* is not required in axons, as the *ATGnull* construct completely rescues the axon growth defects observed in *Tp53inp2* KO neurons (**Fig.2.23).** Moreover, experiments performed in severed axons demonstrate that *Tp53inp2* acts locally to mediate TrkA signalling (**Fig.2.27**), suggesting that retrograde transport of *Tp53inp2* is not required for its function.

mRNA abundance is not necessarily the best indication of the presence of protein, as mRNA levels do not necessarily correlate to protein expression. Post-transcriptional mRNA regulation represents a key factor, given that mRNA can be transcribed and held in a repressive state (de Sousa Abreu *et al.* 2009, Van Der Kelen *et al.* 2009). For example, NGF stimulation of PC12 cells leads to an induction of translation of the eukaryotic elongation factor 1A-1 (eEF1A-1), and axonal injury in sensory neurons results in localised translation of *importin ß1* (Petroulakis and Wang 2002, Perry *et al.* 2012). Ribosome profiling is a more accurate technique that allows global measurement of translation (Ingolia *et al.* 2009), and when combined with sequencing of the transcriptome, it estimates transcripts that are translationally repressed. Parallel ribosome profiling/RNAseq has been used

to demonstrate the translational state of cyclin mRNA during *S. cerevisiae* mitosis and has provided information on miRNA-mediated regulation of mRNA translation in HeLa cells (Guo *et al.* 2010, Brar *et al.* 2012, Ingolia 2014). Ribosome profiling combined with RNAseq performed at various developmental time points in RGC axons, showed that a large proportion of mRNA is not associated with ribosomes (Zivraj *et al.* 2010, Shigeoka *et al.* 2016). Interestingly, *Tp53inp2* was one of the transcripts not found in the translatome, suggesting that *Tp53inp2* may be maintained translationally repressed across a range of neuronal cell types (Zivraj *et al.* 2010, Shigeoka *et al.* 2016).

Polysomal fractionation also revealed that the majority of *Tp53inp2* mRNA co-sedimented with the free and monosomal fractions of the gradient, suggesting inefficient translation and providing a potential explanation for the inability to reliably detect Tp53inp2 protein (**Fig.2.11)**. I detected a small fraction (33.9%) of *Tp53inp2* mRNA associated with the polysomal fractions (**Fig.2.11**). This fraction of mRNA may account for the small amount of Tp53inp2 protein identified in cell bodies by targeted mass-spectrometry. Monosomes have typically been regarded as ribosomes bound to mRNA, yet in a translationally inactive state (Van Der Kelen *et al.* 2009). Unfortunately, these experiments do not provide information on the translational status of transcripts in axons, as polysomal fractionation was performed on sympathetic neuron cell lysates. A recent study from the Kaplan group utilised polysome fractionation on axons of sympathetic neurons to demonstrate the translational status of axonal *Tyrosine hydroxylase* mRNA (Gervasi *et al.* 2016), indicating that the technique is suitable for testing the small amount of

material that can be gathered from cultured axons. Given the enrichment of *Tp53inp2* mRNA in axons, it would be interesting to investigate the translational status of these transcripts. It should be noted that the assumption that transcripts associated with monosomes are not being efficiently translated has been recently challenged in a study that found that in *S. cerevisiae,* the majority of monosomally associated genes (~75%) undergo translational elongation, rather than simply initiation or ribosomal assembly (Heyer and Moore 2016). The monosome-associated transcripts included short ORFs (<590nt, *Tp53inp2* ORF is 666nt) and lowly expressed, regulatory proteins**.** Importantly, this study excluded annotated ncRNA from their analysis, which would likely have influenced the proportion of monosomally associated transcripts undergoing elongation. LncRNA maintain many of the features of mRNA, such as promoter regions and exon-intron boundaries and, interestingly ribosome profiling reveals that a large number of well-annotated lncRNA are associated with ribosomes (Ingolia *et al.* 2011, Guttman *et al.* 2013). However, mass-spectrometry in two human cell-lines failed to identify any products from more than 90% of the ribosome associated long non-coding transcripts (Banfai *et al.* 2012), suggesting that although associated with monosomes, translational elongation is not occurring. A recent study suggests that the association of lncRNA with ribosomes was involved in the degradation of the transcript, rather than its translation, as blocking ribosomal elongation lead to the stabilisation of many of the associated lncRNAs (Carlevaro-Fita *et al.* 2016). Speculatively, the association with ribosomes may facilitate the interaction of the nonsense-mediated decay pathway, allowing targeted degradation of the lncRNA (Lykke-Andersen *et al.* 2014,

Carlevaro-Fita *et al.* 2016). Thus, it is clear that the association of a transcript with monosomal fractions does not unequivocally determine its translational status.

A single-cell, microscopy based-approach, such as TRICK (Translating RNA Imaging by Coat protein Knock-off), could also be utilised to support data obtained from axonal polysome fractionation (Halstead *et al.* 2015). This technique relies on the introduction of MS2 and PP7 stem loops into the CDS and 3'UTR respectively, which associate with different colour-labelled coat proteins. As the ribosome proceeds through the coding sequence, the coat protein associated with the MS2 loops is 'knocked-off', resulting in a colour change and a measure of translation (Halstead *et al.* 2015). This experiment would allow me to determine whether translation is occurring in cell bodies, as suggested by the potential detection of Tp53inp2 by targeted MS and polysome fractionation. In summary, while I cannot completely exclude the possibility that *Tp53inp2* mRNA is translated at extremely low levels, three distinct and highly sensitive experimental approaches - western blotting, polysomal fractionation, and mass-spectrometry - failed to significantly identify the protein in sympathetic neuron axons. Importantly, expression of the *ATGnull Tp53inp2* mRNA is sufficient for axon growth at a stage when the protein is undetectable (**Fig.2.23**), suggesting that translation is not necessary for its function.

The 3'UTR of *Tp53inp2* represses translation

In mammalian cells, 3'UTR length impacts on transcripts' translational efficiency. Studies utilising reporter constructs have demonstrated that for genes expressing 3'UTRs of different length, the transcripts with longer 3'UTR were always more translationally repressed than the ones expressing a shorter 3'UTR (Sandberg *et al.* 2008, Mayr and Bartel 2009). Moreover, recent genome-wide studies that combined RNAseq and polysomal profiling in mammalian cell lines also reported a correlation between 3'UTR length and translational efficiency (Spies *et al.* 2013, Floor and Doudna 2016). Consistent with these findings, I observed that the length of the 3'UTR of *Tp53inp2* had a large impact on translation (**Fig.2.15, 2.16, 2.22**). I found that the full-length 3121bp 3'UTR completely abolished the translation of a reporter gene. The high abundance of *Tp53inp2* transcripts containing the long 3'UTR in sympathetic neuron axons (**Fig.2.13)**, may explain why I was unable to detect the endogenous protein.

3'UTR length varies extensively between cell types; highly differentiated cells, such as neurons, tend to globally express longer 3'UTRs while highly proliferative cells express shorter 3'UTRs (Sandberg *et al.* 2008, Mayr and Bartel 2009, Miura *et al.* 2013, Gruber *et al.* 2014). Therefore, the use of proximal polyA sites can avoid regulation from elements located in the distal parts of the 3'UTR. Tissue specific expression of proteins can be achieved through alternative utilisation of 3'UTR isoforms. This regulatory mechanism is exemplified by *Pax3*, which is a key regulator of myogenesis that expresses three 3'UTR isoforms (Boutet *et al.* 2012). The short isoform is expressed in embryonic muscle progenitor cells, and this ensures that the 3'UTR is not targeted by miR-206. Conversely, the satellite cells of adult muscle tissue

express the long 3'UTR isoform, which is targeted by miR-206 and maintained translationally repressed (Boutet *et al.* 2012). Similarly, the isoform of *Tp53inp2* expressing a shorter 3'UTR (1,200nt) that was identified in sympathetic neurons by RACE did not repress GFP translation (**Fig.2.15, 2.16**). The finding that a shorter 3'UTR isoform of *Tp53inp2* is permissive to translation could explain why endogenous Tp53inp2 protein has been detected in other cell types (Mauvezin *et al.* 2012, Sala *et al.* 2014), and at very low levels in the cell bodies of sympathetic neurons (**Fig.2.8**)**.** An interesting experiment would be to perform either RACE or quantitative polyA sequencing in different tissue types, particularly in those where Tp53inp2 protein has been detected, to investigate potential differences in 3'UTR isoform usage.

Tp53inp2 transcript mediates NGF-TrkA signalling

Retrograde and local TrkA signalling are initiated by the binding of NGF to TrkA, which lead to receptor dimerisation, autophosphorylation and activation of downstream signalling pathways, including PI3K, PLCγ and Ras/MAPK (Yamashita and Kuruvilla 2016). I observed that *Tp53inp2* transcript interacts with TrkA receptor and that the expression of *Tp53inp2* is required for TrkA signalling. In wildtype sympathetic neurons, NGF stimulation following a period of deprivation increases TrkA phosphorylation in axons, along with phosphorylation of its downstream effectors (**Fig.2.27**). In sympathetic neurons lacking *Tp53inp2*, NGF-dependent phosphorylation of TrkA is abolished, strongly supporting a role for *Tp53inp2* in mediating TrkA signalling. Levels of pAkt and pErk1/2 were also significantly reduced in

Tp53inp2 knockout sympathetic neurons. I observed that a non-translatable *Tp53inp2* transcript rescued the axon growth defects observed in *Tp53inp2* knockout mice (**Fig.2.23**). It will be important to investigate if this construct also rescues the axonal loss of TrkA signalling and if, in addition to local signalling, *Tp53inp2* transcript also mediates NGF-TrkA retrograde signalling. Initial attempts to investigate this using an antibody-feeding retrograde trafficking assay were inconclusive. However, on-going experiments performed in the Kuruvilla laboratory indicate that this is the case, as pTrkA immunostaining is dramatically reduced in the cell bodies of sympathetic neurons lacking *Tp53inp2*.

To my knowledge, the data from this study provides the first evidence of an mRNA transcript that interacts with a tyrosine kinase receptor (**Fig.2.24**). Cross-Linking and Immunoprecipitation (CLIP) technique may be suitable to determine whether this interaction is required for *Tp53inp2* function in regulating local TrkA signalling. In this technique a UV-induced crosslinking step is added to conventional RIP, greatly increasing the likelihood of detecting direct interactions between the protein of interest and RNA (Ule *et al.* 2003, Ule *et al.* 2005). CLIP can be combined with high-throughput sequencing to identify multiple transcripts bound to a protein (Licatalosi *et al.* 2008), and it would be suitable to determine if additional transcripts are also involved in the regulation of TrkA signalling. A recent development of the technique - individual-nucleotide resolution CLIP (iCLIP) (Konig *et al.* 2010) - has been used to validate endogenous miRNA target sites of Argonaute in *C. elegans in vivo* (Broughton and Pasquinelli 2013). Identification of the TrkA binding site(s) in *Tp53inp2* mRNA followed by mutation(s) that disrupt binding,

would allow further analysis of the role of *Tp53inp2*'s in regulating TrkA signalling.

Tp53inp2 interaction with the TrkA receptor was observed by using RIP, however TrkA immunofluorescence coupled with *Tp53inp2* mRNA FISH was unsuccessful (**Fig.2.26**). Trk RIP in sympathetic neurons showed an enrichment of *Tp53inp2*, and no enrichment of *IMPA1* mRNA, another highly abundant axonal mRNA (Andreassi *et al.* 2010). Both RIP and ImmunoFISH were performed on neurons grown in the presence of NGF. Given that TrkA phosphorylation increases in response to NGF stimulation after a period of deprivation, it would be interesting to study whether *Tp53inp2*'s interaction with TrkA increases in a similar manner.

Tp53inp2 is required for sympathetic neuron development *in vivo*

We observed that the loss of *Tp53inp2* expression *in vivo* resulted in reduced innervation density and axonal branching of the heart, a target of the SNS, (**Fig.2.20**). Encouragingly, *Tp53inp2* expression was also required to maintain axon growth in sympathetic neurons cultured *in vitro* (**Fig.2.21**). These data strongly suggest that *Tp53inp2* mRNA is directly involved in the regulation of axon growth, and that *Tp53inp2* expression is required for axons to reach their distal targets. Moreover, the ability of an exogenous, non-translatable *Tp53inp2* transcript to sustain axon growth (**Fig.2.23**) demonstrates that the transcript, and not the encoded protein, mediates this function.

Following NGF binding, NGF-TrkA complexes are internalised in endosomes via clathrin-dependent and clathrin-independent endocytosis,

along with activated components of downstream signalling pathways, such as Ras/MAPK and PI3K (Howe *et al.* 2001, Shao *et al.* 2002, Delcroix *et al.* 2003, Valdez *et al.* 2005). Following internalisation, the signalling endosomes promote a rearrangement of the actin cytoskeleton, allowing dynein-dependent retrograde trafficking to the soma (Heerssen *et al.* 2004, Harrington *et al.* 2011). The retrograde propagation of NGF stimulation is essential for survival, as it activates transcription factors including CREB and MEF2D, leading to the expression of pro-survival genes (Riccio *et al.* 1997, Riccio *et al.* 1999, Lonze *et al.* 2002, Pazyra-Murphy *et al.* 2009). We observed a loss in neuronal population in the SCG in *TH-Cre; Tp53inp2*$^{fl/fl}$ mice (**Fig.2.19)**. The developmental time point at which neuronal loss is occurring is important in determining its cause. At E16.5, there is no difference in neuron number between *TH-Cre; Tp53inp2fl*^{fl} and wildtype littermates. However, at this developmental stage, we already observed a reduction of target tissue innervation (**Fig.2.20**). Therefore, when sympathetic neuron survival depends upon target-derived NGF (Glebova and Ginty 2005), *Tp53inp2* loss results in reduced axon growth and their inability to reach the source of NGF (**Fig.2.20**). The neurotrophic hypothesis postulates that developing neurons are overproduced and compete for a limited amount of target-derived survival factor (Davies 1996). Only neurons that successfully reach their targets receive the survival signal, which is retrogradely trafficked and activates gene expression programs essential for promoting survival, differentiation and growth**.** Neurons that do not reach their targets undergo apoptosis, ensuring correct innervation. My findings suggest that the *Tp53inp2* transcript mediates TrkA signaling and facilitates axon growth, and

that the loss of neurons is a consequence of their inability to reach the source of NGF.

A novel, non-coding role for *Tp53inp2*

Since *Tp53inp2* mRNA, but not protein, is essential for axon growth the question remains as to how the transcript is regulating this process. Recent studies have highlighted the potential *trans* acting nature of many RNA species, from canonical ncRNA to dual-functional coding mRNA, suggesting that *Tp53inp2* may function as a regulator of miRNA or as a molecular scaffold.

An alternative function for RNA transcripts may be to act as a 'sponge' for miRNA. Individual miRNA regulate a broad range of targets due to the limited sequence homology required for binding, allowing coordinated gene expression (Pasquinelli 2012). However, as this also means that multiple targets can compete for the same pool of miRNAs, changing the expression levels of a transcript targeted by a miRNA could sequester the activity of the bound miRNA, affecting the expression of other transcripts within the miRNA's regulatory network (Thomson and Dinger 2016). This is known as the competing endogenous RNA (ceRNA) hypothesis and is supported by a growing body of evidence (Salmena *et al.* 2011, Refs within: Thomson and Dinger 2016). For example, the expression of the pseudogene *PTEN* tumour suppressor gene (*PTENP1*) increases the expression of *PTEN* by competing for several *PTEN*-targeting miRNAs (Poliseno *et al.* 2010). mRNA transcripts and in particular their 3'UTRs, can also operate through this mechanism (Fang *et al.* 2013, Valluy *et al.* 2015, Zheng *et al.* 2015, Gao *et al.* 2016). Ube3a is required for dendritic branching in pyramidal neurons (Miao *et al*

2013). Valluy and colleagues identified different isoforms of *Ube3a* mRNA in hippocampal neurons, including one containing a truncated coding sequence utilising a proximal PAS. Rather than protein coding, this isoform appears to act as a reservoir for miR-134, which regulates the dendritic expression of Limk1 and Pum2, two proteins that promote spine maturation (Valluy *et al.* 2015). It should be noted however, that recent studies suggested that changes of ceRNA concentrations would be insufficient to impact on miRNA levels (Denzler *et al.* 2014, Jens and Rajewsky 2015, Denzler *et al.* 2016). Indeed, in many cases the proposed ceRNAs were expressed at non-physiological levels (Poliseno *et al.* 2010, Fang *et al.* 2013, Hansen *et al.* 2013). This counter-argument considers global, cellular changes in both miRNA and mRNA levels, effectively treating the cell as well mixed. It is important to consider that in cell types with spatially restricted compartments, such as neurons, a localised ceRNA concentration could increase to levels sufficient to mediate this “sponge” effect. Bioinformatic prediction suggests that rat *Tp53inp2* mRNA contains putative binding sites for 71 miRNA (www.miRDB.org). Therefore, a possible mechanism of action for *Tp53inp2* could be to regulate the translation of axonal mRNA by altering local miRNA levels. Indeed, mRNA involved in neurotrophic signalling were recently identified as being significantly enriched in axons of sympathetic neurons (Andreassi *et al.* 2017). The binding of *Tp53inp2* to TrkA could induce a conformational change in *Tp53inp2’s* structure, altering the availability of miRNA binding sites and allowing local, acute changes in expression of factors involved in neurotrophic signalling (**Fig.3.1**). The validation and removal of miRNA binding sites within *Tp53inp2* by gene editing to introduce

precise mutations of these sites in their genomic context will reveal whether *Tp53inp2* is acting in this manner.

A separate, but not mutually exclusive, mechanism of action for *Tp53inp2* entails that it acts as a scaffold for the recruitment of proteins. Canonical ncRNA are known to function in this manner. *TERC*, for example, assists in the recruitment of telomerase reverse transcriptase to telomere ends, and *Xist* helps guide the PRC2 complex during X-chromosome inactivation (Zhao *et al.* 2008, Wang and Chang 2011, Engreitz *et al.* 2016). Recent evidence suggests that this mechanism is not restricted to ncRNA, as mRNA transcripts can act as scaffolds to facilitate the regulation of gene expression. In the *Xenopus* oocyte, *Veg-T* mRNA encodes a T-box transcription factor responsible for correct formation of the oocyte endoderm (Zhang and King 1996, Xanthos *et al.* 2001). In addition to its coding function, the mRNA also functions as a scaffold for a subset of mRNAs that are anchored to the vegetal cortex (Heasman *et al.* 2001). In mammalian cells, the *CD47* gene generates alternative isoforms and encodes for a membrane protein that protects cells from autoimmune phagocytosis (Oldenborg *et al.* 2000, Lianoglou *et al.* 2013, Mayr 2016). The mRNA transcript expressing a longer 3'UTR has been shown to act as a scaffold for a protein complex containing HuR and the phosphatase 2A inhibitor SET (Berkovits and Mayr 2015). This RNP complex is transported to the cell membrane where SET is complexed with the newly translated CD47 protein. Thus, RNA scaffolds appear to allow tight spatiotemporal control of gene expression by ensuring components of a process are maintained in the vicinity of one another. It is conceivable that *Tp53inp2* mRNA may act in a similar manner to facilitate local TrkA signalling.

This hypothesis is supported by its binding to the TrkA receptor (**Fig.2.24**) and by the reduction of TrkA signalling pathways following loss of *Tp53inp2* expression. It is possible that *Tp53inp2* mRNA is transported to axons where it interacts initially with the TrkA receptor following NGF stimulation, and later on ensures that components of the TrkA signalling pathway are maintained in proximity to one another to facilitate efficient local signal transduction (**Fig.3.1**). Two recently developed techniques would provide support for this hypothesis. The RNA antisense purification-MS (RAP-MS) and the comprehensive identification of RNA binding proteins by MS (ChIRP-MS) allow the identification of proteins interacting with a transcript of interest, and have been both used to identify interactors of the lncRNA *Xist* (Chu *et al.* 2015, McHugh *et al.* 2015). *Tp53inp2* interacting with members of the TrkA signalling pathway would strongly support a role as structural RNA, facilitating efficient local signalling.

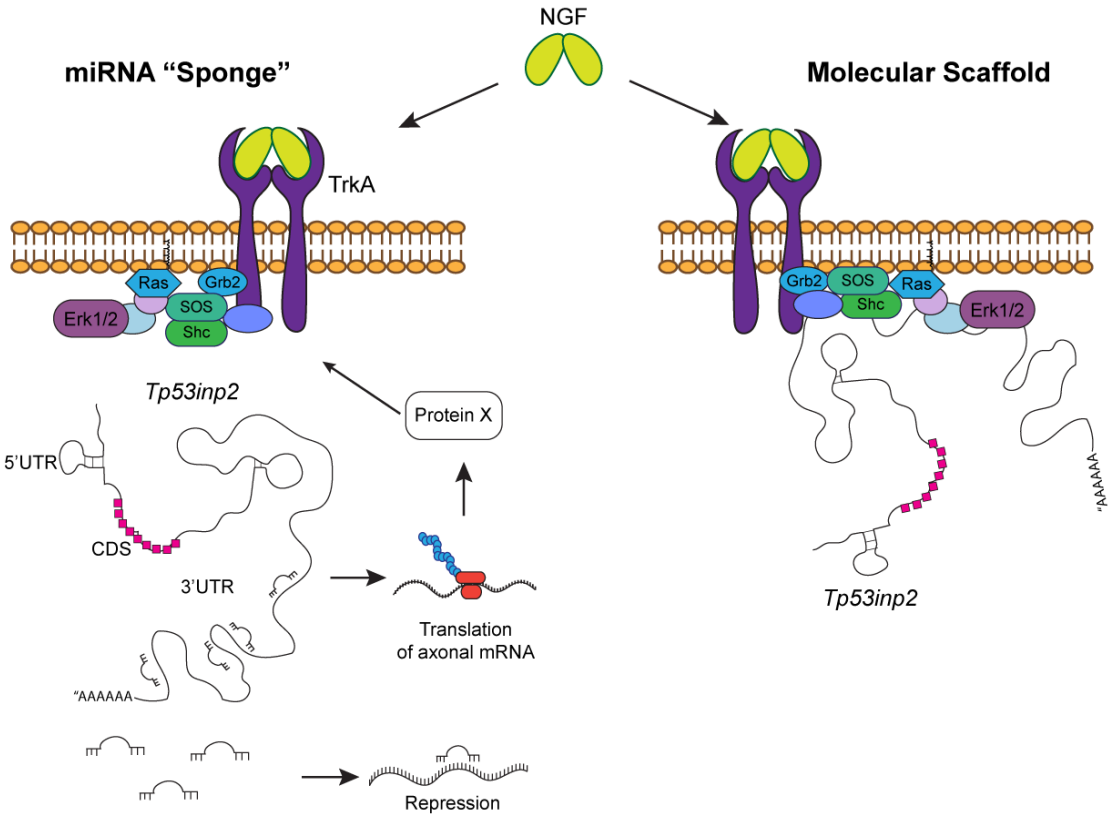

Fig.3.1 Model of *Tp53inp2's* non-coding action in regulating axon growth *Tp53inp2* is translationally repressed and transported to axons where it interacts with TrkA receptor in response to NGF binding. This allows local translation of mRNA involved in neurotrophin signalling through miRNA sequestering (**Left**) and/or efficient activation of downstream effectors of TrkA signalling by acting as molecular scaffold (**Right**). Figure provided by Emily Scott-Solomon (Kuruvilla Laboratory).

It will be important to determine which region of *Tp53inp2* mRNA is responsible for mediating its function in neuronal development. Several studies have shown that the 3'UTRs of protein coding genes may act in *trans* to regulate gene expression. In *D. melanogaster* for example, the embryonic loss of *Oskar* mRNA results in an early arrest of oogenesis. The arrest can be rescued through expression of the 3'UTR alone (Jenny *et al.* 2006). Rescue experiment using vectors that express only the full-length 3'UTR of *Tp53inp2* without the ORF would address whether *Tp53inp2* 3'UTR is sufficient to mediate its function in neuronal development. Moreover, a construct encoding

Tp53inp2 ORF and shorter 3'UTR that is unable to rescue the axon growth defects would provide evidence that two functionally distinct pools of *Tp53inp2* are expressed in sympathetic neurons. It is conceivable that a shorter 3'UTR isoform is translated in the cell bodies and may mediate autophagy (Mauvezin *et al.* 2010, Sala *et al.* 2014), whereas a longer axonal 3'UTR isoform regulates TrkA signalling and utilises the 3'UTR *in trans* in a non-coding manner.

Recent studies have shown that 3'UTRs can be detected independently of their respective CDS in neurons and other cell lines (Mercer *et al.* 2011, Kocabas *et al.* 2015). Importantly, Kocabas and colleagues showed that for dopaminergic and serotonergic neurons, thousands of 3'UTR genes are expressed independently of their CDS during mouse development (Kocabas *et al.* 2015). Excitingly, *Tp53inp2* was identified as one of the genes with a high 3'UTR to CDS expression ratio of (~25:1). How this differential expression is regulated or arises is unknown, however, it does not appear to be dependent on transcription. Through analysis of human ChIP-seq data using antibodies against histone modifications and RNAPII, Mercer and colleagues found no evidence of alternative transcriptional start sites or RNAPII occupancy at the sites of the differentially expressed 3'UTRs (Mercer *et al.* 2011). Therefore, it appears that the mRNA is transcribed as an intact unit and post-transcriptionally cleaved. Though the mechanism for regulating this cleavage is currently unknown, recent work from our laboratory indicates the involvement of a large multi-protein complex containing, among others,

the endonuclease Ago2, the RNA helicase Upf1 and the RBP HuD (Andreassi *et al.* 2017).

The question remains as to what the function of the cleaved 3'UTRs in neurons is. In addition to the aforementioned functions as scaffolds and miRNA regulators, an attractive possibility is that the 3'UTRs may act to regulate large-scale transcriptional programs, perhaps in response to neurotrophin stimuli. Transcription factors are locally translated in axons in response to injury and signalling molecules (Cox *et al.* 2008, Ben-Yaakov *et al.* 2012, Baleriola *et al.* 2014), however it is unknown whether these axonally derived transcription factors differ from the ones transcribed *in loco* and are recruited to specific gene promoters. Recent studies have shown that non-coding transcripts can influence transcription, for example by acting as enhancers (Kim *et al.* 2010, Policarpi *et al.* 2017). It is possible that in response to stimuli, the cleaved 3'UTRs act to guide axonally derived transcription factors to specific genes, facilitating an effective and precise nuclear response.

Closing remarks and perspectives

I discovered that in sympathetic neurons, the transcript *Tp53inp2* is held in a translationally repressed state by its UTRs. The *Tp53inp2* transcript itself acts in *trans* to mediate NGF-TrkA signalling and this function is critical for efficient axon outgrowth. Thus, I have identified a novel role for *Tp53inp2* in the development of the sympathetic nervous system. The implications of my study are not limited to *Tp53inp2* and may extend to many other transcripts. Most work aimed at understanding how mRNA is regulated has focused on transcript localisation, stability and translation (Sandberg *et al.* 2008, Mayr and Bartel 2009, Andreassi *et al.* 2010). The work presented in this study joins a handful of other mRNAs with described roles outside of their coding capacity (Jenny *et al.* 2006, Berkovits and Mayr 2015, Valluy *et al.* 2015, Chao and Vogel 2016). Excitingly, this suggests that mRNA transcripts may have a broader role in the regulation of gene expression in *trans*. As further work combining transcriptomics with analysis of protein output is performed, the list of mRNA that are highly expressed but poorly translated and therefore may represent obvious candidates will likely grow. Therefore, my work presents an example of how, by adapting additional functions for mRNA, organisms have acquired a mechanism to increase the diversity of gene expression without requiring further expansion of the genome.

4. Materials and Methods

Reagents were purchased from Sigma Aldrich unless stated

4.1 Dissection and culture of sympathetic neurons from Superior Cervical Ganglia

All animal studies were approved, where appropriate, by the Institutional Animal Care and Use Committees at University College London, or the Johns Hopkins University Animal Care and Use Committee (ACUC) and NIH guidelines. Superior cervical ganglia (SCG) were dissected from postnatal day 0/1 (P0/1) Sprague Dawley rats or Tp53inp2$^{fl/fl}$ mice and immediately plated as explant tissue or enzymatically dissociated and cultured in compartmentalised chambers, microfluidic chambers or dishes. Enzymatic dissociation was performed at 37°C first for 20 min with 6 mg/ml Collagenase (Worthington), 1 mg/ml hyaluronidase, 0.9 mg/ml DNAseI, 10 mg/ml BSA in HBSS++ (supplemented with 12 mM glucose, 15 mM Hepes), followed by 15 min in 3 mg/ml Trypsin in HBSS++. Dissociated neurons were passed through a 40 μm cell strainer prior to plating. Nunc plastic dishes or glass coverslips were coated beforehand with either 1 μg/ml poly-D-lysine + 5 μ g/ml Laminin (BD Bioscience) or collagen purified rat-tail collagen dissolved in 0.1% acetic acid + 5 μg/ml laminin. Collagen coating was cross-linked by covering the dish with tissue soaked in 100% ammonium hydroxide. Neurons were cultured in DMEM supplemented with 10% foetal bovine serum (FBS), 2 mM glutamine, 1% penicillin/streptomycin (P/S) and 100 ng/ml NGF (in house prepared) and incubated at 37°C 10% CO_2. The antimitotic inhibitor

cytosine arabinoside (AraC) was added at 10 μM from *in vitro* day 1 to minimise growth of non-neuronal, contaminating cell types.

For compartmentalised chamber cultures, Teflon chambers were assembled on collagen-coated Nunc dishes as described previously (Campenot 1977). 80,000 dissociated sympathetic neurons were plated in the central compartment in 80 μl of media. NGF was supplied to both lateral and central compartments until axonal projections were clearly visible in lateral compartments (~4-6 days *in vitro*), at which point NGF was withdrawn from the central compartment.

For surgical separation of cell bodies and axons in explants, the cell body cluster was removed using a scalpel under microscopic dissection.

To withdraw NGF prior to restimulation, neurons were washed with DMEM before addition of high-glucose DMEM containing 0.5% FBS with 1:1000 α-NGF (Sigma N6655) and the anti-apoptopic agent BAF (50 μM; MP Biomedical) for 48 h. Restimulation was achieved by culturing in neurons with standard media + 100 ng/ml NGF for the time period indicated.

4.2 Cell culture of PC12 cells

The PC12 cell line (rat pheochromocytoma) was purchased from ATCC. Cells were grown on Nunc plastic dishes coated with 1 μg/ml poly-D-lysine for naïve cells or 1 μg/ml poly-D-lysine + 2 μg/ml laminin for differentiation. Cells were incubated at 37°C 10% CO_2 and cultured in either 10% FBS, 5% horse serum (HS), 1% glutamine in DMEM for naïve cells or 0.5% FBS, 0.25% HS, 1% glutamine and 50 ng/ml NGF for differentiation. Cells were

passaged at 90-95% confluency and not cultured past passage 20. Responsiveness to NGF was routinely tested.

4.3 Cell culture of HEK293 cells

The HEK293 cell line (human embryonic kidney) was purchased from ATCC. Cells were grown on Nunc plastic dishes, incubated at 37°C 5% CO_2 and cultured in 5% FBS, 1% P/S + 1% glutamine in DMEM. Cells were passaged at 85-90% confluency and not cultured past passage 20.

4.4 Transfection of cell cultures

All transfections were performed using Lipofectamine® 2000 (Invitrogen). Both PC12 cells and HEK293 were passaged to be at 30-40% confluency at point of transfection. DNA/Lipofectamine mix was prepared at a ratio of 1 μg DNA to 3 μl Lipofectamine in Optimem (Thermo) and incubated at room temperature for 20 min. *Tp53inp2* siRNA (Dharmacon) or Allstars negative control siRNA (Qiagen) was added at final concentration of 75 nM. The cell culture media was replaced with Optimem and cells were cultured with transfection mix for 4 h at standard culture conditions before replacing with standard growth media. Cells were typically harvested 48 h post transfection.

4.5 Western Blotting

Plates were washed with PBS and then lysed in 1x NuPAGE LDS buffer + 10% β-mercaptoethanol, homogenised by passing through a 25 G needle 10 times and boiled at 95°C for 5 min to denature proteins before loading. Samples were separated on a 12% polyacrylamide gel with PageRuler™

diluted in 1x LDS buffer as size marker, and transferred onto polyvinylidene difluoride membrane for 90 min 330 mA constant. Membranes were blocked for 1 h RT in 5% milk in tris buffered saline - Tween (TBS-T) (50mM tris-HCl pH7.4, 150 mM NaCl, 0.1%Tween-20) before overnight (O/N) incubation at 4°C in primary antibody diluted in 5% milk TBS-T (see **Table 4.1** for antibodies). Following extensive washing in TBS-T, membranes were incubated 2 h RT with secondary antibody diluted in 5% milk TBS-T, followed by further washing. Signal was detected using ECL or ECL Prime (GE Healthcare Life Science) and exposing membrane to Amersham Hyperfilm (GE Healthcare Life Science).

Antibody Name	**Supplier/Catalogue N°**
Flag	Sigma F7425
Flag M2	Sigma F3165
GFP	Abcam ab6556
HuD	Santa cruz sc-28299
mCherry	Abcam Ab125096
Myc	Upstate 05-724
Myc 9E10	Abcam Ab32
p-Erk1/1	Cell Signalling 9106
p85	Upstate Biotech 06-195
pAkt	Cell Signalling 9271
Rabbit IgG	Santa cruz sc-2027
TH	Millipore AB152
Tp53inp2	Santa cruz sc85972
Tp53inp2 (DOR)	Zorzano Lab
Tp53inp2 (Ig26)	Riccio Lab
Tp53inp2 (N26)	Riccio Lab
Trk	Santa cruz sc-7268
TrkA	Millipore 06-574
Tubulin	Sigma T9026
β-III-tubulin	Sigma

Table 4.1 List of antibodies used in this study

4.6 RNA isolation and reverse transcription

Cells were washed with PBS and lysed using 1 ml of Trizol reagent (Ambion). The lysate was centrifuged 12,000x*g*, 10 min, 4°C to remove debris and the supernatant vigorously mixed with 200 μl chloroform and incubated at 30°C for 5 min. Samples were centrifuged 12,000x*g* 15 min 4°C, the aqueous phase collected (~500 μl) and transferred to a fresh tube. An equal volume of 100% isopropanol was added followed by 10 min incubation at RT to precipitate nucleic acid. Samples were centrifuged 12,000x*g* 10 min 4°C, the supernatant was removed and pellet washed with ice cold 70% EtOH and centrifuged again. The supernatant was carefully removed and the pellet air-dried at RT before resuspension in RNAse free water. The concentration of nucleic acid and presence of impurities within the samples was measured by nanodrop. To remove contaminating genomic and plasmid DNA, total RNA was subjected to DNAse digestion using Turbo™ DNAse (ThermoFisher). Samples were incubated with 3 U of DNAse in 17 μl reaction for 30 min at 37°C. DNAse was subsequently inactivated with 3 μl inactivating reagent for 5 min at 25°C followed by 1,000x*g* 1.5 min RT centrifugation to pellet DNAse bound to the agent. The supernatant was collected and transferred to a new tube. PCR was performed to amplify Actin gDNA or plasmid DNA prior to reverse transcription to confirm DNAse digestion.

500 ng to 1 μg of total RNA was reverse transcribed using SuperScript™ III reverse transcriptase (Invitrogen). The RNA was first incubated at 65°C with 3.75 ng/μl pdN6 random hexamers and 0.5 mM dNTPs, then placed on ice for 2 min. 5 mM DTT, 50 U SuperScript III transcriptase and 40 U

RNaseOUT™ ribonuclease inhibitor (Invitrogen) were added and incubated at 25°C for 5 min, 50°C for 1 h and 70°C for 15 min. Following cDNA synthesis, 2.5 U RNAseH (NEB) was added to the sample and incubated at 37°C 20 min to remove template RNA from cDNA.

4.7 Quantitative RT-PCR

RT-qPCR reaction mixes were prepared to 20 μl volume using SYBR green or SYBR Select master mix and 0.5 μM forward and reverse primers. The reaction was performed in the Mastercycler® ep realplex qPCR machine (Eppendorf). All reactions were performed in triplicate and included a standard curve and no template control. Standard curves were generated through 7 serial 1:10 dilutions of a known concentration of the DNA amplicon for each primer set. PCR conditions as follows: 7 min at 95°C for denaturation and enzyme activation followed by 40 cycles of 10s at 95°C for denaturation then 30s at 60°C for primer annealing, extension and data acquisition. Following 40 cycles a dissociation curve was performed, measuring SYBR fluorescence at 1°C interval between 60°C and 100°C, to assess melting temperature of amplicons. All primer sequences are listed in **Table 4.2**

Primer Name	Sequence
Tp53cds-F	CCT CAT TGA GCA TCC CAG CA
Tp53cds-R	CAG CTC CAT CGC TGA GG
BAct-F	ATG GAT GAC GAT ATC GCT GCG
BAct-R	GGT GAC AAT GCC GTG TTC AAT
IVT-F	GTG TTA ACT TCC GAC TCC TCG C
IVT-R	GTG ATG TCA AAC GAC GCA GC
Terc-F	GCG CAT TCT GGA ACC TCA AA
Terc-R	GTT CCG TTA CTG TCC TTG CG
GFP-F	CGA CAA CCA CTA CCT GA
GFP-R	ATC ATC CTG CTC CTC CAC CT
mCherryF	GAG GGC ACC CAG ACC GCC AA
mCherryR	ACG CCG CCG TCC TCG AAG TT
msTp53-F	ATG TTC CAG CGC TTC ACC AGC
msTp53-R	CTG ATC AGG CAA GGC AGC TTC A
msGAPDH-F	CCT GCA CCA CCA ACT GCT TA
msGAPDH-R	CCA CGA TGC CAA AGT TGT CA
18S-F	CGC CGC TAG AGG TGA AAT TC
18S-R	TTG GCA AAT GCT TTC GCT C
TpUTR-F	AAC CTT GTT GCT GTC CCA AG
TpUTR-R	GAG CCA AAT GCC CTA TCA AA
Impa1-F	AAG GTC TTG GGC CTC TCA AA
Impa1-R	TTG CAC GGT CCA AAT CAG AG
Tp53Loxp3-F	GAT CAG GAC CTC AGC GAT GG
Tp53Loxp3-R	GCA CCT GGC ACA GGT AAC TA

Table 4.2 Sequences for primers used for RT-qPCR and genotyping analysis

4.8 Mass Spectrometry

PC12 cells transfected with a plasmid expressing Myc-Tp53inp2 were washed with cold PBS and lysed in cold RIPA buffer (50 mM tris-HCl pH 7.4, 150 mM NaCl, 0.5% sodium deoxycholate, 1% NP40, 1:100 protease inhibitor cocktail) manually sheared with a 25G needle and protein content quantified by BCA assay according to manufacturers instructions (Thermo Fisher). 2 μg Myc 9E10 antibody (Abcam) was conjugated to protein G-sepharose beads (GE Healthcare Life Science) O/N rotating at 4°C. The antibody was then cross-linked to the beads with 2x 30 min RT rotation with

6.5 mg/ml dimethyl pimelimidate (DMP) (Thermo Fisher) in 0.2 M pH8.2 triethanolamine-HCl, followed by 30 min RT blocking in 100 mM pH 8.2 ethanolamine-HCl. Beads washed extensively with PBS to remove unbound antibody. Following washing of beads, 300 μg of PC12 lysate was added and incubated O/N 4°C. Beads were washed 3 times for 10 min at RT in wash buffer (10 mM tris-HCl pH7.4, 150 mM NaCl, 1 mM EDTA pH8, 1 mM EGTA pH8, 0.1% TritonX-100) followed by final PBS wash. Samples were then subjected to on-bead digestion using 200 ng sequencing grade trypsin in 300 μl of 100 mM tris pH8 for 15 min at 37°C. Beads were pelleted by centrifugation and supernatant collected. The immunoprecipitated sample was submitted for mass-spectrometry analysis at the University of Catanzaro by Dr. Marco Gaspari as follows. Lyophilised samples were reconstituted in HPLC-grade water and reduced with 10 mM DTT 1 h at 37° C, followed by cysteine alkylation (25 mM iodoacetamide, 1 h at 37 ° C in the dark); excess iodoacetamide was quenched by 1 μl of 100 mM DTT. Full tryptic digestion was achieved by an additional overnight incubation in presence of 200 ng of trypsin proteomics grade. Peptides were purified by strong cation exchange (SCX) extraction tips, and eluted in 7 μL of 500 mM ammonium acetate containing 20% acetonitrile v/v. A 10% aliquot of the IP digest was injected for nanoLC-MS/MS analysis in data-dependent mode.

SCG explants were cultured under NGF stimulation for 7 days and axons surgically dissected. Axon and cell body samples from 50 explants were lysed in cold RIPA buffer, quantified by BCA and 150 μg of total protein for each sample was analysed by mass-spectrometry by Dr. Marco Gaspari as

follows. Proteins were precipitated by adding four volumes of cold acetone, and by incubating the solution at -20°C for one hour. After a centrifugation step carried out at 12,000x*g* for 20 min 4°C, the supernatant was discarded, and the pellet was resuspended in buffer containing 8 M urea, 100 mM tris-HCl pH 8.5 and 0.2% w/v SDS. Protein reduction and alkylation was performed as described above. The protein solution was brought to a final volume of 400 μL by adding HPLC-grade water to reduce urea and SDS concentrations. Finally, 2 μg of trypsin proteomics grade was added to each sample and incubated O/N at 37 $^{\circ}$ C with agitation. The digests were diluted 8-fold in 80% acetonitrile/0.5% formic acid before being loaded onto SCX extraction tips. For targeted analysis, 30 μL of the initial digest solutions were loaded on SCX extraction tips and then eluted in 7 μL of 500 mM ammonium acetate containing 20% acetonitrile (v/v); the eluate was evaporated to dryness and reconstituted in 20 μL of mobile phase A (0.1% formic acid, 2% acetonitrile); a 3 μL aliquot was then injected for nanoscale liquid chromatography coupled to tandem mass spectrometry (nanoLC-MS/MS) analysis.

Peptides were loaded directly on-column at 500 nL/min, and separated at 300 nL/min via a 60-min gradient ramped from 5% to 35% mobile phase B (80% acetonitrile, 0,1% formic acid); mobile phase A was 2% acetonitrile, 0.1% formic acid. The analytical column, a pulled 75 μm i.d capillary in-house packed to a length of 12 cm, was connected to a liquid chromatography system (EasyLC 1000, Thermo Fisher Scientific) and directly interfaced to a quadrupole-orbitrap mass spectrometer Q-Exactive

(Thermo Fisher Scientific) via a nanoelectrospray interface operating in positive ion mode. Data-dependent acquisition was performed using a top-12 method. Full scan parameters were: resolution 70,000, m/z range 350-1800. Tandem mass spectrometry parameters were: resolution 17,500, isolation window 1.6 m/z, maximum injection time 60 ms, AGC target 100,000, normalized collision energy 25, dynamic exclusion 30 s. Data were processed using Proteome Discoverer 1.3 (Thermo Fisher Scientific). Tandem mass spectrometry data were searched against the Rattus norvegicus Uniprot database (downloaded on 03/2015) merged with a list of common contaminating proteins (albumin, trypsin, human keratins). Sequest search parameters were: MS tolerance 20 ppm; MS/MS tolerance 0.02 Da; oxidised methionine (variable); carbamidomethyl cysteine (static); enzyme trypsin; maximum missed cleavages 2. Search results were filtered by Percolator, integrated in Proteome Discoverer, using default parameters. Protein hits based on two high-confidence peptide identifications (q-value<0.01) were considered valid.

For targeted mode of analysis, the Orbitrap analyser was operated in targeted MS/MS mode: a single full MS scan (17,500 resolution, 500,000 target ions) was followed by three targeted MS/MS events on precursors at 420.2 (ALHHAAAPMoxPAR, z=3), 507.6 (HQGSFIYQPCQR, z=3), 414.9 (ALHHAAAPMPAR, z=3) m/z. MS/MS conditions were, in all cases, the following: MS resolution 70,000, maximum injection time 250 ms, isolation window 2.0 m/z, AGC target 200,000, normalized collision energy 25.

4.9 Polysomal Fractionation and Denaturing Agarose Gel Electrophoresis

Rat sympathetic neurons were cultured for 7 days under NGF stimulation, then 0.1 mg/ml cyclohexamide was added directly to growth media for 3 min at 37°C to immobilise ribosomal progression on RNA. The cells were washed 2x on ice with ice-cold PBS + 0.1 mg/ml cyclohexamide followed by lysis in Lysis buffer (10 mM tris-HCl pH8, 150 mM NaCl, 5 mM $MgCl_2$, 1% NP40, 10 mM vanadyl ribonucleoside complex, 1% sodium deoxycholate, 40 mM DTT, 500 U RNAseOUT (Thermo Fisher Scientific)). Nuclei were removed by brief centrifugation and lysis buffer supplemented with extraction buffer (0.1 M tris-HCl pH7.5, 150 mM NaCl, 75 μg/ml cyclohexamide, 1:100 protease inhibitor cocktail) followed by further centrifugation to remove insoluble material. 15%-40% sucrose gradients were prepared in gradient buffer (10 mM tris-HCl pH7.5, 140 mM NaCl, 1.5 mM $MgCl_2$, 10 mM DTT, 0.1 mg/ml cyclohexamide). Lysates were loaded on top of the gradient and subjected to ultracentrifugation in Beckman SW41Ti rotor for 2 h at 4°C 25,000x*g*. 19 fractions were collected and subjected to proteinase digestion (100 μg proteinase K, 0.1% SDS, 10 mM EDTA) for 20 min at 37°C. To normalise for potential RNA loss during extraction, 2.5 ng of *in vitro* transcribed RNA was spiked into each fraction prior to phenol: chloroform extraction. 25% of sample was precipitated and resuspended in H_2O for RT-qPCR, and the remainder was precipitated for denaturing agarose gel electrophoresis to assess quality of fractionation.

The RNA pellet was resuspended in 20 μl gel loading buffer (50% formamide, 16.2% formaldehyde, 1X MOPS) followed by denaturing at 70°C

for 5 min. Denatured samples were run in denaturing conditions on 1% agarose MOPS gel (16.2% formaldehyde, 1X MOPS) in 1X MOPS buffer. Prior to imaging, the agarose gel was stained with SYBRGold (ThermoFisher) and imaged with a GeneFlash Imaging Gel system (Syngene).

4.10 Cloning

Rat Tp53inp2 coding sequence (CDS) was amplified from SCG neuron cDNA and ligated into pCMV-Myc to generate Myc-Tp53inp2CDS plasmid. Tp53inp2CDS-Flag was amplified from Myc-Tp53inp2CDS plasmid, using primers that encode 2xFlag tag at the C-terminus. Tp53inp2 3'UTR 1.2, 2.2 and 3.1Kb and 5'UTR were amplified from RACE clones and used to replace the IMPA UTRs in myrdEGFP-IMPA1-L (Andreassi *et al.* 2010). Mutation of the ATG codons to generate ATGNullCDS was done using the QuikChange Site-Directed Mutagenesis kit (Agilent) according to manufacturers instructions. The ATGNullTp53inp2 CDS was PCR amplified and used to replace the myrdEGFP sequence in the 3.1Kb myrdEGFP-Tp53inp2 UTR vector to create ATGNull Tp53inp2. Rat Tp53inp2 5'UTR+CDS was amplified from SCG neuron cDNA to include endogenous Kozack sequence, and cloned in place of the ATGNull CDS to generate Wildtype Tp53inp2 vector. Adenoviral vectors were generated using the AdEasy Adenoviral Vector system (Agilent) according to manufacturers instructions.

4.11 Whole mount *In situ* hybridisation

In situ hybridisation was performed using a digoxigenin-labelled probe spanning a 450-bp region within exons 1-2 of mouse *Tp53inp2*. Mice at

various developmental ages were flash frozen in OCT and serially sectioned (12 μ m) using a cryostat. A section of SCG from mice of each developmental age was placed on every slide. Sections were post-fixed in 4% paraformaldehyde (PFA), washed in PBS and acetylated with 0.25% acetic anhydride in 0.1 M triethanolamine with 0.9% NaCl. After hybridisation with the digoxigenin-labelled RNA probe (2 μ g per ml) at 68 °C O/N, sections were washed with 0.2 $\times$ SSC buffer at 65 °C, blocked with TBS containing 1% normal goat serum and then incubated with alkaline phosphatase-labeled anti-DIG antibody (1:5,000; Roche) O/N at 4 °C. The alkaline phosphatase reaction was visualised with NBT/BCIP, slides were then rinsed in PBS, fixed in 4% PFA and mounted in AquaMount (EMD Chemicals).

4.12 Generation of conditional *Tp53inp2* mutant mice

ES cells containing the *Tp53inp2*$^{tm1a(KOMP)Mbp}$ targeting vector were obtained from the trans-NIH Knock-Out Mouse Project (KOMP) Repository (www.komp.org) and used by transgenic core facility at Johns Hopkins University to generate chimeric mice carrying the *Tp53inp2*^{tm1a} allele. *Tp53inp2*^{tm1a} chimeric male mice were mated to wild type albino mice (Jackson Laboratory Stock No: 000058). *Tp53inp2*^{tm1a} mice carry a knockout-first allele, in which a promoterless cassette including LacZ and neo genes were inserted in intron 1 of the *Tp53inp2* gene. For the sympathetic neuron-specific conditional knockout mice, *Tp53inp2*^{tm1a} mice were crossed with a ubiquitously expressing Flippase line 129S4/SvJaeSor-*Gt(ROSA)26Sortm1(FLP1)Dym/J* (Jackson Lab) to excise the LacZ/neo cassette. These mice were then crossed with *Th-Cre* transgenic mice (kindly

gifted by Dr. C. Gerfen, NIH Bethesda USA) to generate mice lacking *Tp53inp2* in sympathetic neurons. The offspring of these mice were then backcrossed for 2-3 generations to *C57/BL6* mice to obtain offspring of several genotypes including *Th-Cre;Tp53inp2*$^{fl/fl}$ mice and control *Tp53inp2*$^{fl/fl}$ littermates. Primers Tp53Loxp3F and Tp53Loxp3R (**Table 4.2**) which span the third *loxP* site, were used to genotype the *Tp53inp2* allele by PCR.

4.13 SCG neuronal counts

The SCG of Tp53inp2$^{fl/fl}$ or TH-Cre Tp53inp2$^{fl/fl}$ E16.5, P0.5 and P21 mice were surgically dissected and fixed in 4% PFA (PBS) for 4 h at 4°C (E16.5, P0.5), or O/N (P21) respectively. The heads were then cryoprotected O/N (for E16.5 and P0.5) or 2 days (P21) in 30% sucrose-PBS, frozen in OCT and then serially sectioned (12 μm) using a cryostat. The sections were stained with a solution containing 0.5% cresyl violet (Nissl). Cells with characteristic neuronal morphology and visible nucleoli were counted in every fifth Nissl-stained section.

4.14 Whole-mount diaminobenzidine-tyrosine hydroxylase immunohistochemistry

4% PFA-fixed E16.5 embryonic organs were dehydrated by methanol series (50-80%) and incubated O/N in 20% dimethylsulfoxide (DMSO)/80% methanol solution containing 3% H_2O_2 to quench endogenous peroxidase activity. Tissues were then re-hydrated, blocked O/N in blocking solution (4% BSA/1% Triton X-100 in PBS) and then incubated with α-TH (Millipore) 1:200 in blocking solution for 72 h at 4°C. Detection was performed with

horseradish peroxidase-conjugated α-rabbit IgG (GE Healthcare) at 1:200 in blocking solution and incubated O/N at 4 °C. Visualisation was accomplished with diaminobenzidine. Tissues were re-fixed in 4% PFA (PBS), dehydrated by methanol series and cleared with a 2:1 mixture of benzyl benzoate/benzyl alcohol to allow visualisation of staining inside the tissue followed by clearing.

4.15 Adenovirus stock generation

Adenoviral vectors were transfected into HEK293 cells to prepare a stock of primary AV. Due to their large size (>35 Kb), the recombinant adenoviral plasmids were linearised with *PacI* prior to transfection to increase insertion efficiency. HEK293 cells were plated at 70% confluency in 6 cm Nunc treated culture dish and transfected using 15 μl Lipofectamine 2000 and 3 μg linearised plasmid DNA. Transfected cells were monitored daily for detachment, indicative of viral infection, with media gently changed every 72 h. Upon detachment (~10 days post transfection), cells were harvested in 2 ml PBS and ruptured using four rounds of freeze-thaw: placed in methanol/dry-ice bath until frozen before rapidly transferring to 37°C water bath until defrosted. Cell debris was removed by centrifugation, 12,000x*g* 10 min 4°C, and the supernatant containing the mature adenovirus collected. 1 ml of supernatant was transferred to a fresh 10 cm plate of 80-90% confluent HEK293 cells to further amplify the virus, and this process was repeated twice. To generate high-titer final viral stocks, five x 25 cm plates containing HEK293 cells at 80-90% confluency were infected with 200 μl each of the passaged, mature virus and monitored for detachment (~1-2 days). Cells were combined and centrifuged 5 min 500x*g* RT. The pellet was

resuspended in 2 ml of 0.1 M tris-HCl pH8 and subjected to freeze-thaw as above. The supernatant was laid on top of a two-step CsCl gradient (1.25 g/ml + 1.4 g/ml) and ultracentrifuged 120,000x*g* 1 hr 15°C. The bottom of the centrifuge tube was punctured and the lower, mature virus band was collected, which was subsequently equilibrated through further centrifugation on a 1.35 g/ml CsCl column at 120,000x*g* 15 h 15°C. The lower band was collected as before treated with two rounds of dialysis in 6 L of TD buffer (137 mM NaCl, 6 mM KCl, 0.7 mM Na_2HPO_4, 1 mM $MgCl_2$, 25 mM tris-HCl pH7.5). The high-titre, pure virus stocks were stored at -80°C in freezing solution (2mM tris-HCl pH8.0, 0.02% BSA, 10% glycerol, 0.02 mM $MgCl_2$).

4.16 Axonal outgrowth assay

Compartmentalised chamber cultures were prepared using sympathetic neurons isolated from P0.5 Tp53inp2$^{fl/fl}$ mice SCGs. Following 7-10 days *in vitro*, dependent on the detection of axons in the side chambers, cell bodies within the central compartment were infected with a high-titer adenovirus expressing either Cre to abolish *Tp53inp2* expression, or expressing LacZ or GFP as controls. Neurons were either totally deprived of NGF or NGF (100 ng/ml) was added only to distal axons. 50 μM BAF was also added to the cell body compartment to allow assessment of axon growth without the complications of cell death. For the rescue experiment, Cre-infected neurons were also infected with adenovirus expressing full-length Tp53inp2 or full-length ATGNull Tp53inp2. After 48 h, axon growth was measured by capturing phase contrast images of the distal axons over consecutive 24 h intervals for 3 days, using a Zeiss Axiovert 200 microscope with a Retiga EXi

camera. The rate of axonal growth (μ m/day) was quantified using Openlab 4.04. Measurements from 30–50 neurons were averaged for each condition for a single experiment. For representative images, neurons were immunostained with β -III-tubulin 48 h after beginning measurement of growth (1:200; Sigma-Aldrich).

4.17 RNA Immunoprecipitation

4 μ g rabbit α -Trk antibody (Santa cruz), rabbit α -HuD antibody (Santa cruz) or Rabbit IgG antibody (Santa cruz) were incubated with 30 μ l PBS prewashed protein A/G agarose beads (Santa Cruz) and 1 mg/ml heparin in 1%BSA for 2 h 4°C, then washed 3 times 10 min at 4°C with wash buffer (50 mM tris-HCl pH8, 150 mM NaCl, 1% Triton X-100). ~2.5 million rat sympathetic neurons were cultured 7 days *in vitro*, washed with PBS and then lysed in 1 ml of Buffer A (50 mM tris pH8, 150 mM NaCl, 1% Triton X-100, 1:100 protease inhibitor cocktail, 500 U/ml RNAseOUT) for 10 min at 4°C. Insoluble material was removed by centrifugation at 1,000x*g* 10 min 4°C, the supernatant was collected then centrifuged again 10,000x*g* 10 min 4°C. 300 μ l of lysate was made up to 500 μ l volume with Buffer A plus 0.2 mg/ml heparin and then incubated with the antibody conjugated beads for 1 h 4°C rotating mix. Beads were collected by centrifugation 1,500x*g* 3 min 4°C then washed 3 times for 10 min 4°C with 1 ml wash buffer. In the final wash, the Eppendorf tube was replaced with a fresh tube to reduce aspecific RNA binding. RNA was eluted from beads in 150 μ l extraction buffer (0.2 M NaAcetate, 1 mM EDTA, 0.2% SDS) for 5 min at 70°C, followed by centrifugation 17,000x*g* 1 min RT. RNA was purified from the

immunocomplexes and the remaining 100 µl of lysate as total input using PureLink® RNA Micro Scale Kit (ThermoFisher) according to manufacturers instructions. The RNA was treated to DNAse digestion and RT-qPCR as described.

4.18 smFISH and Immunofluorescence

Cy5 labelled *Tp53inp2* and Cy3 labelled *Impa1* probe sets (Stellaris probes, Biosearch technologies) were generated using the Stellaris probe-set designer, targeting the *R. norvegicus* ORF and 3'UTR of both genes. Probes were reconstituted at 12.5 µM in TE buffer (10 mM tris-HCl pH8, 1 mM EDTA pH8).

For siRNA-mediated knockdown of *Tp53inp2* in neurons, the Cellaxess CX1 system (Cellectricon) was used (Andreassi *et al.* 2010). Sympathetic neurons were maintained *in vitro* for 6 days and then electroporated with 5 µM *Tp53inp2* siRNA (Dharmacon) or Allstars negative control siRNA (Qiagen) and 20 ng/µl GFP expression vector.

SCG neurons were cultured 3-7 days *in vitro* on glass coverslips, washed with RT PBS and fixed using 3.7% PFA at RT for 10 min. Cells were permeabilised with 70% EtOH at 4°C for 3 h and then pre-hybridised in 2x SSC 10% formamide for 5 min at RT. 1 µl of 12.5 µl probe stock was added to 100 µl Hybridisation buffer (10% Dextran Sulfate, 2x SSC, 10% formamide, 200 mM vanadyl ribonucleoside) and coverslips incubated O/N at 37°C in humidified chamber. Coverslips were then washed 2x in warm 2x SSC 10% formamide at 37°C 30 min in the dark. For smFISH+IMF, coverslips were then prehybridised in 1% BSA 2x SSC for 30 min RT before

O/N incubation with α-TrkA (Millipore) 1:400 or α-GFP (Abcam) 1:400 in 1% BSA 2x SSC at 4°C. Coverslips were then washed 3x5 min RT in 2x SSC before incubation with 1:1000 α-Rabbit conjugated to Alexafluor488 in 2x SSC 45 min 37°C, followed by 3x5 min RT in 2x SSC washes. Coverslips were then mounted to slides with homemade mounting solution (0.4% glucose, 10 mM tris-HCl pH8, 2x SSC, 3.7 μg/ml glucose oxidase, 3 U catalase). Samples were imaged using an Ultraview Vox spinning disc microscope within 24 h of staining and images analysed using the JACoP colocalisation plugin for ImageJ.

4.19 Immunodetection of p-Trk, p-Akt and p-Erk

SCGs were isolated from P0.5 Tp53inp2$^{fl/fl}$ mice and plated on as explant cultures. After 7 days *in vitro*, neurons were infected with adenovirus expressing Cre or Lac-Z as a control. At the same time, neurons were deprived of NGF and 50 μM BAF supplied to prevent apoptosis. Following a 48 h infection to ensure efficient knockout of *Tp53inp2* expression, cell bodies were surgically removed and the axons treated with either 50ng/mL NGF or 1:1000 anti-NGF for 30 min. The axons from 3-7 explants per condition were lysed in RIPA buffer (50 mM tris-HCl pH8, 150 mM NaCl, 1 mM EDTA, 1% NP-40, 0.25% sodium deoxycholate, 1:100 protease inhibitor) with phosphatase inhibitor cocktail (2.5 mM sodium pyrophosphate, 50 mM sodium fluoride, 1 mM sodium orthovanadate). Lysate was then either directly immunoblotted or immunoprecipitated to detect phosphorylated TrkA. The axonal lysate was incubated with 4 μl α-p-Tyrosine (Sigma P4110) and 20 μl Protein G-Plus beads (Santa Cruz) for 2.5 h at 4°C. The beads were

spun down 1,500x*g* 3 min 4°C and washed 3 times with 1 ml RIPA buffer containing phosphatase inhibitors and protease inhibitors. Protein was eluted from beads by boiling at 95°C for 5 min in 50 μl loading buffer (100 mM tris-HCl pH6.8, 4% SDS, 0.2% bromophenol blue, 20% glycerol, 200 mM β-mercaptoethanol) and separated on a 12% polyacrylamide gel for western blotting as described above.

5. References

Aakalu, G., W. B. Smith, N. Nguyen, C. Jiang and E. M. Schuman (2001). "Dynamic visualization of local protein synthesis in hippocampal neurons." Neuron **30**(2): 489-502.

Ainger, K., D. Avossa, A. S. Diana, C. Barry, E. Barbarese and J. H. Carson (1997). "Transport and Localization Elements in Myelin Basic Protein mRNA." The Journal of Cell Biology **138**(5): 1077-1087.

Alvarez, J., A. Giuditta and E. Koenig (2000) “Protein synthesis in axons and terminals: significance for maintenance, plasticity and regulation of phenotype: With a critique of slow transport theory.” Progress in Neurobiology **63**(1):1-62

An, J. J., K. Gharami, G. Y. Liao, N. H. Woo, A. G. Lau, F. Vanevski, E. R. Torre, K. R. Jones, Y. Feng, B. Lu and B. Xu (2008). "Distinct role of long 3' UTR BDNF mRNA in spine morphology and synaptic plasticity in hippocampal neurons." Cell **134**(1): 175-187.

Anderson, P. and N. Kedersha (2006). "RNA granules." The Journal of Cell Biology **172**(6): 803-808.

Anderson, P. and N. Kedersha (2008). "Stress granules: the Tao of RNA triage." Trends in Biochemical Sciences **33**(3): 141-150.

Andreassi, C., R. Luisier, H. Crerar, S. Franke, N. M. Luscombe, G. Cuda, M. Gaspari and A. Riccio (2017). "3'UTR Remodelling of Axonal Transcripts in Sympathetic Neurons." bioRxiv.

Andreassi, C. and A. Riccio (2009). "To localize or not to localize: mRNA fate is in 3'UTR ends." Trends in Cell Biology **19**(9): 465-474.

Andreassi, C., C. Zimmermann, R. Mitter, S. Fusco, S. De Vita, A. Saiardi and A. Riccio (2010). "An NGF-responsive element targets myo-inositol monophosphatase-1 mRNA to sympathetic neuron axons." Nature Neuroscience **13**(3): 291-301.

Antar, L. N., R. Afroz, J. B. Dictenberg, R. C. Carroll and G. J. Bassell (2004). "Metabotropic glutamate receptor activation regulates fragile x mental retardation protein and FMR1 mRNA localization differentially in dendrites and at synapses." Journal of Neuroscience **24**(11): 2648-2655.

Antar, L. N., J. B. Dictenberg, M. Plociniak, R. Afroz and G. J. Bassell (2005). "Localization of FMRP-associated mRNA granules and requirement of microtubules for activity-dependent trafficking in hippocampal neurons." Genes Brain and Behaviour **4**(6): 350-359.

Ascano, M., D. Bodmer and R. Kuruvilla (2012). "Endocytic trafficking of neurotrophins in neural development." Trends in Cell Biology **22**(5): 266-273.

Ascano, M., Jr., N. Mukherjee, P. Bandaru, J. B. Miller, J. D. Nusbaum, D. L. Corcoran, C. Langlois, M. Munschauer, S. Dewell, M. Hafner, Z. Williams, U. Ohler and T. Tuschl (2012). "FMRP targets distinct mRNA sequence elements to regulate protein expression." Nature **492**(7429): 382-386.

Aschrafi, A., O. Natera-Naranjo, A. E. Gioio and B. B. Kaplan (2010). "Regulation of axonal trafficking of cytochrome c oxidase IV mRNA." Molecular and Cellular Neuroscience **43**(4): 422-430.

Atwal, J. K., B. Massie, F. D. Miller and D. R. Kaplan (2000). "The TrkB-Shc site signals neuronal survival and local axon growth via MEK and P13-kinase." Neuron **27**(2): 265-277.

Baleriola, J., C. A. Walker, Y. Y. Jean, J. F. Crary, C. M. Troy, P. L. Nagy and U. Hengst (2014). "Axonally synthesized ATF4 transmits a neurodegenerative signal across brain regions." Cell **158**(5): 1159-1172.

Baloh, R. H., M. G. Tansey, P. A. Lampe, T. J. Fahrner, H. Enomoto, K. S. Simburger, M. L. Leitner, T. Araki, E. M. Johnson, Jr. and J. Milbrandt (1998). "Artemin, a novel member of the GDNF ligand family, supports peripheral and central neurons and signals through the GFRalpha3-RET receptor complex." Neuron **21**(6): 1291-1302.

Bamji, S. X., M. Majdan, C. D. Pozniak, D. J. Belliveau, R. Aloyz, J. Kohn, C. G. Causing and F. D. Miller (1998). "The p75 neurotrophin receptor mediates neuronal apoptosis and is essential for naturally occurring sympathetic neuron death." The Journal of Cell Biology **140**(4): 911-923.

Banfai, B., H. Jia, J. Khatun, E. Wood, B. Risk, W. E. Gundling, Jr., A. Kundaje, H. P. Gunawardena, Y. Yu, L. Xie, K. Krajewski, B. D. Strahl, X. Chen, P. Bickel, M. C. Giddings, J. B. Brown and L. Lipovich (2012). "Long noncoding RNAs are rarely translated in two human cell lines." Genome Research **22**(9): 1646-1657.

Barnes, A. P. and F. Polleux (2009). "Establishment of axon-dendrite polarity in developing neurons." Annual Review of Neuroscience **32**: 347-381.

Bartel, D. P. (2009). "MicroRNAs: target recognition and regulatory functions." Cell **136**(2): 215-233.

Bartlett, S. E., A. J. Reynolds, M. Weible, K. Heydon and I. A. Hendry (1997). "In sympathetic but not sensory neurones, phosphoinositide-3 kinase is important for NGF-dependent survival and the retrograde transport of 125I-βNGF." Brain Research **761**(2): 257-262.

Bassell, G. J., H. Zhang, A. L. Byrd, A. M. Femino, R. H. Singer, K. L. Taneja, L. M. Lifshitz, I. M. Herman and K. S. Kosik (1998). "Sorting of beta-actin mRNA and protein to neurites and growth cones in culture." Journal of Neuroscience **18**(1): 251-265.

Baumgartner, B. G., M. Orpinell, J. Duran, V. Ribas, H. E. Burghardt, D. Bach, A. V. Villar, J. C. Paz, M. Gonzalez, M. Camps, J. Oriola, F. Rivera, M. Palacin and A. Zorzano (2007). "Identification of a novel modulator of thyroid hormone receptor-mediated action." PLoS One **2**(11): e1183.

Belliveau, D. J., I. Krivko, J. Kohn, C. Lachance, C. Pozniak, D. Rusakov, D. Kaplan and F. D. Miller (1997). "NGF and neurotrophin-3 both activate TrkA on sympathetic neurons but differentially regulate survival and neuritogenesis." The Journal of Cell Biology **136**(2): 375-388.

Ben-Yaakov, K., S. Y. Dagan, Y. Segal-Ruder, O. Shalem, D. Vuppalanchi, D. E. Willis, D. Yudin, I. Rishal, F. Rother, M. Bader, A. Blesch, Y. Pilpel, J. L. Twiss and M. Fainzilber (2012). "Axonal transcription factors signal retrogradely in lesioned peripheral nerve." EMBO J **31**(6): 1350-1363.

Bennetts, J. S., L. F. Fowles, N. C. Butterfield, J. L. Berkman, R. D. Teasdale, F. Simpson and C. Wicking (2006). "Identification and analysis of novel genes expressed in the mouse embryonic facial primordia." Frontiers in Bioscience **11**: 2631-2646.

Bennetts, J. S., N. D. Rendtorff, F. Simpson, L. Tranebjaerg and C. Wicking (2007). "The coding region of TP53INP2, a gene expressed in the developing nervous system, is not altered in a family with autosomal recessive non-progressive infantile ataxia on chromosome 20q11-q13." Developmental Dynamics **236**(3): 843-852.

Berkovits, B. D. and C. Mayr (2015). "Alternative 3' UTRs act as scaffolds to regulate membrane protein localization." Nature **522**(7556): 363-367.

Bicker, S., S. Khudayberdiev, K. Weiss, K. Zocher, S. Baumeister and G. Schratt (2013). "The DEAH-box helicase DHX36 mediates dendritic localization of the neuronal precursor-microRNA-134." Genes and Development **27**(9): 991-996.

Bird, L. M. (2014). "Angelman syndrome: review of clinical and molecular aspects." The Application of Clinical Genetics **7**: 93-104.

Bodmer, D., M. Ascano and R. Kuruvilla (2011). "Isoform-specific dephosphorylation of dynamin1 by calcineurin couples neurotrophin receptor endocytosis to axonal growth." Neuron **70**(6): 1085-1099.

Bonni, A., A. Brunet, A. E. West, S. R. Datta, M. A. Takasu and M. E. Greenberg (1999). "Cell survival promoted by the Ras-MAPK signaling pathway by transcription-dependent and -independent mechanisms." Science **286**(5443): 1358-1362.

Boutet, S. C., T. H. Cheung, N. L. Quach, L. Liu, S. L. Prescott, A. Edalati, K. Iori and T. A. Rando (2012). "Alternative polyadenylation mediates microRNA regulation of muscle stem cell function." Cell Stem Cell **10**(3): 327-336.

Brar, G. A., M. Yassour, N. Friedman, A. Regev, N. T. Ingolia and J. S. Weissman (2012). "High-Resolution View of the Yeast Meiotic Program Revealed by Ribosome Profiling." Science **335**(6068): 552-557.

Broughton, J. P. and A. E. Pasquinelli (2013). "Identifying Argonaute binding sites in Caenorhabditis elegans using iCLIP." Methods **63**(2): 119-125.

Bueker, E. D. (1948). "Implantation of tumors in the hind limb field of the embryonic chick and the developmental response of the lumbosacral nervous system." The Anatomical Record **102**(3): 369-389.

Cajigas, I. J., G. Tushev, T. J. Will, S. tom Dieck, N. Fuerst and E. M. Schuman (2012). "The local transcriptome in the synaptic neuropil revealed by deep sequencing and high-resolution imaging." Neuron **74**(3): 453-466.

Campbell, D. S. and C. E. Holt (2001). "Chemotropic responses of retinal growth cones mediated by rapid local protein synthesis and degradation." Neuron **32**(6): 1013-1026.

Campenot, R. B. (1977). "Local control of neurite development by nerve growth factor." PNAS **74**(10): 4516-4519.

Carlevaro-Fita, J., A. Rahim, R. Guigó, L. A. Vardy and R. Johnson (2016). "Cytoplasmic long noncoding RNAs are frequently bound to and degraded at ribosomes in human cells." RNA **22**(6): 867-882.

Casaccia-Bonnefil, P., B. D. Carter, R. T. Dobrowsky and M. V. Chao (1996). "Death of oligodendrocytes mediated by the interaction of nerve growth factor with its receptor p75." Nature **383**(6602): 716-719.

Chanas-Sacre, G., C. Mazy-Servais, R. Wattiez, S. Pirard, B. Rogister, J. G. Patton, S. Belachew, B. Malgrange, G. Moonen and P. Leprince (1999). "Identification of PSF, the polypyrimidine tract-binding protein-associated splicing factor, as a developmentally regulated neuronal protein." Journal of Neuroscience Research **57**(1): 62-73.

Chang, N., J. Yi, G. Guo, X. Liu, Y. Shang, T. Tong, Q. Cui, M. Zhan, M. Gorospe and W. Wang (2010). "HuR uses AUF1 as a cofactor to promote p16INK4 mRNA decay." Molecular Cell Biology **30**(15): 3875-3886.

Chao, Y. and J. Vogel (2016). "A 3' UTR-Derived Small RNA Provides the Regulatory Noncoding Arm of the Inner Membrane Stress Response." Molecular Cell **61**(3): 352-363.

Chen, B. P., C. D. Wolfgang and T. Hai (1996). "Analysis of ATF3, a transcription factor induced by physiological stresses and modulated by gadd153/Chop10." Molecular and Cellular Biology **16**(3): 1157-1168.

Cheng, Y., R. M. Miura and B. Tian (2006). "Prediction of mRNA polyadenylation sites by support vector machine." Bioinformatics **22**(19): 2320-2325.

Chu, C., Qiangfeng C. Zhang, Simão T. da Rocha, Ryan A. Flynn, M. Bharadwaj, J. M. Calabrese, T. Magnuson, E. Heard and Howard Y. Chang (2015). "Systematic Discovery of Xist RNA Binding Proteins." Cell **161**(2): 404-416.

Cohen, S. (1960). "Purification of a Nerve-Growth Promoting Protein from the Mouse Salivary Gland and Its Neuro-Cytotoxic Antiserum." PNAS **46**(3): 302-311.

Cohen, S. and R. Levi-Montalcini (1956). "A Nerve Growth-Stimulating Factor Isolated from Snake Venom." PNAS **42**(9): 571-574.

Corish, P. and C. Tyler-Smith (1999). "Attenuation of green fluorescent protein half-life in mammalian cells." Protein Engineering, Design and Selection **12**(12): 1035-1040.

Cosker, K. E., S. J. Fenstermacher, M. F. Pazyra-Murphy, H. L. Elliott and R. A. Segal (2016). "The RNA-binding protein SFPQ orchestrates an RNA regulon to promote axon viability." Nature Neuroscience **19**(5): 690-696.

Cosker, K. E., M. F. Pazyra-Murphy, S. J. Fenstermacher and R. A. Segal (2013). "Target-derived neurotrophins coordinate transcription and transport of bclw to prevent axonal degeneration." Journal of Neuroscience **33**(12): 5195-5207.

Costa, W. and Willia D. (2017). “To the End of the Line: Axonal mRNA Transport and Local Translation in Health and Neurodegenerative Disease.” Developmental Neurobiology **78**:209-220

Cox, L. J., U. Hengst, N. G. Gurskaya, K. A. Lukyanov and S. R. Jaffrey (2008). "Intra-axonal translation and retrograde trafficking of CREB promotes neuronal survival." Nature Cell Biology **10**(2): 149-159.

Crowder, R. J. and R. S. Freeman (1998). "Phosphatidylinositol 3-Kinase and Akt Protein Kinase Are Necessary and Sufficient for the Survival of Nerve Growth Factor-Dependent Sympathetic Neurons." Journal of Neuroscience **18**(8): 2933-2943.

Crowley, C., S. D. Spencer, M. C. Nishimura, K. S. Chen, S. Pitts-Meek, M. P. Armaninl, L. H. Ling, S. B. McMahon, D. L. Shelton, A. D. Levinson and H. S. Phillips (1994). "Mice lacking nerve growth factor display perinatal loss of sensory and sympathetic neurons yet develop basal forebrain cholinergic neurons." Cell **76**(6): 1001-1011.

Cunningham, M. E., R. M. Stephens, D. R. Kaplan and L. A. Greene (1997). "Autophosphorylation of Activation Loop Tyrosines Regulates Signaling by the TRK Nerve Growth Factor Receptor." Journal of Biological Chemistry **272**(16): 10957-10967.

Dajas-Bailador, F., B. Bonev, P. Garcez, P. Stanley, F. Guillemot and N. Papalopulu (2012). "microRNA-9 regulates axon extension and branching by targeting Map1b in mouse cortical neurons." Nature Neuroscience **15** 697-699.

Dale, L., G. Matthews and A. Colman (1993). "Secretion and mesoderm-inducing activity of the TGF-beta-related domain of Xenopus Vg1." EMBO J **12**(12): 4471-4480.

Darnell, J. C., K. B. Jensen, P. Jin, V. Brown, S. T. Warren and R. B. Darnell (2001). "Fragile X mental retardation protein targets G quartet mRNAs important for neuronal function." Cell **107**(4): 489-499.

Darnell, J. C., S. J. Van Driesche, C. Zhang, K. Y. Hung, A. Mele, C. E. Fraser, E. F. Stone, C. Chen, J. J. Fak, S. W. Chi, D. D. Licatalosi, J. D. Richter and R. B. Darnell (2011). "FMRP stalls ribosomal translocation on mRNAs linked to synaptic function and autism." Cell **146**(2): 247-261.

Davies, A. M. (1996). "The neurotrophic hypothesis: where does it stand?" Philos Trans R Soc Lond B Biol Sci **351**(1338): 389-394.

de Sousa Abreu, R., L. O. Penalva, E. M. Marcotte and C. Vogel (2009). "Global signatures of protein and mRNA expression levels." Molecular Biosystems **5**(12): 1512-1526.

Del Prete, M. J., R. Vernal, H. Dolznig, E. W. Müllner and J. A. Garcia-Sanz (2007). "Isolation of polysome-bound mRNA from solid tissues amenable for RT-PCR and profiling experiments." RNA **13**(3): 414-421.

Delcroix, J. D., J. S. Valletta, C. Wu, S. J. Hunt, A. S. Kowal and W. C. Mobley (2003). "NGF signaling in sensory neurons: evidence that early endosomes carry NGF retrograde signals." Neuron **39**(1): 69-84.

Denzler, R., V. Agarwal, J. Stefano, D. P. Bartel and M. Stoffel (2014). "Assessing the ceRNA hypothesis with quantitative measurements of miRNA and target abundance." Molecular Cell **54**(5): 766-776.

Denzler, R., Sean E. McGeary, Alexandra C. Title, V. Agarwal, David P. Bartel and M. Stoffel (2016). "Impact of MicroRNA Levels, Target-Site Complementarity, and Cooperativity on Competing Endogenous RNA-Regulated Gene Expression." Molecular Cell **64**(3): 565-579.

Deppmann, C. D., S. Mihalas, N. Sharma, B. E. Lonze, E. Niebur and D. D. Ginty (2008). "A model for neuronal competition during development." Science **320**(5874): 369-373.

Derti, A., P. Garrett-Engele, K. D. Macisaac, R. C. Stevens, S. Sriram, R. Chen, C. A. Rohl, J. M. Johnson and T. Babak (2012). "A quantitative atlas of polyadenylation in five mammals." Genome Research **22**(6): 1173-1183.

Dong, X., J. Sweet, J. R. G. Challis, T. Brown and S. J. Lye (2007). "Transcriptional Activity of Androgen Receptor Is Modulated by Two RNA Splicing Factors, PSF and p54nrb." Molecular and Cellular Biology **27**(13): 4863-4875.

Donnelly, C. J., D. E. Willis, M. Xu, C. Tep, C. Jiang, S. Yoo, N. C. Schanen, C. B. Kirn-Safran, J. van Minnen, A. English, S. O. Yoon, G. J. Bassell and J. L. Twiss (2011). "Limited availability of ZBP1 restricts axonal mRNA localization and nerve regeneration capacity." EMBO J **30**(22): 4665-4677.

Doyle, M. and M. A. Kiebler (2011). "Mechanisms of dendritic mRNA transport and its role in synaptic tagging." EMBO J **30**(17): 3540-3552.

Elkon, R., A. P. Ugalde and R. Agami (2013). "Alternative cleavage and polyadenylation: extent, regulation and function." Nature Review Genetics **14**(7): 496-506.

Elvira, G., S. Wasiak, V. Blandford, X. K. Tong, A. Serrano, X. Fan, M. del Rayo Sanchez-Carbente, F. Servant, A. W. Bell, D. Boismenu, J. C. Lacaille, P. S. McPherson, L. DesGroseillers and W. S. Sossin (2006). "Characterization of an RNA granule from developing brain." Molecular & Cellular Proteomics **5**(4): 635-651.

Emili, A., M. Shales, S. McCracken, W. Xie, P. W. Tucker, R. Kobayashi, B. J. Blencowe and C. J. Ingles (2002). "Splicing and transcription-associated proteins PSF and p54nrb/nonO bind to the RNA polymerase II CTD." RNA **8**(9): 1102-1111.

Engreitz, J. M., N. Ollikainen and M. Guttman (2016). "Long non-coding RNAs: spatial amplifiers that control nuclear structure and gene expression." Nature Reviews Molecular Cell Biology **17**(12): 756-770.

Enomoto, H., P. A. Crawford, A. Gorodinsky, R. O. Heuckeroth, E. M. Johnson, Jr. and J. Milbrandt (2001). "RET signaling is essential for migration, axonal growth and axon guidance of developing sympathetic neurons." Development **128**(20): 3963-3974.

Eom, T., L. N. Antar, R. H. Singer and G. J. Bassell (2003). "Localization of a beta-actin messenger ribonucleoprotein complex with zipcode-binding protein modulates the density of dendritic filopodia and filopodial synapses." Journal of Neuroscience **23**(32): 10433-10444.

Ephrussi, A., L. K. Dickinson and R. Lehmann (1991). "Oskar organizes the germ plasm and directs localization of the posterior determinant nanos." Cell **66**(1): 37-50.

Ephrussi, A. and R. Lehmann (1992). "Induction of germ cell formation by oskar." Nature **358**(6385): 387-392.

Ernsberger, U., E. Reissmann, I. Mason and H. Rohrer (2000). "The expression of dopamine β-hydroxylase, tyrosine hydroxylase, and Phox2 transcription factors in sympathetic neurons: evidence for common regulation during noradrenergic induction and diverging regulation later in development." Mechanisms of Development **92**(2): 169-177.

Fagan, A. M., H. Zhang, S. Landis, R. J. Smeyne, I. Silos-Santiago and M. Barbacid (1996). "TrkA, But Not TrkC, Receptors Are Essential for Survival of Sympathetic Neurons In Vivo." Journal of Neuroscience **16**(19): 6208-6218.

Fang, L., W. W. Du, X. Yang, K. Chen, A. Ghanekar, G. Levy, W. Yang, A. J. Yee, W. Y. Lu, J. W. Xuan, Z. Gao, F. Xie, C. He, Z. Deng and B. B. Yang (2013). "Versican 3'-untranslated region (3'-UTR) functions as a ceRNA in inducing the development of hepatocellular carcinoma by regulating miRNA activity." FASEB J **27**(3): 907-919.

Farina, K. L., S. Huttelmaier, K. Musunuru, R. Darnell and R. H. Singer (2003). "Two ZBP1 KH domains facilitate beta-actin mRNA localization, granule formation, and cytoskeletal attachment." The Journal of Cell Biology **160**(1): 77-87.

Farinas, I., K. R. Jones, C. Backus, X. Y. Wang and L. F. Reichardt (1994). "Severe sensory and sympathetic deficits in mice lacking neurotrophin-3." Nature **369**(6482): 658-661.

Fineberg, S. K., K. S. Kosik and B. L. Davidson (2009). "MicroRNAs potentiate neural development." Neuron **64**(3): 303-309.

Fiore, R., S. Khudayberdiev, M. Christensen, G. Siegel, S. W. Flavell, T. K. Kim, M. E. Greenberg and G. Schratt (2009). "Mef2-mediated transcription of the miR379-410 cluster regulates activity-dependent dendritogenesis by fine-tuning Pumilio2 protein levels." EMBO J **28**(6): 697-710.

Flavell, S. W., C. W. Cowan, T. K. Kim, P. L. Greer, Y. Lin, S. Paradis, E. C. Griffith, L. S. Hu, C. Chen and M. E. Greenberg (2006). "Activity-dependent regulation of MEF2 transcription factors suppresses excitatory synapse number." Science **311**(5763): 1008-1012.

Flavell, S. W., T. K. Kim, J. M. Gray, D. A. Harmin, M. Hemberg, E. J. Hong, E. Markenscoff-Papadimitriou, D. M. Bear and M. E. Greenberg (2008). "Genome-wide analysis of MEF2

transcriptional program reveals synaptic target genes and neuronal activity-dependent polyadenylation site selection." Neuron **60**(6): 1022-1038.

Floor, S. N. and J. A. Doudna (2016). "Tunable protein synthesis by transcript isoforms in human cells." eLife **5**: e10921.

Francis, N., I. Farinas, C. Brennan, K. Rivas-Plata, C. Backus, L. Reichardt and S. Landis (1999). "NT-3, like NGF, is required for survival of sympathetic neurons, but not their precursors." Developmental Biology **210**(2): 411-427.

Gao, S., C. Cheng, H. Chen, M. Li, K. Liu and G. Wang (2016). "IGF1 3'UTR functions as a ceRNA in promoting angiogenesis by sponging miR-29 family in osteosarcoma." Journal of Molecular Histology **47**(2): 135-143.

Geisberg, J. V., Z. Moqtaderi, X. Fan, F. Ozsolak and K. Struhl (2014). "Global analysis of mRNA isoform half-lives reveals stabilizing and destabilizing elements in yeast." Cell **156**(4): 812-824.

Gervasi, N. M., S. S. Scott, A. Aschrafi, J. Gale, S. N. Vohra, M. A. MacGibeny, A. N. Kar, A. E. Gioio and B. B. Kaplan (2016). "The local expression and trafficking of tyrosine hydroxylase mRNA in the axons of sympathetic neurons." RNA **22**(6): 883-895.

Gilbert, C. and J. Q. Svejstrup (2006). "RNA immunoprecipitation for determining RNA-protein associations in vivo." Current Protocols in Molecular Biology **Chapter 27**: Unit 27.24.

Ginty, D. D., A. Bonni and M. E. Greenberg (1994). "Nerve growth factor activates a Ras-dependent protein kinase that stimulates c-fos transcription via phosphorylation of CREB." Cell **77**(5): 713-725.

Giuditta, A., W. D. Dettbarn and M. Brzin (1968). "Protein synthesis in the isolated giant axon of the squid." PNAS **59**(4): 1284-1287.

Glebova, N. O. and D. D. Ginty (2005). "Growth and survival signals controlling sympathetic nervous system development." Annual Review of Neuroscience **28**: 191-222.

Glock, C., M. Heumuller and E. M. Schuman (2017). "mRNA transport & local translation in neurons." Current Opinion in Neurobiology **45**: 169-177.

González, C. and A. Couve (2014). "The axonal endoplasmic reticulum and protein trafficking: Cellular bootlegging south of the soma." Seminars in Cell & Developmental Biology **27**: 23-31.

Graef, I. A., F. Wang, F. Charron, L. Chen, J. Neilson, M. Tessier-Lavigne and G. R. Crabtree (2003). "Neurotrophins and netrins require calcineurin/NFAT signaling to stimulate outgrowth of embryonic axons." Cell **113**(5): 657-670.

Greene, L. A. and A. S. Tischler (1976). "Establishment of a noradrenergic clonal line of rat adrenal pheochromocytoma cells which respond to nerve growth factor." PNAS **73**(7): 2424-2428.

Gruber, A. R., G. Martin, P. Muller, A. Schmidt, A. J. Gruber, R. Gumienny, N. Mittal, R. Jayachandran, J. Pieters, W. Keller, E. van Nimwegen and M. Zavolan (2014). "Global 3' UTR shortening has a limited effect on protein abundance in proliferating T cells." Nature Communications **5**: 5465.

Gumy, L. F., G. S. Yeo, Y. C. Tung, K. H. Zivraj, D. Willis, G. Coppola, B. Y. Lam, J. L. Twiss, C. E. Holt and J. W. Fawcett (2011). "Transcriptome analysis of embryonic and adult sensory axons reveals changes in mRNA repertoire localization." RNA **17**(1): 85-98.

Guo, H., N. T. Ingolia, J. S. Weissman and D. P. Bartel (2010). "Mammalian microRNAs predominantly act to decrease target mRNA levels." Nature **466**(7308): 835-840.

Guttman, M., P. Russell, N. T. Ingolia, J. S. Weissman and E. S. Lander (2013). "Ribosome profiling provides evidence that large noncoding RNAs do not encode proteins." Cell **154**(1): 240-251.

Ha, M. and V. N. Kim (2014). "Regulation of microRNA biogenesis." Nature Reviews Molecular Cell Biology **15**(8): 509-524.

Hafezparast, M., R. Klocke, C. Ruhrberg, A. Marquardt, A. Ahmad-Annuar, S. Bowen, G. Lalli, A. S. Witherden, H. Hummerich, S. Nicholson, P. J. Morgan, R. Oozageer, J. V. Priestley, S. Averill, V. R. King, S. Ball, J. Peters, T. Toda, A. Yamamoto, Y. Hiraoka, M. Augustin, D. Korthaus, S. Wattler, P. Wabnitz, C. Dickneite, S. Lampel, F. Boehme, G. Peraus, A. Popp, M. Rudelius, J. Schlegel, H. Fuchs, M. Hrabe de Angelis, G. Schiavo, D. T. Shima, A. P. Russ, G. Stumm, J. E. Martin and E. M. Fisher (2003). "Mutations in dynein link motor neuron degeneration to defects in retrograde transport." Science **300**(5620): 808-812.

Hai, T., C. D. Wolfgang, D. K. Marsee, A. E. Allen and U. Sivaprasad (1999). "ATF3 and stress responses." Gene Expression **7**(4-6): 321-335.

Halstead, J. M., T. Lionnet, J. H. Wilbertz, F. Wippich, A. Ephrussi, R. H. Singer and J. A. Chao (2015). "Translation. An RNA biosensor for imaging the first round of translation from single cells to living animals." Science **347**(6228): 1367-1671.

Hamanoue, M., G. Middleton, S. Wyatt, E. Jaffray, R. T. Hay and A. M. Davies (1999). "p75-Mediated NF-κB Activation Enhances the Survival Response of Developing Sensory Neurons to Nerve Growth Factor." Molecular and Cellular Neuroscience **14**(1): 28-40.

Hancock, M. L., N. Preitner, J. Quan and J. G. Flanagan (2014). "MicroRNA-132 is enriched in developing axons, locally regulates Rasa1 mRNA, and promotes axon extension." Journal of Neuroscience **34**(1): 66-78.

Hansen, T. B., T. I. Jensen, B. H. Clausen, J. B. Bramsen, B. Finsen, C. K. Damgaard and J. Kjems (2013). "Natural RNA circles function as efficient microRNA sponges." Nature **495**(7441): 384-388.

Hanz, S., E. Perlson, D. Willis, J. Q. Zheng, R. Massarwa, J. J. Huerta, M. Koltzenburg, M. Kohler, J. van-Minnen, J. L. Twiss and M. Fainzilber (2003). "Axoplasmic importins enable retrograde injury signaling in lesioned nerve." Neuron **40**(6): 1095-1104.

Harrington, A. W. and D. D. Ginty (2013). "Long-distance retrograde neurotrophic factor signalling in neurons." Nature Reviews Neuroscience **14**(3): 177-187.

Harrington, A. W., C. St Hillaire, L. S. Zweifel, N. O. Glebova, P. Philippidou, S. Halegoua and D. D. Ginty (2011). "Recruitment of actin modifiers to TrkA endosomes governs retrograde NGF signaling and survival." Cell **146**(3): 421-434.

He, T.-C., S. Zhou, L. T. da Costa, J. Yu, K. W. Kinzler and B. Vogelstein (1998). "A simplified system for generating recombinant adenoviruses." PNAS **95**(5): 2509-2514.

Heasman, J., O. Wessely, R. Langland, E. J. Craig and D. S. Kessler (2001). "Vegetal localization of maternal mRNAs is disrupted by VegT depletion." Developmental Biology **240**(2): 377-386.

Heerssen, H. M., M. F. Pazyra and R. A. Segal (2004). "Dynein motors transport activated Trks to promote survival of target-dependent neurons." Nature Neuroscience **7**(6): 596-604.

Heiman, M., A. Schaefer, S. Gong, J. D. Peterson, M. Day, K. E. Ramsey, M. Suarez-Farinas, C. Schwarz, D. A. Stephan, D. J. Surmeier, P. Greengard and N. Heintz (2008). "A translational profiling approach for the molecular characterization of CNS cell types." Cell **135**(4): 738-748.

Hendry, I. A. (1975). "The response of adrenergic neurones to axotomy and nerve growth factor." Brain Research **94**(1): 87-97.

Hengst, U., A. Deglincerti, H. J. Kim, N. L. Jeon and S. R. Jaffrey (2009). "Axonal elongation triggered by stimulus-induced local translation of a polarity complex protein." Nature Cell Biology **11**(8): 1024-1030.

Heumann, R., S. Korsching, J. Scott and H. Thoenen (1984). "Relationship between levels of nerve growth factor (NGF) and its messenger RNA in sympathetic ganglia and peripheral target tissues." EMBO J **3**(13): 3183-3189.

Heyer, E. E. and M. J. Moore (2016). "Redefining the Translational Status of 80S Monosomes." Cell **164**(4): 757-769.

Honma, Y., T. Araki, S. Gianino, A. Bruce, R. Heuckeroth, E. Johnson and J. Milbrandt (2002). "Artemin is a vascular-derived neurotropic factor for developing sympathetic neurons." Neuron **35**(2): 267-282.

Hoque, M., Z. Ji, D. Zheng, W. Luo, W. Li, B. You, J. Y. Park, G. Yehia and B. Tian (2013). "Analysis of alternative cleavage and polyadenylation by 3' region extraction and deep sequencing." Nature Methods **10**(2): 133-139.

Horton, A., G. Laramee, S. Wyatt, A. Shih, J. Winslow and A. M. Davies (1997). "NGF binding to p75 enhances the sensitivity of sensory and sympathetic neurons to NGF at different stages of development." Molecular and Cellular Neuroscience **10**(3-4): 162-172.

Howard, M. J. (2005). "Mechanisms and perspectives on differentiation of autonomic neurons." Developmental Biology **277**(2): 271-286.

Howe, C. L., J. S. Valletta, A. S. Rusnak and W. C. Mobley (2001). "NGF Signaling from Clathrin-Coated Vesicles: Evidence that Signaling Endosomes Serve as a Platform for the Ras-MAPK Pathway." Neuron **32**(5): 801-814.

Howe, C. L., J. S. Valletta, A. S. Rusnak and W. C. Mobley (2001). "NGF signaling from clathrin-coated vesicles: evidence that signaling endosomes serve as a platform for the Ras-MAPK pathway." Neuron **32**(5): 801-814.

Hu, Y., X. Li, W. Xue, J. Pang, Y. Meng, Y. Shen and Q. Xu (2017). "TP53INP2-related basal autophagy is involved in the growth and malignant progression in human liposarcoma cells." Biomedicine & Pharmacotherapy **88**: 562-568.

Huang, E. J. and L. F. Reichardt (2003). "Trk receptors: roles in neuronal signal transduction." Annual Review of Biochemistry **72**: 609-642.

Huang, Y. S., J. H. Carson, E. Barbarese and J. D. Richter (2003). "Facilitation of dendritic mRNA transport by CPEB." Genes & Development **17**(5): 638-653.

Hunke, S., R. Keller and V. S. Müller (2012). "Signal integration by the Cpx-envelope stress system." FEMS Microbiology Letters **326**(1): 12-22.

Hurt, J. A., A. D. Robertson and C. B. Burge (2013). "Global analyses of UPF1 binding and function reveal expanded scope of nonsense-mediated mRNA decay." Genome Research **23**(10): 1636-1650.

Huttelmaier, S., D. Zenklusen, M. Lederer, J. Dictenberg, M. Lorenz, X. Meng, G. J. Bassell, J. Condeelis and R. H. Singer (2005). "Spatial regulation of beta-actin translation by Src-dependent phosphorylation of ZBP1." Nature **438**(7067): 512-515.

Im, H.-I. and P. J. Kenny (2012). "MicroRNAs in neuronal function and dysfunction." Trends in Neurosciences **35**(5): 325-334.

Ingolia, N. T. (2014). "Ribosome profiling: new views of translation, from single codons to genome scale." Nature Reviews Genetics **15**(3): 205-213.

Ingolia, N. T., S. Ghaemmaghami, J. R. Newman and J. S. Weissman (2009). "Genome-wide analysis in vivo of translation with nucleotide resolution using ribosome profiling." Science **324**(5924): 218-223.

Ingolia, N. T., L. F. Lareau and J. S. Weissman (2011). "Ribosome profiling of mouse embryonic stem cells reveals the complexity and dynamics of mammalian proteomes." Cell **147**(4): 789-802.

Isaac, D. D., J. S. Pinkner, S. J. Hultgren and T. J. Silhavy (2005). "The extracytoplasmic adaptor protein CpxP is degraded with substrate by DegP." PNAS **102**(49): 17775-17779.

Iyengar, B. R., A. Choudhary, M. A. Sarangdhar, K. V. Venkatesh, C. J. Gadgil and B. Pillai (2014). "Non-coding RNA interact to regulate neuronal development and function." Frontiers in Cellular Neuroscience **8**: 47.

Jambhekar, A. and J. L. DeRisi (2007). "Cis-acting determinants of asymmetric, cytoplasmic RNA transport." RNA **13**(5): 625-642.

Jenny, A., O. Hachet, P. Zavorszky, A. Cyrklaff, M. D. Weston, D. S. Johnston, M. Erdelyi and A. Ephrussi (2006). "A translation-independent role of oskar RNA in early Drosophila oogenesis." Development **133**(15): 2827-2833.

Jens, M. and N. Rajewsky (2015). "Competition between target sites of regulators shapes post-transcriptional gene regulation." Nature Review Genetics **16**(2): 113-126.

Ji, S.-J. and S. R. Jaffrey (2012). "Intra-Axonal Translation of SMAD1/5/8 Mediates Retrograde Regulation of Trigeminal Ganglia Subtype Specification." Neuron **74**(1): 95-107.

Ji, Z., J. Y. Lee, Z. Pan, B. Jiang and B. Tian (2009). "Progressive lengthening of 3' untranslated regions of mRNAs by alternative polyadenylation during mouse embryonic development." PNAS **106**(17): 7028-7033.

Johnstone, O. and P. Lasko (2001). "Translational regulation and RNA localization in Drosophila oocytes and embryos." Annual Review of Genetics **35**: 365-406.

Jung, H., C. G. Gkogkas, N. Sonenberg and C. E. Holt (2014). "Remote control of gene function by local translation." Cell **157**(1): 26-40.

Kádár, A., G. Wittmann, Z. Liposits and C. Fekete (2009). "Improved method for combination of immunocytochemistry and Nissl staining." Journal of Neuroscience Methods **184**(1): 115-118.

Kanke, M., H. Jambor, J. Reich, B. Marches, R. Gstir, Y. H. Ryu, A. Ephrussi and P. M. Macdonald (2015). "oskar RNA plays multiple noncoding roles to support oogenesis and maintain integrity of the germline/soma distinction." RNA **21**(6): 1096-1109.

Kao, S.-c., R. K. Jaiswal, W. Kolch and G. E. Landreth (2001). "Identification of the Mechanisms Regulating the Differential Activation of the MAPK Cascade by Epidermal

Growth Factor and Nerve Growth Factor in PC12 Cells." Journal of Biological Chemistry **276**(21): 18169-18177.

Kaplan, D. R., B. L. Hempstead, D. Martin-Zanca, M. V. Chao and L. F. Parada (1991). "The trk proto-oncogene product: a signal transducing receptor for nerve growth factor." Science **252**(5005): 554-558.

Kar, A. N., J. N. S. Vargas, C.-Y. Chen, J. A. Kowalak, A. E. Gioio and B. B. Kaplan (2017). "Molecular determinants of cytochrome C oxidase IV mRNA axonal trafficking." Molecular and Cellular Neuroscience **80**: 32-43.

Kaur, J. and J. Debnath (2015). "Autophagy at the crossroads of catabolism and anabolism." Nature Reviews Molecular Cell Biology **16**: 461.

Kiebler, M. A. and G. J. Bassell (2006). "Neuronal RNA granules: movers and makers." Neuron **51**(6): 685-690.

Kim, T. K., M. Hemberg, J. M. Gray, A. M. Costa, D. M. Bear, J. Wu, D. A. Harmin, M. Laptewicz, K. Barbara-Haley, S. Kuersten, E. Markenscoff-Papadimitriou, D. Kuhl, H. Bito, P. F. Worley, G. Kreiman and M. E. Greenberg (2010). "Widespread transcription at neuronal activity-regulated enhancers." Nature **465**(7295): 182-187.

Kim-Ha, J., J. L. Smith and P. M. Macdonald (1991). "oskar mRNA is localized to the posterior pole of the Drosophila oocyte." Cell **66**(1): 23-35.

Kishino, T., M. Lalande and J. Wagstaff (1997). "UBE3A/E6-AP mutations cause Angelman syndrome." Nature Genetics **15**(1): 70-73.

Kislauskis, E. H., X. Zhu and R. H. Singer (1994). "Sequences responsible for intracellular localization of beta-actin messenger RNA also affect cell phenotype." The Journal of Cell Biology **127**(2): 441-451.

Klein, R., S. Jing, V. Nanduri, E. O'Rourke and M. Barbacid (1991). "The trk proto-oncogene encodes a receptor for nerve growth factor." Cell **65**(1): 189-197.

Kocabas, A., T. Duarte, S. Kumar and M. A. Hynes (2015). "Widespread Differential Expression of Coding Region and 3' UTR Sequences in Neurons and Other Tissues." Neuron **88**(6): 1149-1156.

Koenig, E. (1967). "Synthetic mechanisms in the axon. IV. In vitro incorporation of [3H]precursors into axonal protein and RNA." Journal of Neurochemistry **14**(4): 437-446.

Kole, A. J., V. Swahari, S. M. Hammond and M. Deshmukh (2011). "miR-29b is activated during neuronal maturation and targets BH3-only genes to restrict apoptosis." Genes & Development **25**(2): 125-130.

Konig, J., K. Zarnack, G. Rot, T. Curk, M. Kayikci, B. Zupan, D. J. Turner, N. M. Luscombe and J. Ule (2010). "iCLIP reveals the function of hnRNP particles in splicing at individual nucleotide resolution." Nature Structural & Molecular Biology **17**(7): 909-915.

Kosik, K. S. (2006). "The neuronal microRNA system." Nature Reviews Neuroscience **7**(12): 911-920.

Krichevsky, A. M., K. S. King, C. P. Donahue, K. Khrapko and K. S. Kosik (2003). "A microRNA array reveals extensive regulation of microRNAs during brain development." RNA **9**(10): 1274-1281.

Kundel, M., K. J. Jones, C. Y. Shin and D. G. Wells (2009). "Cytoplasmic Polyadenylation Element-Binding Protein Regulates Neurotrophin-3-Dependent β-Catenin mRNA

Translation in Developing Hippocampal Neurons." Journal of Neuroscience **29**(43): 13630-13639.

Kuruvilla, R., H. Ye and D. D. Ginty (2000). "Spatially and functionally distinct roles of the PI3-K effector pathway during NGF signaling in sympathetic neurons." Neuron **27**(3): 499-512.

Kuruvilla, R., L. S. Zweifel, N. O. Glebova, B. E. Lonze, G. Valdez, H. Ye and D. D. Ginty (2004). "A neurotrophin signaling cascade coordinates sympathetic neuron development through differential control of TrkA trafficking and retrograde signaling." Cell **118**(2): 243-255.

Lagos-Quintana, M., R. Rauhut, A. Yalcin, J. Meyer, W. Lendeckel and T. Tuschl (2002). "Identification of Tissue-Specific MicroRNAs from Mouse." Current Biology **12**(9): 735-739.

Lasek, R., C. Dabrowski and R. Nordlander (1973) “Analysis of axoplasmic RNA from invertebrate giant axons” Nature New Biology **244**: 162-165

Lawrence, J. B. and R. H. Singer (1986). "Intracellular localization of messenger RNAs for cytoskeletal proteins." Cell **45**(3): 407-415.

Lecuyer, E., H. Yoshida, N. Parthasarathy, C. Alm, T. Babak, T. Cerovina, T. R. Hughes, P. Tomancak and H. M. Krause (2007). "Global analysis of mRNA localization reveals a prominent role in organizing cellular architecture and function." Cell **131**(1): 174-187.

Lee, D. H. and A. L. Goldberg (1998). "Proteasome inhibitors: valuable new tools for cell biologists." Trends in Cell Biology **8**(10): 397-403.

Lee, J. Y., I. Yeh, J. Y. Park and B. Tian (2007). "PolyA_DB 2: mRNA polyadenylation sites in vertebrate genes." Nucleic Acids Research **35**(Database issue): D165-168.

Leung, K. M., F. P. van Horck, A. C. Lin, R. Allison, N. Standart and C. E. Holt (2006). "Asymmetrical beta-actin mRNA translation in growth cones mediates attractive turning to netrin-1." Nature Neuroscience **9**(10): 1247-1256.

Levi-Montalcini, R. (1987). "The nerve growth factor 35 years later." Science **237**(4819): 1154-1162.

Levi-Montalcini, R. and B. Booker (1960). "Destruction of the Sympathetic Ganglia in Mammals by an Antiserum to a Nerve-Growth Protein." PNAS **46**(3): 384-391.

Levi-Montalcini, R. and S. Cohen (1956). "In Vitro and in Vivo Effects of a Nerve Growth-Stimulating Agent Isolated from Snake Venom." PNAS **42**(9): 695-699.

Levi-Montalcini, R. and V. Hamburger (1951). "Selective growth stimulating effects of mouse sarcoma on the sensory and sympathetic nervous system of the chick embryo." Journal of Experimental Zoology **116**(2): 321-361.

Lewis, B. P., C. B. Burge and D. P. Bartel (2005). "Conserved Seed Pairing, Often Flanked by Adenosines, Indicates that Thousands of Human Genes are MicroRNA Targets." Cell **120**(1): 15-20.

Li, X., X. Zhao, Y. Fang, X. Jiang, T. Duong, C. Fan, C.-C. Huang and S. R. Kain (1998). "Generation of Destabilized Green Fluorescent Protein as a Transcription Reporter." Journal of Biological Chemistry **273**(52): 34970-34975.

Lianoglou, S., V. Garg, J. L. Yang, C. S. Leslie and C. Mayr (2013). "Ubiquitously transcribed genes use alternative polyadenylation to achieve tissue-specific expression." Genes & Development **27**(21): 2380-2396.

Licatalosi, D. D., A. Mele, J. J. Fak, J. Ule, M. Kayikci, S. W. Chi, T. A. Clark, A. C. Schweitzer, J. E. Blume, X. Wang, J. C. Darnell and R. B. Darnell (2008). "HITS-CLIP yields genome-wide insights into brain alternative RNA processing." Nature **456**(7221): 464-469.

Lim, L. P., N. C. Lau, P. Garrett-Engele, A. Grimson, J. M. Schelter, J. Castle, D. P. Bartel, P. S. Linsley and J. M. Johnson (2005). "Microarray analysis shows that some microRNAs downregulate large numbers of target mRNAs." Nature **433**(7027): 769-773.

Lo, L., X. Morin, J.-F. Brunet and D. J. Anderson (1999). "Specification of Neurotransmitter Identity by Phox2 Proteins in Neural Crest Stem Cells." Neuron **22**(4): 693-705.

Lo, L., L. Sommer and D. J. Anderson (1997). "MASH1 maintains competence for BMP2-induced neuronal differentiation in post-migratory neural crest cells." Current Biology **7**(6): 440-450.

Lo, L. C., J. E. Johnson, C. W. Wuenschell, T. Saito and D. J. Anderson (1991). "Mammalian achaete-scute homolog 1 is transiently expressed by spatially restricted subsets of early neuroepithelial and neural crest cells." Genes & Development **5**(9): 1524-1537.

Loeb, D. M., R. M. Stephens, T. Copeland, D. R. Kaplan and L. A. Greene (1994). "A Trk nerve growth factor (NGF) receptor point mutation affecting interaction with phospholipase C-gamma 1 abolishes NGF-promoted peripherin induction but not neurite outgrowth." Journal of Biological Chemistry **269**(12): 8901-8910.

Long, R. M., R. H. Singer, X. Meng, I. Gonzalez, K. Nasmyth and R. P. Jansen (1997). "Mating type switching in yeast controlled by asymmetric localization of ASH1 mRNA." Science **277**(5324): 383-387.

Lonze, B. E., A. Riccio, S. Cohen and D. D. Ginty (2002). "Apoptosis, Axonal Growth Defects, and Degeneration of Peripheral Neurons in Mice Lacking CREB." Neuron **34**(3): 371-385.

Lugli, G., J. Larson, M. E. Martone, Y. Jones and N. R. Smalheiser (2005). "Dicer and eIF2c are enriched at postsynaptic densities in adult mouse brain and are modified by neuronal activity in a calpain-dependent manner." Journal of Neurochemistry **94**(4): 896-905.

Lugli, G., V. I. Torvik, J. Larson and N. R. Smalheiser (2008). "Expression of microRNAs and their precursors in synaptic fractions of adult mouse forebrain." Journal of Neurochemistry **106**(2): 650-661.

Lykke-Andersen, S., Y. Chen, B. R. Ardal, B. Lilje, J. Waage, A. Sandelin and T. H. Jensen (2014). "Human nonsense-mediated RNA decay initiates widely by endonucleolysis and targets snoRNA host genes." Genes & Development **28**(22): 2498-2517.

Macdonald, P. M. and G. Struhl (1988). "cis-acting sequences responsible for anterior localization of bicoid mRNA in Drosophila embryos." Nature **336**(6199): 595-598.

Maisonpierre, P. C., L. Belluscio, S. Squinto, N. Y. Ip, M. E. Furth, R. M. Lindsay and G. D. Yancopoulos (1990). "Neurotrophin-3: a neurotrophic factor related to NGF and BDNF." Science **247**(4949 Pt 1): 1446-1451.

Mandai, K., T. Guo, C. St. Hillaire, J. S. Meabon, K. C. Kanning, M. Bothwell and D. D. Ginty (2009). "LIG Family Receptor Tyrosine Kinase-Associated Proteins Modulate Growth Factor Signals during Neural Development." Neuron **63**(5): 614-627.

Markus, A., A. v. Holst, H. Rohrer and R. Heumann (1997). "NGF-Mediated Survival Depends on p21ras in Chick Sympathetic Neurons from the Superior Cervical but Not from Lumbosacral Ganglia." Developmental Biology **191**(2): 306-310.

Martin, K. C. and A. Ephrussi (2009). "mRNA localization: gene expression in the spatial dimension." Cell **136**(4): 719-730.

Masiero, E., L. Agatea, C. Mammucari, B. Blaauw, E. Loro, M. Komatsu, D. Metzger, C. Reggiani, S. Schiaffino and M. Sandri (2009). "Autophagy Is Required to Maintain Muscle Mass." Cell Metabolism **10**(6): 507-515.

Matoulkova, E., E. Michalova, B. Vojtesek and R. Hrstka (2012). "The role of the 3' untranslated region in post-transcriptional regulation of protein expression in mammalian cells." RNA Biology **9**(5): 563-576.

Matsuura, T., J. S. Sutcliffe, P. Fang, R. J. Galjaard, Y. H. Jiang, C. S. Benton, J. M. Rommens and A. L. Beaudet (1997). "De novo truncating mutations in E6-AP ubiquitin-protein ligase gene (UBE3A) in Angelman syndrome." Nature Genetics **15**(1): 74-77.

Mauvezin, C., M. Orpinell, V. A. Francis, F. Mansilla, J. Duran, V. Ribas, M. Palacin, P. Boya, A. A. Teleman and A. Zorzano (2010). "The nuclear cofactor DOR regulates autophagy in mammalian and Drosophila cells." EMBO Reports **11**(1): 37-44.

Mauvezin, C., A. Sancho, S. Ivanova, M. Palacin and A. Zorzano (2012). "DOR undergoes nucleo-cytoplasmic shuttling, which involves passage through the nucleolus." FEBS Lett **586**(19): 3179-3186.

Mayr, C. (2016). "Evolution and Biological Roles of Alternative 3'UTRs." Trends in Cell Biology **26**(3): 227-237.

Mayr, C. and D. P. Bartel (2009). "Widespread shortening of 3'UTRs by alternative cleavage and polyadenylation activates oncogenes in cancer cells." Cell **138**(4): 673-684.

McHugh, C. A., C.-K. Chen, A. Chow, C. F. Surka, C. Tran, P. McDonel, A. Pandya-Jones, M. Blanco, C. Burghard, A. Moradian, M. J. Sweredoski, A. A. Shishkin, J. Su, E. S. Lander, S. Hess, K. Plath and M. Guttman (2015). "The Xist lncRNA interacts directly with SHARP to silence transcription through HDAC3." Nature **521**(7551): 232-236.

McHugh, L. and J. W. Arthur (2008). "Computational Methods for Protein Identification from Mass Spectrometry Data." PLoS Computational Biology **4**(2): e12.

Mendez, R., L. E. Hake, T. Andresson, L. E. Littlepage, J. V. Ruderman and J. D. Richter (2000). "Phosphorylation of CPE binding factor by Eg2 regulates translation of c-mos mRNA." Nature **404**(6775): 302-307.

Mercer, T. R., D. Wilhelm, M. E. Dinger, G. Solda, D. J. Korbie, E. A. Glazov, V. Truong, M. Schwenke, C. Simons, K. I. Matthaei, R. Saint, P. Koopman and J. S. Mattick (2011). "Expression of distinct RNAs from 3' untranslated regions." Nucleic Acids Research **39**(6): 2393-2403.

Merianda, T. T., C. Gomes, S. Yoo, D. Vuppalanchi and J. L. Twiss (2013). "Axonal localization of neuritin/CPG15 mRNA in neuronal populations through distinct 5' and 3' UTR elements." Journal of Neuroscience **33**(34): 13735-13742.

Michaelevski, I., Y. Segal-Ruder, M. Rozenbaum, K. F. Medzihradszky, O. Shalem, G. Coppola, S. Horn-Saban, K. Ben-Yaakov, S. Y. Dagan, I. Rishal, D. H. Geschwind, Y. Pilpel, A. L. Burlingame and M. Fainzilber (2010). "Signaling to transcription networks in the neuronal retrograde injury response." Science Signaling **3**(130): ra53.

Mili, S., K. Moissoglu and I. G. Macara (2008). "Genome-wide screen reveals APC-associated RNAs enriched in cell protrusions." Nature **453**(7191): 115-119.

Ming, G. L., S. T. Wong, J. Henley, X. B. Yuan, H. J. Song, N. C. Spitzer and M. M. Poo (2002). "Adaptation in the chemotactic guidance of nerve growth cones." Nature **417**(6887): 411-418.

Mischel, P. S., S. G. Smith, E. R. Vining, J. S. Valletta, W. C. Mobley and L. F. Reichardt (2001). "The Extracellular Domain of p75NTR Is Necessary to Inhibit Neurotrophin-3 Signaling through TrkA." Journal of Biological Chemistry **276**(14): 11294-11301.

Miura, P., S. Shenker, C. Andreu-Agullo, J. O. Westholm and E. C. Lai (2013). "Widespread and extensive lengthening of 3' UTRs in the mammalian brain." Genome Research **23**(5): 812-825.

Miyashiro, K., M. Dichter and J. Eberwine (1994). "On the nature and differential distribution of mRNAs in hippocampal neurites: implications for neuronal functioning." PNAS **91**(23): 10800-10804.

Moughamian, A. J., G. E. Osborn, J. E. Lazarus, S. Maday and E. L. Holzbaur (2013). "Ordered recruitment of dynactin to the microtubule plus-end is required for efficient initiation of retrograde axonal transport." Journal of Neuroscience **33**(32): 13190-13203.

Mowry, K. L. and D. A. Melton (1992). "Vegetal messenger RNA localization directed by a 340-nt RNA sequence element in Xenopus oocytes." Science **255**(5047): 991-994.

Nalavadi, V. C., R. S. Muddashetty, C. Gross and G. J. Bassell (2012). "Dephosphorylation-induced ubiquitination and degradation of FMRP in dendrites: a role in immediate early mGluR-stimulated translation." Journal of Neuroscience **32**(8): 2582-2587.

Natera-Naranjo, O., A. Aschrafi, A. E. Gioio and B. B. Kaplan (2010). "Identification and quantitative analyses of microRNAs located in the distal axons of sympathetic neurons." RNA **16**(8): 1516-1529.

Nielsen, C. B., N. Shomron, R. Sandberg, E. Hornstein, J. Kitzman and C. B. Burge (2007). "Determinants of targeting by endogenous and exogenous microRNAs and siRNAs." RNA **13**(11): 1894-1910.

Nishino, J., K. Mochida, Y. Ohfuji, T. Shimazaki, C. Meno, S. Ohishi, Y. Matsuda, H. Fujii, Y. Saijoh and H. Hamada (1999). "GFRα3, a Component of the Artemin Receptor, Is Required for Migration and Survival of the Superior Cervical Ganglion." Neuron **23**(4): 725-736.

Nowak, J., C. Archange, J. Tardivel-Lacombe, P. Pontarotti, M. J. Pebusque, M. I. Vaccaro, G. Velasco, J. C. Dagorn and J. L. Iovanna (2009). "The TP53INP2 protein is required for autophagy in mammalian cells." Molecular Biology of the Cell **20**(3): 870-881.

Nowak, J., D. Depetris, J. L. Iovanna, M. G. Mattei and M. J. Pebusque (2005). "Assignment of the tumor protein p53 induced nuclear protein 2 (TP53INP2) gene to human chromosome band 20q11.2 by in situ hybridization." Cytogenetic and Genome Research **108**(4): 362.

Obermeier, A., H. Halfter, K. H. Wiesmuller, G. Jung, J. Schlessinger and A. Ullrich (1993). "Tyrosine 785 is a major determinant of Trk--substrate interaction." EMBO J **12**(3): 933-941.

Oldenborg, P.-A., A. Zheleznyak, Y.-F. Fang, C. F. Lagenaur, H. D. Gresham and F. P. Lindberg (2000). "Role of CD47 as a Marker of Self on Red Blood Cells." Science **288**(5473): 2051-2054.

Oldenborg, P. A., A. Zheleznyak, Y. F. Fang, C. F. Lagenaur, H. D. Gresham and F. P. Lindberg (2000). "Role of CD47 as a marker of self on red blood cells." Science **288**(5473): 2051-2054.

Oppenheim, R. W. (1991). "Cell death during development of the nervous system." Annual Review of Neuroscience **14**: 453-501.

Palay S. and G. Palade (1955). " The fine structure of neurons." Journal of Biophysical and Biochemical Cytology **1**:69-88

Pan, Y. X., H. Chen and M. S. Kilberg (2005). "Interaction of RNA-binding proteins HuR and AUF1 with the human ATF3 mRNA 3'-untranslated region regulates its amino acid limitation-induced stabilization." The Journal of Biological Chemistry **280**(41): 34609-34616.

Paquin, N. and P. Chartrand (2008). "Local regulation of mRNA translation: new insights from the bud." Trends in Cell Biology **18**(3): 105-111.

Pasquinelli, A. E. (2012). "MicroRNAs and their targets: recognition, regulation and an emerging reciprocal relationship." Nature Reviews Genetics **13**(4): 271-282.

Pazyra-Murphy, M. F., A. Hans, S. L. Courchesne, C. Karch, K. E. Cosker, H. M. Heerssen, F. L. Watson, T. Kim, M. E. Greenberg and R. A. Segal (2009). "A retrograde neuronal survival response: target-derived neurotrophins regulate MEF2D and bcl-w." Journal of Neuroscience **29**(20): 6700-6709.

Perez, P., P. M. Coll, B. L. Hempstead, D. Martin-Zanca and M. V. Chao (1995). "NGF binding to the trk tyrosine kinase receptor requires the extracellular immunoglobulin-like domains." Molecular and Cellular Neuroscience **6**(2): 97-105.

Perrone-Bizzozero, N. and C. W. Bird (2013). "Role of HuD in nervous system function and pathology." Frontiers in Bioscience **5**: 554-563.

Perry, R. B., E. Doron-Mandel, E. Iavnilovitch, I. Rishal, S. Y. Dagan, M. Tsoory, G. Coppola, M. K. McDonald, C. Gomes, D. H. Geschwind, J. L. Twiss, A. Yaron and M. Fainzilber (2012). "Subcellular knockout of importin beta1 perturbs axonal retrograde signaling." Neuron **75**(2): 294-305.

Perry, R. B.-T., I. Rishal, E. Doron-Mandel, A. L. Kalinski, K. F. Medzihradszky, M. Terenzio, S. Alber, S. Koley, A. Lin, M. Rozenbaum, D. Yudin, P. K. Sahoo, C. Gomes, V. Shinder, W. Geraisy, E. A. Huebner, C. J. Woolf, A. Yaron, A. L. Burlingame, J. L. Twiss and M. Fainzilber (2016). "Nucleolin-Mediated RNA Localization Regulates Neuron Growth and Cycling Cell Size." Cell Reports **16**(6): 1664-1676.

Petroulakis, E. and E. Wang (2002). "Nerve Growth Factor Specifically Stimulates Translation of Eukaryotic Elongation Factor 1A-1 (eEF1A-1) mRNA by Recruitment to Polyribosomes in PC12 Cells." Journal of Biological Chemistry **277**(21): 18718-18727.

Pichardo-Casas, I., L. A. Goff, M. R. Swerdel, A. Athie, J. Davila, M. Ramos-Brossier, M. Lapid-Volosin, W. J. Friedman, R. P. Hart and L. Vaca (2012). "Expression profiling of synaptic microRNAs from the adult rat brain identifies regional differences and seizure-induced dynamic modulation." Brain Research **1436**: 20-33.

Piper, M., R. Anderson, A. Dwivedy, C. Weinl, F. van Horck, K. M. Leung, E. Cogill and C. Holt (2006). "Signaling mechanisms underlying Slit2-induced collapse of Xenopus retinal growth cones." Neuron **49**(2): 215-228.

Policarpi, C., L. Crepaldi, E. Brookes, J. Nitarska, S. French, A. Coatti and A. Riccio (2017). "Enhancer SINEs Link Pol III to Pol II Transcription in Neurons." Cell Reports **21**: 1-16.

Poliseno, L., L. Salmena, J. Zhang, B. Carver, W. J. Haveman and P. P. Pandolfi (2010). "A coding-independent function of gene and pseudogene mRNAs regulates tumour biology." Nature **465**(7301): 1033-1038.

Poon, M. M., S.-H. Choi, C. A. M. Jamieson, D. H. Geschwind and K. C. Martin (2006). "Identification of Process-Localized mRNAs from Cultured Rodent Hippocampal Neurons." Journal of Neuroscience **26**(51): 13390-13399.

Proudfoot, N. J. (2011). "Ending the message: poly(A) signals then and now." Genes & Development **25**(17): 1770-1782.

Rangaraju, V., S. Tom Dieck and E. M. Schuman (2017). "Local translation in neuronal compartments: how local is local?" EMBO Reports **18**(5): 693-711.

Reichardt, L. F. (2006). "Neurotrophin-regulated signalling pathways." Philos Trans R Soc Lond B Biol Sci **361**(1473): 1545-1564.

Riccio, A., S. Ahn, C. M. Davenport, J. A. Blendy and D. D. Ginty (1999). "Mediation by a CREB family transcription factor of NGF-dependent survival of sympathetic neurons." Science **286**(5448): 2358-2361.

Riccio, A., B. A. Pierchala, C. L. Ciarallo and D. D. Ginty (1997). "An NGF-TrkA-mediated retrograde signal to transcription factor CREB in sympathetic neurons." Science **277**(5329): 1097-1100.

Rodriguez-Tebar, A., G. Dechant and Y. A. Barde (1990). "Binding of brain-derived neurotrophic factor to the nerve growth factor receptor." Neuron **4**(4): 487-492.

Rodriguez-Tebar, A., G. Dechant, R. Gotz and Y. A. Barde (1992). "Binding of neurotrophin-3 to its neuronal receptors and interactions with nerve growth factor and brain-derived neurotrophic factor." EMBO J **11**(3): 917-922.

Ross, A. F., Y. Oleynikov, E. H. Kislauskis, K. L. Taneja and R. H. Singer (1997). "Characterization of a beta-actin mRNA zipcode-binding protein." Molecular and Cellular Biology **17**(4): 2158-2165.

Ross, R. A., D. L. Lazarova, G. T. Manley, P. S. Smitt, B. A. Spengler, J. B. Posner and J. L. Biedler (1997). "HuD, a neuronal-specific RNA-binding protein, is a potential regulator of MYCN expression in human neuroblastoma cells." Eur J Cancer **33**(12): 2071-2074.

Roufa, D., M. B. Bunge, M. I. Johnson and C. J. Cornbrooks (1986). "Variation in content and function of non-neuronal cells in the outgrowth of sympathetic ganglia from embryos of differing age." Journal of Neuroscience **6**(3): 790-802.

Rubin, E. (1985). "Development of the rat superior cervical ganglion: ganglion cell maturation." Journal of Neuroscience **5**(3): 673-684.

Rubin, E. (1985). "Development of the rat superior cervical ganglion: ingrowth of preganglionic axons." Journal of Neuroscience **5**(3): 685-696.

Ryu, Y. K., S. E. Collins, H. Y. Ho, H. Zhao and R. Kuruvilla (2013). "An autocrine Wnt5a-Ror signaling loop mediates sympathetic target innervation." Developmental Biology **377**(1): 79-89.

Saba, R., P. H. Storchel, A. Aksoy-Aksel, F. Kepura, G. Lippi, T. D. Plant and G. M. Schratt (2012). "Dopamine-regulated microRNA MiR-181a controls GluA2 surface expression in hippocampal neurons." Molecular and Cellular Biology **32**(3): 619-632.

Sala, D., S. Ivanova, N. Plana, V. Ribas, J. Duran, D. Bach, S. Turkseven, M. Laville, H. Vidal, M. Karczewska-Kupczewska, I. Kowalska, M. Straczkowski, X. Testar, M. Palacin, M. Sandri, A. L. Serrano and A. Zorzano (2014). "Autophagy-regulating TP53INP2 mediates muscle wasting and is repressed in diabetes." J Clin Invest **124**(5): 1914-1927.

Sala, D. and A. Zorzano (2015). "Is TP53INP2 a critical regulator of muscle mass?" Curr Opin Clin Nutr Metab Care **18**(3): 234-239.

Salmena, L., L. Poliseno, Y. Tay, L. Kats and P. P. Pandolfi (2011). "A ceRNA hypothesis: the Rosetta Stone of a hidden RNA language?" Cell **146**(3): 353-358.

Sambandan, S., G. Akbalik, L. Kochen, J. Rinne, J. Kahlstatt, C. Glock, G. Tushev, B. Alvarez-Castelao, A. Heckel and E. M. Schuman (2017). "Activity-dependent spatially localized miRNA maturation in neuronal dendrites." Science **355**(6325): 634-637.

Sancho, A., J. Duran, A. Garcia-Espana, C. Mauvezin, E. A. Alemu, T. Lamark, M. J. Macias, R. DeSalle, M. Royo, D. Sala, J. U. Chicote, M. Palacin, T. Johansen and A. Zorzano (2012). "DOR/Tp53inp2 and Tp53inp1 constitute a metazoan gene family encoding dual regulators of autophagy and transcription." PLoS One **7**(3): e34034.

Sandberg, R., J. R. Neilson, A. Sarma, P. A. Sharp and C. B. Burge (2008). "Proliferating cells express mRNAs with shortened 3' untranslated regions and fewer microRNA target sites." Science **320**(5883): 1643-1647.

Sasaki, Y., C. Gross, L. Xing, Y. Goshima and G. J. Bassell (2014). "Identification of axon-enriched microRNAs localized to growth cones of cortical neurons." Developmetal Neurobiology **74**(3): 397-406.

Scarisbrick, I. A., E. G. Jones and P. J. Isackson (1993). "Coexpression of mRNAs for NGF, BDNF, and NT-3 in the cardiovascular system of the pre- and postnatal rat." Journal of Neuroscience **13**(3): 875-893.

Schratt, G. M., F. Tuebing, E. A. Nigh, C. G. Kane, M. E. Sabatini, M. Kiebler and M. E. Greenberg (2006). "A brain-specific microRNA regulates dendritic spine development." Nature **439**(7074): 283-289.

Schreiber, R. C., S. A. Vaccariello, K. Boeshore, A. M. Shadiack and R. E. Zigmond (2002). "A comparison of the changes in the non-neuronal cell populations of the superior cervical ganglia following decentralization and axotomy." Journal of Neurobiology **53**(1): 68-79.

Schwanhausser, B., D. Busse, N. Li, G. Dittmar, J. Schuchhardt, J. Wolf, W. Chen and M. Selbach (2011). "Global quantification of mammalian gene expression control." Nature **473**(7347): 337-342.

Sempere, L. F., S. Freemantle, I. Pitha-Rowe, E. Moss, E. Dmitrovsky and V. Ambros (2004). "Expression profiling of mammalian microRNAs uncovers a subset of brain-expressed microRNAs with possible roles in murine and human neuronal differentiation." Genome Biology **5**(3): R13-R13.

Sen, G. L. and H. M. Blau (2005). "Argonaute 2/RISC resides in sites of mammalian mRNA decay known as cytoplasmic bodies." Nature Cell Biology **7**(6): 633-636.

Sephton, C. F. and G. Yu (2015). "The function of RNA-binding proteins at the synapse: implications for neurodegeneration." Cellular and Molecular Life Sciences **72**(19): 3621-3635.

Shao, Y., W. Akmentin, J. J. Toledo-Aral, J. Rosenbaum, G. Valdez, J. B. Cabot, B. S. Hilbush and S. Halegoua (2002). "Pincher, a pinocytic chaperone for nerve growth factor/TrkA signaling endosomes." The Journal of Cell Biology **157**(4): 679-691.

Shelton, D. L. and L. F. Reichardt (1984). "Expression of the beta-nerve growth factor gene correlates with the density of sympathetic innervation in effector organs." PNAS **81**(24): 7951-7955.

Shepard, P. J., E. A. Choi, J. Lu, L. A. Flanagan, K. J. Hertel and Y. Shi (2011). "Complex and dynamic landscape of RNA polyadenylation revealed by PAS-Seq." RNA **17**(4): 761-772.

Shi, Y. (2012). "Alternative polyadenylation: new insights from global analyses." RNA **18**(12): 2105-2117.

Shi, Y., D. C. Di Giammartino, D. Taylor, A. Sarkeshik, W. J. Rice, J. R. Yates, J. Frank and J. L. Manley (2009). "Molecular Architecture of the Human Pre-mRNA 3′ Processing Complex." Molecular Cell **33**(3): 365-376.

Shigeoka, T., H. Jung, J. Jung, B. Turner-Bridger, J. Ohk, J. Q. Lin, P. S. Amieux and C. E. Holt (2016). "Dynamic Axonal Translation in Developing and Mature Visual Circuits." Cell **166**(1): 181-192.

Smeyne, R. J., R. Klein, A. Schnapp, L. K. Long, S. Bryant, A. Lewin, S. A. Lira and M. Barbacid (1994). "Severe sensory and sympathetic neuropathies in mice carrying a disrupted Trk/NGF receptor gene." Nature **368**(6468): 246-249.

Spiegelman, B. M., S. M. Penningroth and M. W. Kirschner (1977). "Turnover of tubulin and the N site GTP in Chinese hamster ovary cells." Cell **12**(3): 587-600.

Spies, N., C. B. Burge and D. P. Bartel (2013). "3' UTR-isoform choice has limited influence on the stability and translational efficiency of most mRNAs in mouse fibroblasts." Genome Research **23**(12): 2078-2090.

Stephens, R. M., D. M. Loeb, T. D. Copeland, T. Pawson, L. A. Greene and D. R. Kaplan (1994). "Trk receptors use redundant signal transduction pathways involving SHC and PLC-γ1 to mediate NGF responses." Neuron **12**(3): 691-705.

Subhojit, R. (2014). "Seeing the Unseen." The Neuroscientist **20**(1): 71-81.

Takizawa, P. A., A. Sil, J. R. Swedlow, I. Herskowitz and R. D. Vale (1997). "Actin-dependent localization of an RNA encoding a cell-fate determinant in yeast." Nature **389**(6646): 90-93.

Taliaferro, J. M., M. Vidaki, R. Oliveira, S. Olson, L. Zhan, T. Saxena, E. T. Wang, B. R. Graveley, F. B. Gertler, M. S. Swanson and C. B. Burge (2016). "Distal Alternative Last Exons Localize mRNAs to Neural Projections." Molecular Cell **61**(6): 821-833.

Tasdemir-Yilmaz, O. E. and R. A. Segal (2016). "There and back again: coordinated transcription, translation and transport in axonal survival and regeneration." Current Opinion in Neurobiology **39**(Supplement C): 62-68.

Taylor, A. M., N. C. Berchtold, V. M. Perreau, C. H. Tu, N. Li Jeon and C. W. Cotman (2009). "Axonal mRNA in uninjured and regenerating cortical mammalian axons." Journal of Neuroscience **29**(15): 4697-4707.

Tcherkezian, J., P. A. Brittis, F. Thomas, P. P. Roux and J. G. Flanagan (2010). "Transmembrane receptor DCC associates with protein synthesis machinery and regulates translation." Cell **141**(4): 632-644.

Thelen, K., B. Maier, M. Faber, C. Albrecht, P. Fischer and G. E. Pollerberg (2012). "Translation of the cell adhesion molecule ALCAM in axonal growth cones - regulation and functional importance." Journal of Cell Science **125**(Pt 4): 1003-1014.

Thomsen, G. H. and D. A. Melton (1993). "Processed Vg1 protein is an axial mesoderm inducer in xenopus." Cell **74**(3): 433-441.

Thomson, D. W. and M. E. Dinger (2016). "Endogenous microRNA sponges: evidence and controversy." Nature Reviews Genetics **17**(5): 272-283.

Tian, B., J. Hu, H. Zhang and C. S. Lutz (2005). "A large-scale analysis of mRNA polyadenylation of human and mouse genes." Nucleic Acids Research **33**(1): 201-212.

Tian, B. and J. L. Manley (2017). "Alternative polyadenylation of mRNA precursors." Nature Reviews Molecular Cell Biology **18**(1): 18-30.

Twiss, J. L., D. S. Smith, B. Chang and E. M. Shooter (2000). "Translational control of ribosomal protein L4 mRNA is required for rapid neurite regeneration." Neurobiology of Disease **7**(4): 416-428.

Ule, J., K. Jensen, A. Mele and R. B. Darnell (2005). "CLIP: a method for identifying protein-RNA interaction sites in living cells." Methods **37**(4): 376-386.

Ule, J., K. B. Jensen, M. Ruggiu, A. Mele, A. Ule and R. B. Darnell (2003). "CLIP identifies Nova-regulated RNA networks in the brain." Science **302**(5648): 1212-1215.

Valdez, G., W. Akmentin, P. Philippidou, R. Kuruvilla, D. D. Ginty and S. Halegoua (2005). "Pincher-Mediated Macroendocytosis Underlies Retrograde Signaling by Neurotrophin Receptors." Journal of Neuroscience **25**(21): 5236-5247.

Valluy, J., S. Bicker, A. Aksoy-Aksel, M. Lackinger, S. Sumer, R. Fiore, T. Wust, D. Seffer, F. Metge, C. Dieterich, M. Wohr, R. Schwarting and G. Schratt (2015). "A coding-independent function of an alternative Ube3a transcript during neuronal development." Nature Neuroscience **18**(5): 666-673.

Van Der Kelen, K., R. Beyaert, D. Inze and L. De Veylder (2009). "Translational control of eukaryotic gene expression." Critical Reviews in Biochemistry and Molecular Biology **44**(4): 143-168.

Van Minnen, J., J.J. Bergman, E.R. Van Kesteren, A.B. Smit, W.P. Geraerts, K. Lukowiak, S.U. Hasan and N.I. Syed (1997) “De novo protein synthesis in isolated axons of identified neurons.” Neuroscience **80:**1-7

Wang, B., L. Pan, M. Wei, Q. Wang, W. W. Liu, N. Wang, X. Y. Jiang, X. Zhang and L. Bao (2015). "FMRP-Mediated Axonal Delivery of miR-181d Regulates Axon Elongation by Locally Targeting Map1b and Calm1." Cell Reports **13**(12): 2794-2807.

Wang, E. T., J. M. Taliaferro, J.-A. Lee, I. P. Sudhakaran, W. Rossoll, C. Gross, K. R. Moss and G. J. Bassell (2016). "Dysregulation of mRNA Localization and Translation in Genetic Disease." Journal of Neuroscience **36**(45): 11418-11426.

Wang, K. C. and H. Y. Chang (2011). "Molecular mechanisms of long noncoding RNAs." Molecular Cell **43**(6): 904-914.

Wang, P. and S. R. Wilson (2013). "Mass spectrometry-based protein identification by integrating de novo sequencing with database searching." BMC Bioinformatics **14**(Suppl 2): S24-S24.

Watson, F. L., H. M. Heerssen, D. B. Moheban, M. Z. Lin, C. M. Sauvageot, A. Bhattacharyya, S. L. Pomeroy and R. A. Segal (1999). "Rapid nuclear responses to target-derived neurotrophins require retrograde transport of ligand-receptor complex." Journal of Neuroscience **19**(18): 7889-7900.

Welshhans, K. and G. J. Bassell (2011). "Netrin-1-induced local beta-actin synthesis and growth cone guidance requires zipcode binding protein 1." Journal of Neuroscience **31**(27): 9800-9813.

Will, T. J., G. Tushev, L. Kochen, B. Nassim-Assir, I. J. Cajigas, S. tom Dieck and E. M. Schuman (2013). "Deep Sequencing and High-Resolution Imaging Reveal Compartment-Specific Localization of Bdnf mRNA in Hippocampal Neurons." Science signaling **6**(306): rs16-rs16.

Willis, D. E., E. A. van Niekerk, Y. Sasaki, M. Mesngon, T. T. Merianda, G. G. Williams, M. Kendall, D. S. Smith, G. J. Bassell and J. L. Twiss (2007). "Extracellular stimuli specifically regulate localized levels of individual neuronal mRNAs." The Journal of Cell Biology **178**(6): 965-980.

Willis, D. E., M. Xu, C. J. Donnelly, C. Tep, M. Kendall, M. Erenstheyn, A. W. English, N. C. Schanen, C. B. Kirn-Safran, S. O. Yoon, G. J. Bassell and J. L. Twiss (2011). "Axonal Localization of transgene mRNA in mature PNS and CNS neurons." Journal of Neuroscience **31**(41): 14481-14487.

Wolozin, B. (2012). "Regulated protein aggregation: stress granules and neurodegeneration." Molecular Neurodegeneration **7**: 56.

Wu, K. Y., U. Hengst, L. J. Cox, E. Z. Macosko, A. Jeromin, E. R. Urquhart and S. R. Jaffrey (2005). "Local translation of RhoA regulates growth cone collapse." Nature **436**(7053): 1020-1024.

Wyatt, S. and A. M. Davies (1995). "Regulation of nerve growth factor receptor gene expression in sympathetic neurons during development." The Journal of Cell Biology **130**(6): 1435-1446.

Xanthos, J. B., M. Kofron, C. Wylie and J. Heasman (2001). "Maternal VegT is the initiator of a molecular network specifying endoderm in Xenopus laevis." Development **128**(2): 167-180.

Xing, J., D. D. Ginty and M. E. Greenberg (1996). "Coupling of the RAS-MAPK Pathway to Gene Activation by RSK2, a Growth Factor-Regulated CREB Kinase." Science **273**(5277): 959-963.

Xu, Y., W. Wan, X. Shou, R. Huang, Z. You, Y. Shou, L. Wang, T. Zhou and W. Liu (2016). "TP53INP2/DOR, a mediator of cell autophagy, promotes rDNA transcription via facilitating the assembly of the POLR1/RNA polymerase I preinitiation complex at rDNA promoters." Autophagy **12**(7): 1118-1128.

Yamashita, N. and R. Kuruvilla (2016). "Neurotrophin signaling endosomes: biogenesis, regulation, and functions." Current Opinion in Neurobiology **39**: 139-145.

Yamashita, T. and M. Tohyama (2003). "The p75 receptor acts as a displacement factor that releases Rho from Rho-GDI." Nature Neuroscience **6**(5): 461-467.

Yamashita, T., K. L. Tucker and Y. A. Barde (1999). "Neurotrophin binding to the p75 receptor modulates Rho activity and axonal outgrowth." Neuron **24**(3): 585-593.

Yao, J., Y. Sasaki, Z. Wen, G. J. Bassell and J. Q. Zheng (2006). "An essential role for beta-actin mRNA localization and translation in Ca2+-dependent growth cone guidance." Nature Neuroscience **9**(10): 1265-1273.

Ye, H., R. Kuruvilla, L. S. Zweifel and D. D. Ginty (2003). "Evidence in support of signaling endosome-based retrograde survival of sympathetic neurons." Neuron **39**(1): 57-68.

Yoon, B. C., H. Jung, A. Dwivedy, C. M. O'Hare, K. H. Zivraj and C. E. Holt (2012). "Local translation of extranuclear lamin B promotes axon maintenance." Cell **148**(4): 752-764.

Young, H. M., K. N. Cane and C. R. Anderson (2011). "Development of the autonomic nervous system: a comparative view." Auton Neurosci **165**(1): 10-27.

Yudin, D., S. Hanz, S. Yoo, E. Iavnilovitch, D. Willis, T. Gradus, D. Vuppalanchi, Y. Segal-Ruder, K. Ben-Yaakov, M. Hieda, Y. Yoneda, J. L. Twiss and M. Fainzilber (2008). "Localized regulation of axonal RanGTPase controls retrograde injury signaling in peripheral nerve." Neuron **59**(2): 241-252.

Zhang, H., J. Y. Lee and B. Tian (2005). "Biased alternative polyadenylation in human tissues." Genome Biology **6**(12): R100.

Zhang, H. L., T. Eom, Y. Oleynikov, S. M. Shenoy, D. A. Liebelt, J. B. Dictenberg, R. H. Singer and G. J. Bassell (2001). "Neurotrophin-induced transport of a beta-actin mRNP complex increases beta-actin levels and stimulates growth cone motility." Neuron **31**(2): 261-275.

Zhang, J. and M. L. King (1996). "Xenopus VegT RNA is localized to the vegetal cortex during oogenesis and encodes a novel T-box transcription factor involved in mesodermal patterning." Development **122**(12): 4119-4129.

Zhao, J., B. K. Sun, J. A. Erwin, J. J. Song and J. T. Lee (2008). "Polycomb proteins targeted by a short repeat RNA to the mouse X chromosome." Science **322**(5902): 750-756.

Zheng, J. Q., T. K. Kelly, B. Chang, S. Ryazantsev, A. K. Rajasekaran, K. C. Martin and J. L. Twiss (2001). "A functional role for intra-axonal protein synthesis during axonal regeneration from adult sensory neurons." Journal of Neuroscience **21**(23): 9291-9303.

Zheng, T., J. Chou, F. Zhang, Y. Liu, H. Ni, X. Li, L. Zheng, T. Tang, L. Jin and T. Xi (2015). "CXCR4 3'UTR functions as a ceRNA in promoting metastasis, proliferation and survival of MCF-7 cells by regulating miR-146a activity." European Journal of Cell Biology **94**(10): 458-469.

Zhou, F.-Q., J. Zhou, S. Dedhar, Y.-H. Wu and W. D. Snider (2004). "NGF-Induced Axon Growth Is Mediated by Localized Inactivation of GSK-3β and Functions of the Microtubule Plus End Binding Protein APC." Neuron **42**(6): 897-912.

Zivraj, K. H., Y. C. Tung, M. Piper, L. Gumy, J. W. Fawcett, G. S. Yeo and C. E. Holt (2010). "Subcellular profiling reveals distinct and developmentally regulated repertoire of growth cone mRNAs." Journal of Neuroscience **30**(46): 15464-15478.

Zweifel, L. S., R. Kuruvilla and D. D. Ginty (2005). "Functions and mechanisms of retrograde neurotrophin signalling." Nature Reviews Neuroscience **6**(8): 615-625.